

Copyright Warning & Restrictions

The copyright law of the United States (Title 17, United States Code) governs the making of photocopies or other reproductions of copyrighted material.

Under certain conditions specified in the law, libraries and archives are authorized to furnish a photocopy or other reproduction. One of these specified conditions is that the photocopy or reproduction is not to be “used for any purpose other than private study, scholarship, or research.” If a user makes a request for, or later uses, a photocopy or reproduction for purposes in excess of “fair use” that user may be liable for copyright infringement,

This institution reserves the right to refuse to accept a copying order if, in its judgment, fulfillment of the order would involve violation of copyright law.

Please Note: The author retains the copyright while the New Jersey Institute of Technology reserves the right to distribute this thesis or dissertation

Printing note: If you do not wish to print this page, then select “Pages from: first page # to: last page #” on the print dialog screen



The Van Houten library has removed some of the personal information and all signatures from the approval page and biographical sketches of theses and dissertations in order to protect the identity of NJIT graduates and faculty.

2)
=
INVESTIGATION OF MIXED - MODE
=
FRACTURE IN CONCRETE
=

BY

)
STYLIANOS C. ANIFTOS
=

This thesis is submitted to the faculty of
Graduate School of New Jersey Institute of Technology
in partial fulfillment of the requirements for the degree of
Master of Science in Civil Engineering
1990

APPROVAL SHEET

Title of Thesis : Investigation of Mixed -
Mode Frature in Concrete

Name of Candidate : STYLIANOS C. ANIFTOS
Master of Science in
Civil Engineering

Thesis and Abstract
Approved :

2/5/90

Dr. Methi Wecharatana Date
Associate Professor
Department of Civil
Engineering

Signature of other members
of Thesis Committee :

2/4/90

Dr. Ala Saadehvazivi Date
Assistant Professor

2/5/90

Dr. Namunu meegoda Date
Assistant Professor

VITA

NAME : Stylianos C. Aniftos

DEGREE AND DATE OF
CONFERRED : MSCE, May 1990

SECONDARY & HIGH SCHOOL
EDUCATION : Lanitioy Gymnasium, Limassol,
Cyprus

COLLEGIATE INSTITUTIONS
ATTENDED :

	DATE	DEGREE	DATE OF DEGREE
ESSEX COUNTY COLLEGE NEWARK NJ	1/84 12/85	-----	-----
NEW JERSEY INST. OF TECHNOLOGY, NEWARK NJ	1/86 5/90	BSCE MSCE	May 1990

MAJOR : CIVIL ENGINEERING

ABSTRACT

Title of Thesis : Investigation of Mixed - Mode Fracture in Concrete

Stylianos Anifetos, Master of Science in Civil Engineering, 1989

Thesis Directed by : Dr. Methi Wecharatana, Associate Professor of Civil Engineering

This study is aimed at evaluating the failure characteristics of concrete in the notched beam configuration. In general, for Mode I failure tension is commonly encountered. However, in the area of high shear stress, it remains to be a question whether shear or Mode II failure exists. Researches carried out in the past decade confirmed the existance of both Mode I and Mode II failure. It is the objective of this investigation to clarify this failure characteristics using FRANC an interactive fracture mechanics software.

The investigation carried out in this study used the experimental results of Bazant and Pfeiffer (3) and Jeng and Shah (5) as the input data to the FRANC software. Stress analysis, stress intensity factors, the load-CMOD, and the load CMOD were analyzed and plotted and compared with the experimental data. The results indicate that a good correlation (89% accuracy) between FRANC's results and the experimental data. Also observed in this study are the effects of specimen size, notch depth, and notch off-set distance on the P-CMOD in the single notch specimen reported by Jeng and Shah (5). These effects are less pronounced for the double notch specimen of Bazant and Pfeiffer (3).

Blank Page

ACKNOWLEDGEMENTS

I wish to thank Dr. Methi Wecharatana for his guidance and valuable assistance throughout the entire project.

The participation of S. Chimamphant, S. Ratanalert and L. Leary during the casting and testing is gratefully appreciated.

I also thank T. Hernandez for her help in typing this thesis.

TABLE OF CONTENTS

Chapter	Page
Abstract	i
Acknowledgements	ii
Table of Contents	iii
List of Figures	iv
List of Tables	vi
1) Introduction	
1.1 General.....	1
1.2 Literature Review.....	2
1.3 Objectives.....	11
2) Experimental and Theoretical Investigations	
2.1 Testing Procedure used by Bazant and Pfeiffer.....	15
2.2 Testing Procedure used by Jeng and Shah.....	16
2.3 Fracture Analysis Code (FRANC) Program.....	18
3) Results and Discussion	
3.1 Solution of Beams with Double Notch.....	24
3.2 Solution of Beams with Single Notch.....	26
3.3 Comparison of results with other studies.....	29
4) Conclusion.....	83
Appendix A.....	84
Appendix B.....	100
References.....	121

LIST OF FIGURES

Figures	Page
1.1	Specimen used by Arrea and Ingraffea(1)..... 13
1.2	Specimen used by Bazant and Pfeiffer(3) and Swartz and Taha(8)..... 12
1.3	Specimen used by Jeng and Shah(5)..... 13
1.4	Specimen used by Barr, Hasso, and Khalifa(2)..... 14
1.5	Crack pattern for Beams used by Swartz and Taha(8). 13
2.1	Mixed-Mode fracture specimen and loading apparatus. used by Bazant and Pfeiffer (3).....20
2.2	Typical CMSD vs LOAD relationship for Bazant and Pfeiffer test.....21
2.3	Specimen used by Jeng and Shah (5).....22
2.4	Typical CMOD vs LOAD relationship for Jeng and Shah's test.....23
3.1	Dimensions of double notch specimen..... 34
3.2	Loading conditions..... 35
3.3	Sliding displacement for the double notched beam #5 33
3.4	Sliding displacement for the double notched beam #6 34
3.5	Mesh Configuration..... 38
3.6	Deformed Mesh..... 39
3.7	Sx on Section 1-1..... 40
3.8	Sy on Section 1-1..... 41
3.9	Sxy on Section 1-1..... 42
3.10	Sx on Section 2-2..... 43
3.11	Sxy on Section 2-2..... 44
3.12	Sx on Section 3-3..... 45
3.13	Sxy on Section 3-3..... 46
3.14	Tensile Principal Stress Vectors..... 47
3.15	Dimension of Single Notch Specimen..... 48
3.16	Crack mouth opening displacement for the single notched beam #C1M2..... 49
3.17	Crack mouth opening displacement for the single notched beam #M256..... 50
3.18	Crack mouth opening displacement for the single notched beam #C1S3..... 51
3.19	Mesh Configuration for x=9..... 52
3.20	Mesh Configuration for x=6..... 53
3.21	Mesh Configuration for x=3..... 54
3.22	Deformed Mesh (x=9)..... 55
3.23	Deformed Mesh (x=6)..... 56
3.24	Deformed Mesh (x=3)..... 57
3.25	Sx on Section 1-1 (x=9)..... 58
3.26	Sx on Section 1-1 (x=6)..... 59
3.27	Sx on Section 1-1 (x=3)..... 60
3.28	Sy on Section 1-1 (x=9)..... 61
3.29	Sy on Section 1-1 (x=6)..... 62

LIST OF FIGURES (CONT.)

Figures		Page
3.30	S_y on Section 1-1 ($x=3$).....	63
3.31	S_{xy} on Section 1-1 ($x=9$).....	64
3.32	S_{xy} on Section 1-1 ($x=6$).....	65
3.33	S_{xy} on Section 1-1 ($x=3$).....	66
3.34	S_x on Section 2-2 ($x=9$).....	67
3.35	S_x on Section 2-2 ($x=6$).....	68
3.36	S_x on Section 2-2 ($x=3$).....	69
3.37	S_{xy} on section 2-2 ($x=9$).....	70
3.38	S_{xy} on Section 2-2 ($x=6$).....	71
3.39	S_{xy} on Section 2-2 ($x=3$).....	72
3.40	Tensile Principal Stress Vectors ($x=9$).....	73
3.41	Tensile Principal Stress Vectors ($x=6$).....	74
3.42	Tensile Principal Stress Vectors ($x=3$).....	75
3.43	Stress Normal to Line 1-1 ($x=9$).....	76
3.44	Stress Normal to Line 1-1 ($x=6$).....	77
3.45	Stress Normal to Line 1-1 ($x=3$).....	78
3.46	Shear Stress Along Line 1-1 ($x=9$).....	79
3.47	Shear Stress Along Line 1-1 ($x=6$).....	80
3.48	Shear Stress Along Line 1-1 ($x=3$).....	81

LIST OF TABLES

Table		Page
1	Input data given to FRANC for single and double notched beams.....	31
2	Stress Intensity Factors for the double notched beams.....	32
3	Stress Intensity Factors for the single notched beams.	33

CHAPTER 1

INTRODUCTION

1.1 General

In Fracture Mechanics there are three basic fracture modes: a) Mode I, crack opening mode; b) Mode II, sliding shear mode; and c) Mode III, tearing shear mode. In Mode I, the internal surfaces of the crack move perpendicularly to each other. In Mode II, the surfaces move in the same plane and in a direction parallel to the crack. For Mode III, the surfaces move in the same plane in a direction perpendicular to the crack. Most of the research studies reported to date on the application of Fracture Mechanics to concrete have concentrated on the Mode I type of failure, and few on the Mode II. In most cases, however, cracks in the concrete structure do not propagate in pure Mode I or pure Mode II and fracture mechanics of the Mixed-Mode which is a combination of both has also been studied.

Despite decades of research which have been carried out at various research centers around the world on the evaluation of shear performance of concrete members, current design is still based on empirical results. Many researchers have indicated the difficulties of performing a Mode II test and the results obtained

from different experiments show wide variation and disagreement on the cause of failure, that is, whether the failure was due to shear or tensile stresses. Most of the available data has been obtained from normal strength concrete. At present, there is a trend to use higher strength concrete and its fracture behavior should also be investigated.

1.2 Literature Review

Mixed-mode fracture in concrete was first studied by Arrea and Ingraffea (1) using a single notch beam. Bazant and Pfeiffer (3) later introduced a double notch beam for mixed-mode testing resulting in a straight crack plane. Arrea and Ingraffea observed a crack at the top of the notch which propagated at a certain angle into the material and proceeded subsequently more or less vertically and ended under the Load Point. (Fig. 1.1) They concluded that shear failure as such does not exist.

Bazant and Pfeiffer disagreed strongly with the idea of non-existence of shear failure. They argued that the crack path observed by Arrea and Ingraffea (1) was due to the wide zone of shear force. For their tests they used beams of constant rectangular cross section and constant length-to-depth ratio of 8:3. To determine the size effect, a crucial aspect of fracture mechanics, geometrically similar specimens of various depths, 1.5, 3, 6, and 12 in., were tested.

A pair of symmetric notches, of depth $d/6$ and thickness of 2.5 mm was cut on all the specimens (Fig. 1.2).

The tests were carried out in a 10-ton servo-controlled closed-loop MTS testing machine. The shear loading was produced by a system of steel beams, which applied concentrated vertical loads onto the specimens. Note that the loads were applied relatively close to the notches so as to produce a narrow region of a high shear force.

The test results showed that the cracks propagate as shown in Fig. 1.2. For that reason they believe that shear fracture exists, (i.e., the crack can propagate in Mode II). They concluded that the shear fracture is likely to form as a zone of tensile microcracks with a predominantly 45 degree inclination which only later connects by shearing; but the fact is that in the microscopic sense the observed fractures must be described as Mode II.

Bazant and Pfeiffer's (3) test differed from Arrea and Ingraffea's (1) by its wider separation of the loading points. In that case the cracks propagated from the notch tip basically in the direction normal to the maximum principal stress, as observed by Ingraffea.

Bazant and Pfeiffer (3) concluded that, shear fracture of concrete exists.

The direction normal to the maximum principal stress cannot be considered generally as a criteria of crack propagation direction in concrete. Rather, fracture seems to propagate in the direction for which the energy release rate from the fracture is maximized.

Ingraffea and Panthaki (4) tried to show that although shear fracture can occur under certain conditions, tensile and not shear fracture occurred in Bazant and Pfeiffer's specimens.

By employing classical elasticity solutions, linear finite element analysis and non-linear fracture mechanics analysis they reached the following conclusions: Limited tensile cracking from the notch tips was likely to occur. By moving the load points closer together than in the Arrea and Ingraffea tests, the intensity of the shear stress in the region between the notch tips was decreased rather than increased.

The major principal stress in the region between the notches is tensile, and its direction is roughly constant at about 10 degrees above the horizontal. This means that the plane of principal shear is far from being vertical. The stress state between the notch tips, despite the existence of the notches and the minor loads, is similar to an element in the central region of a cylinder in the Brazilian test. By treating a beam element the

same as an element from the center of a Brazilian test specimen, Ingraffea and Panthaki were able to predict the peak loads with acceptable accuracy. Based on the above considerations they concluded that the beams failed in tension and not in shear, with the tension crack nucleating in the central region of the beam, roughly vertical and propagating towards the notch tips. Additional cracking also occurred at the notch tips at relatively low load levels. However, this cracking occurred in a direction normal to principal tensile stresses and became stable.

Bazant and Pfeiffer (3) responded saying that the symmetric loading produced a symmetric stress singularity at the tips of each of the notches and the cracks emanating from them. This singularity is characterized by non-zero Mode I stress intensity factor K_I . However, K_I is negative because the transverse normal stresses near the notch or crack tips are compressive. Thus, a linearly elastic calculation indicated horizontal displacements which imply overlapping of the material on the cracks. Such overlapping is impossible and instead of it compressive stresses are generated across the cracks. These stresses eliminate the singularity and cause that $K_I=0$ at the crack tip. Thus, there can be no Mode I fracture and so the tests cannot involve mixed mode failure but rather a pure Mode II situation at the crack tip.

Bazant and Pfeiffer (3) supported their ideas with a linearly elastic finite element analysis using elements larger than the aggregate size which were too coarse to represent stress singularities. These results indicated that the maximum principal stress, which was tensile near the notch or crack tip and occurred in an inclined direction, was much larger in magnitude than the maximum principal stress (tensile) in the center of the ligament. Thus, the crack cannot be assumed to start at the center of the cross section but must initiate from the notch tips and propagate continuously toward the center. From the tests it was observed that the cracks propagated straight along the ligament section rather than in inclined directions from the notches. Since the maximum principal tensile stress should be inclined, the cracks which begin at the notches cannot be considered as tensile. They represent shear cracks, although microscopically they may consist of a row of inclined tensile microcracks prior to the formation of the final continuous fracture. The same results were obtained by nonlinear analysis. Although this analysis indicates a somewhat smaller inclination of the tensile microcracks, the inclination of the microcracks is still significant. Thus, the band of microcracks emanating from the notches cannot be considered as tensile fracture but as shear fracture affected by tensile stresses.

The analysis done by S.E. Swartz and N.M. Taha (8) is a combined experimental and analytical investigation of mixed mode crack propagation on four-point-loading concrete beams (Fig. 1.2, 1.5). The experimental program consisted of tests on beams with double notches, beams without notches, beams with an applied axial force, and also tests of tensile strength following the Brazilian method.

For beams without axial force, both crack mouth sliding displacement (CMSD) and load point displacement (LPD) versus the applied load were recorded. For beams with axial force, both CMSD and mid-depth longitudinal deformation (LD) were recorded throughout the test.

The specimens used in the experiment had length to depth ratio 8:3, the same dimensions as those used by Bazant and Pfeiffer (3). Swartz and Taha (8) concluded that the failure mechanism was due to tensile splitting for the following three reasons. First, the crack was not exactly vertical, but inclined in the direction of the center lines of the two middle supports in a manner similar to that of the tensile splitting test (Fig. 1.5). Second, the surface of the crack was rough and there was no sign of any crushed material which must have been found if the failure were due to shear. Third, the crack surface was exactly

the same as that of pure Mode I of other experiments.

For beams without axial force the initial crack angle results and showed that the initial angle is about 65 degrees. For the cross section connecting the two notch tips, neither the tensile stress nor the shear stress exceeded the concrete strength. That is why the specimen did not fail along that line.

For beams with axial force the state of stresses around the predicted by both ANSYS and CRACKER agreed with the experimental notch tips was tensile which caused cracks to propagate with the same initial crack angle as the beams without axial loads. The crack surfaces of the beams with high axial force were different from that of beams without axial force. Crushed material was found and the aggregate interlock was broken which caused the crack surface to be smoother.

Jeng and Shah (5) for their analysis of mixed mode fracture in concrete used three-point-bend notched beams with notches at different off-sets (x) (Fig. 1.3). It can be seen that when the off-set (x) equals zero the notch is in the center of the beam and the test is reduced to pure Mode I three-point bend tests. Thus, pure Mode I and mixed mode tests can be performed using similar specimens and the same testing setup. When the off-set is not equal to zero, both K_{II} and K_I exist and mixed mode type of failure is expected to occur.

Three different mix proportions and two different specimen sizes were used in their mixed-mode experiments. The dimensions of the specimens were 24 in. x 6 in. x 2.25 in and 12 in. x 3 in. x 1.125 in. for large and small beams respectively. The off-sets varied from 0 to 9 in. with increments of 3 in. with notch-depth ratio equal to 1/3, was used to study the shear effect. Another set of specimens with fixed off-set (6 in.) and different notch-depth ratios (ranging from 0.5 to 2/3) was used to study the notch-depth effects on mixed mode failure. All beams were tested in a closed-loop testing machine with CMOD or load-line deflection as feedback signal to maintain a "stable" failure. The quarter-point singular element approach was used to calculate the stress intensity factors. It was found that the values of K_{II} were close to zero and K_I was close to its maximum value along the direction of the theoretical initiation angle regardless of the length of the branch. From their experimental results they found that the crack initiation angles are difficult to measure due to the tortuosity of crack paths. However, they assumed that the crack initiates and propagates in a straight line along the predicted initiation angle. The initiation angle was then assumed as the final failure point. Depending on the off-set the final failure angle ranges from 1 degree to 33 degrees. The theoretical prediction of the crack initiation angles always underestimated

the final crack angle for small specimens. This is possible due to the aggregate arresting mechanism which forces the crack to deviate from the original initiation angle. They also observed that the experimentally measured final failure angles were scattered about the theoretical predictions for large specimens. Perhaps this was because the uncracked ligaments of large specimens were long enough for the crack to correct its crack path and go back to the original initiation path. Moreover, since the specimens were relatively large compared to the grain size, these specimens exhibited more homogenous behavior. Despite the large scatter of the experimental results, the theoretical predictions of crack initiation angles seemed to be reasonable compared to the accuracy of the experimental measurements.

Izumi (6) and his co-workers in their study measured the fracture toughness of concrete for Mode II. In their tests a normal compressive force was applied to the cracked plane to prevent any microcracking in Mode I around the crack tip. The stress distribution on the critical section was found to be not quite uniform. They concluded that Mode II fracture may occur at the angle of 15 degrees.

Barr, Hasso and Khalifa (2) added side groove for their specimen test to avoid high compressive stress under the supports

(Fig. 1.4). They indicated that; 1. Manufacturing of perfect specimens was very difficult; 2. A great deal of care was necessary during the test preparations concerning the depth of the notches and position of the applied load; 3. Tension was developed in the area adjacent to the roots of the notches, which may result in a Mode I failure. They argue that since the tensile stress is less than the shear stress at the middle of the cross section connecting the notch tips, failure due to tension is unlikely to occur.

1.3 Objectives

After reviewing the previous work on Mixed-Mode fracture and noting the disagreement on the nature of the failure it was decided to investigate further to see if a conclusion to the matter might be reached. To verify these findings, two approaches were used in this study. An experimental program using double notched beams and techniques similar to Bazant and Pfeiffer's (3) was carried out. Additionally, a computer study on single and double notched beams using the Cornell FRacture ANalysis Code (FRANC) was done. FRANC is a fracture analysis software that models the normal and shear stresses as well as determines the stress intensity factors for a given fracture structure. Based on the results of these studies it is hoped that a determination of the type of failure, i.e., whether the failure is one of tension, shear or a combination of both can be reached.

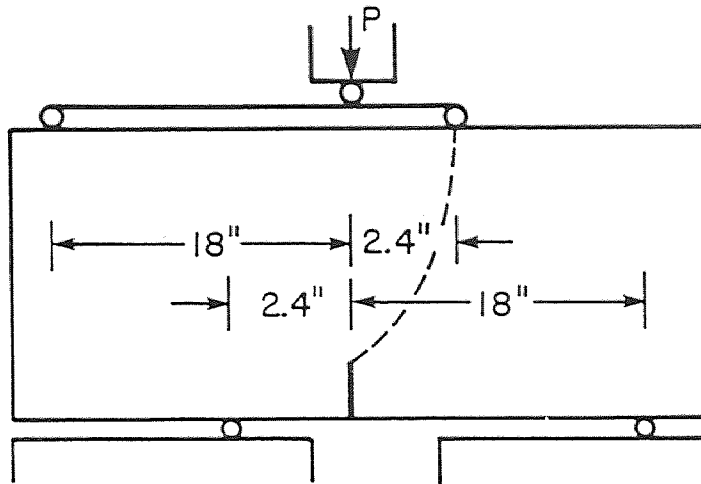


FIG. I.1 – SPECIMEN USED BY ARREA AND INGRAFFEN (1)

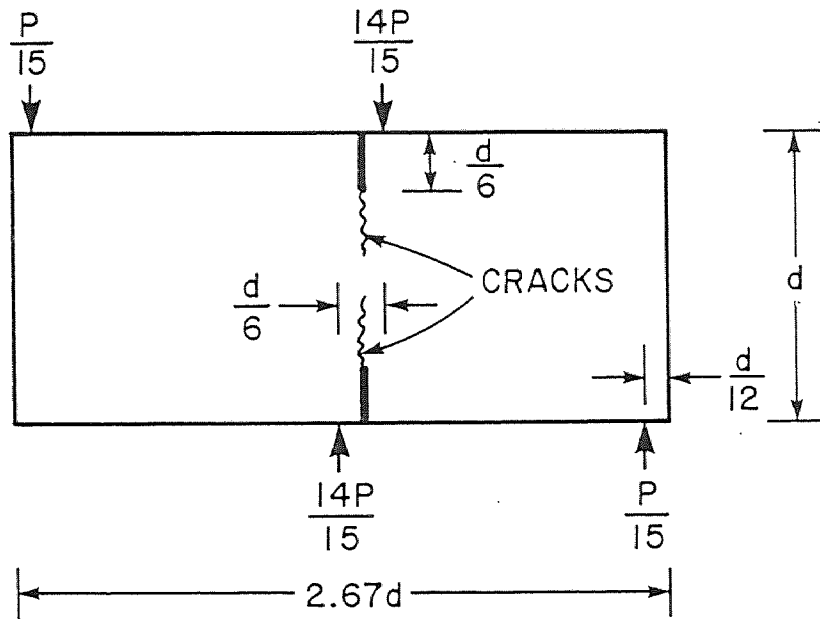


FIG. I.2 – SPECIMEN USED BY BAŽANT AND PFEIFFER (3)
AND SWARTZ AND TAHA (8)

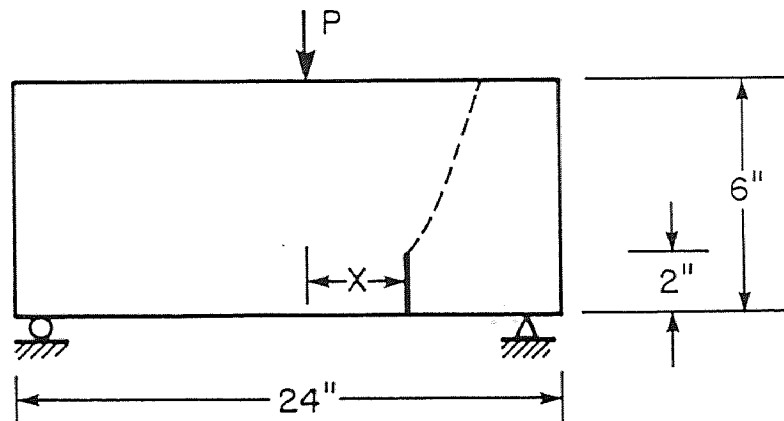


FIG. I.3 – SPECIMEN USED BY JENG AND SHAH (5)

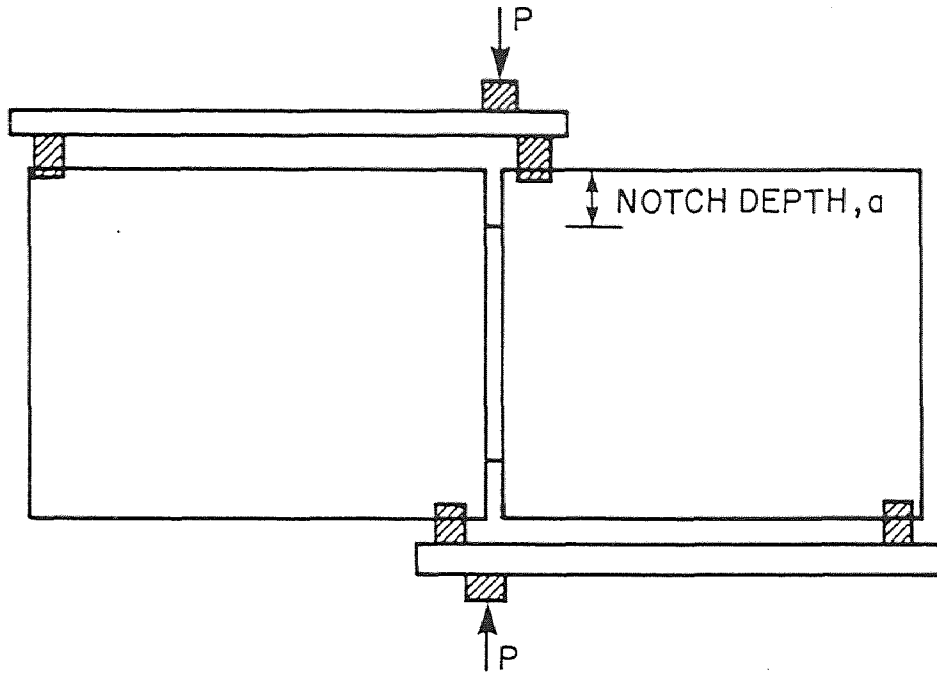


FIG.1.4 – SPECIMEN USED BY BARR, HUSSO AND KHALIFU (2)

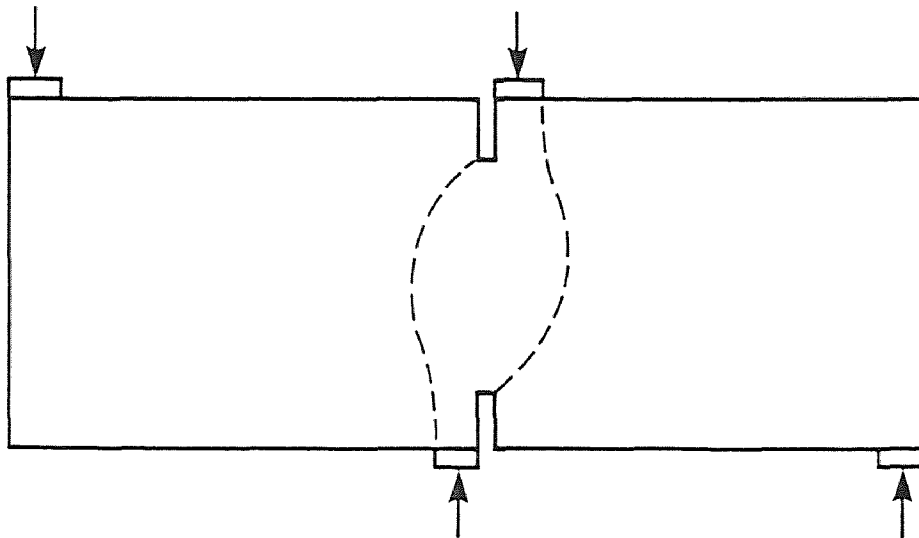


FIG.1.5 – CRACK PATTERN FOR BEAMS USED BY SWARTZ AND TAHA (8)

CHAPTER 2

EXPERIMENTAL AND THEORETICAL INVESTIGATIONS

An experimental program, similar to that used by Bazant and Pfeiffer (3), was initially planned and carried out using the hydraulic servo-controlled MTS testing machine. The test was controlled by crack mouth sliding displacement (CMSD) as the feedback signal. Unfortunately, due to the insensitivity of the clip gauge used in CMSD measurement, the experiment carried out failed to provide reliable experimental results. It was then decided that the experimental results for mixed-mode fracture of concrete by Bazant and Pfeiffer (3) and Jeng and Shah (5) cited in the literature would be used instead of the planned experiment.

The theoretical analysis of the mixed-mode fracture problems was analysed employing the FRacture ANalysis Code (FRANC) program, which was developed by A. R. Ingraffea at Cornell University. FRANC was used to analyze the behavior of both double notched beams and single notched beams used by Bazant and Pfeiffer (3) and Jeng and Shah (5) respectively. All needed input data, which included specimen configurations, loading and fixity conditions, were obtained from the references (3) and (5).

To provide a better understanding of how a mixed-mode experiment in concrete is carried out, a brief discussion of the

experimental programs of Bazant and Pfeiffer (3) and Jeng and Shah (5) is summarized in the next two sections.

2.1 Testing Procedure used by Bazant and Pfeiffer (3)

The test specimens used were beams of rectangular cross section with a constant length-to-depth ratio of 8:3. To determine the size effect, geometrically similar specimens of various depths, $d=1.5, 3, 6$ and 12 in., were tested. The specimens of all sizes were cast from the same batch of concrete or mortar, and their thickness (b) were the same ($b=1.5$ in.). A pair of symmetric notches, of depth $d/6$ and thickness of 2.5 mm was cut on all the specimens. The specimens were cast using a water-cement ratio of 0.6 , and 0.5 and cement-sand-gravel ratio of $1:2:2$, and $1:2:0$ for concrete and mortar respectively. The maximum gravel size was 0.5 in. for concrete and 0.19 in. for mortar. The specimens were removed from the plywood forms after one day and were subsequently cured until the moment of the test for 28 days, in a moist room of 95% relative humidity and 78 F temperature.

The tests were carried out in a 10-ton servo-controlled closed-loop MTS testing machine. The shear loading was produced by a system of steel beams which applied concentrated vertical loads onto the specimen. Three of the loads were applied through

rollers, and one through a hinge, which produced a statically determinate support arrangement. The loads were applied relatively close to the notches, so as to produce a narrow region of a high shear force. However, the loads could not be too close to the notch, or else the concrete under the support would shear off locally before the overall shear fracture could be produced.

The specimens were tested at constant displacement rate of the machine so as to achieve the maximum load in about 5 minutes. The crack mouth sliding displacement (CMSD), as well as the load point displacement (LPD) were measured. The specimen dimensions test set up and loading apparatus for Bazant and Pfeiffer's test are presented in figure 2.1 and a typical CMSD vs LOAD relationship is also shown in figure 2.2.

2.2 Testing Procedure used by Jeng and Shah (5)

The test specimens used were beams of two different sizes. The dimensions (span x depth x thickness) were 24 in. x 6 in. x 2.25 in. and 12 in. x 3 in. x 1.125 in. for large and small beams respectively. Three different mix-proportions were cast. The water-cement ration was 0.55, 0.45 and 0.35 and the cement-sand-gravel ration was 1:2.6:2.6, 1:2.6:0 and 1:0.5:0 for C, M and F series respectively. The maximum gravel size was 0.375 in. for C series, 0.1875 in. for M series and 0.1875 for F series.

Jeng and Shah (5) used three-point-bend notched beams with notches at different off-set ratios ($p=2x/s$) (Fig. 2.3). It can be seen that when the off-set ratio equals zero the notch is in the center of the beam and the test is reduced to pure Mode I three-point-bend tests. Thus, pure Mode I and mixed mode tests can be performed using similar specimens and the same testing setup.

The off-set ratio varied from 0 to $2/3$ by an increment of $1/6$ with a notch-depth ratio equal to $1/3$. Another set of specimens with fixed off-set ratio (0.5) and different notch-depth ratios (ranging from 0.5 to $2/3$) was used to study the notch-depth effects on mixed-mode failure.

The beams were tested in a closed-loop testing machine with crack mouth opening displacement (CMOD) or load-line deflection as feedback signal to maintain a stable failure. The CMOD and the load-line deflection were measured. The specimen configurations, test setup and loading apparatus for Jeng and Shah's test are shown in Figure 2.3 and a typical CMOD vs LOAD graph is shown in Figure 2.4.

2.3 FRacture ANalysis Code (FRANC) Program

The FRacture ANalysis Code (FRANC) is an interactive workstation-based program which was designed to perform discrete crack modeling of two dimensional fracture processes. Structural behavior is modeled by means of the finite element method. Integral remeshing routines allow the finite element mesh to be modified semi-automatically to represent new crack configurations. The program is now a general purpose finite element and fracture analysis package.

The FRANC program is menu driven; each page lists a number of menu options. To activate a menu option the user uses the mouse to move the cursor to the menu option box and pushes the pick button. When FRANC is activated, two partially overlapping windows appear on the screen. One window contains the menu and the problem mesh, the other window is initially blank. This window is used for displaying x-y plots and miscellaneous information. When the program is computing something and is not sensitive to input requests, the button is highlighted and a "working" message is displayed. When none of the buttons are highlighted and a "Select a menu option" message prompts the user to take action. To select a menu option, the user is required to place the cursor on the menu button and click the mouse.

To start analysis of a problem one must have an input file. Before an analysis can be performed, loads and fixities must be applied to the structure. Fixities can be applied individually or along a structural boundary. When fixities are to be applied individually the user points to the nodes to be fixed. When fixities are to be applied along an edge the user first points to the starting node. The user then points to an adjacent node on the edge. This specified adjacent node specifies the direction in which the fixity will be applied. Finally the user specifies the node at which the fixity will stop. Loads can be applied in a similar manner.

After boundary conditions have been specified an analysis can be performed. FRANC has a linear equation solver.

The post-processing functions are accessed by the "Post Process" menu. Each post-processing function can be operational for a given load case or, by default, for the net response for all loads.

"Line plot" displays stresses along a line specified by two end points.

"Circle plot" creates a stress plot around a circle.

"Radial plot" is similar to "Line plot" except that the first point is a node rather than an arbitrary point in space.

"Surf plot" creates a pseudo-3-D surface plot of the response over a square region. Stress intensities are computed by means of the "Sif" command.

A crack can be nucleated in one of two ways, either as an edge crack or as an internal crack. An edge crack starts from a structural boundary and must start from an element corner node. An internal crack is nucleated by specifying the two crack tip locations.

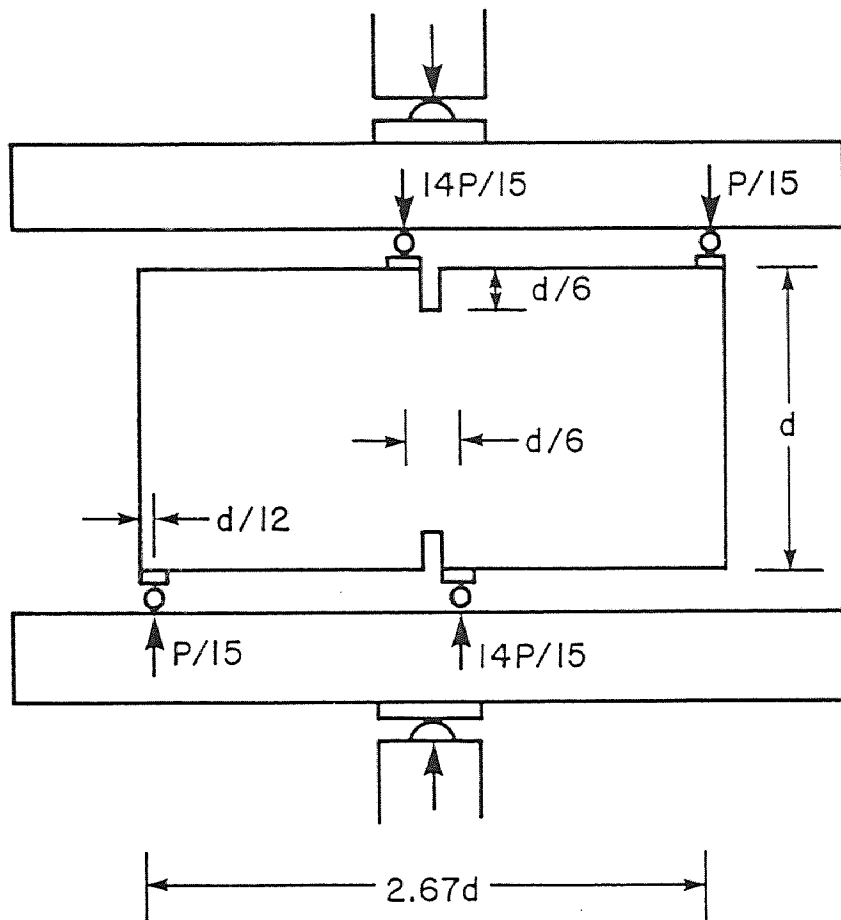


FIG.2.1 – MIXED-MODE FRACTURE SPECIMEN AND LOADING APPARATUS USED BY BAZANT AND PFEIFFER (3)

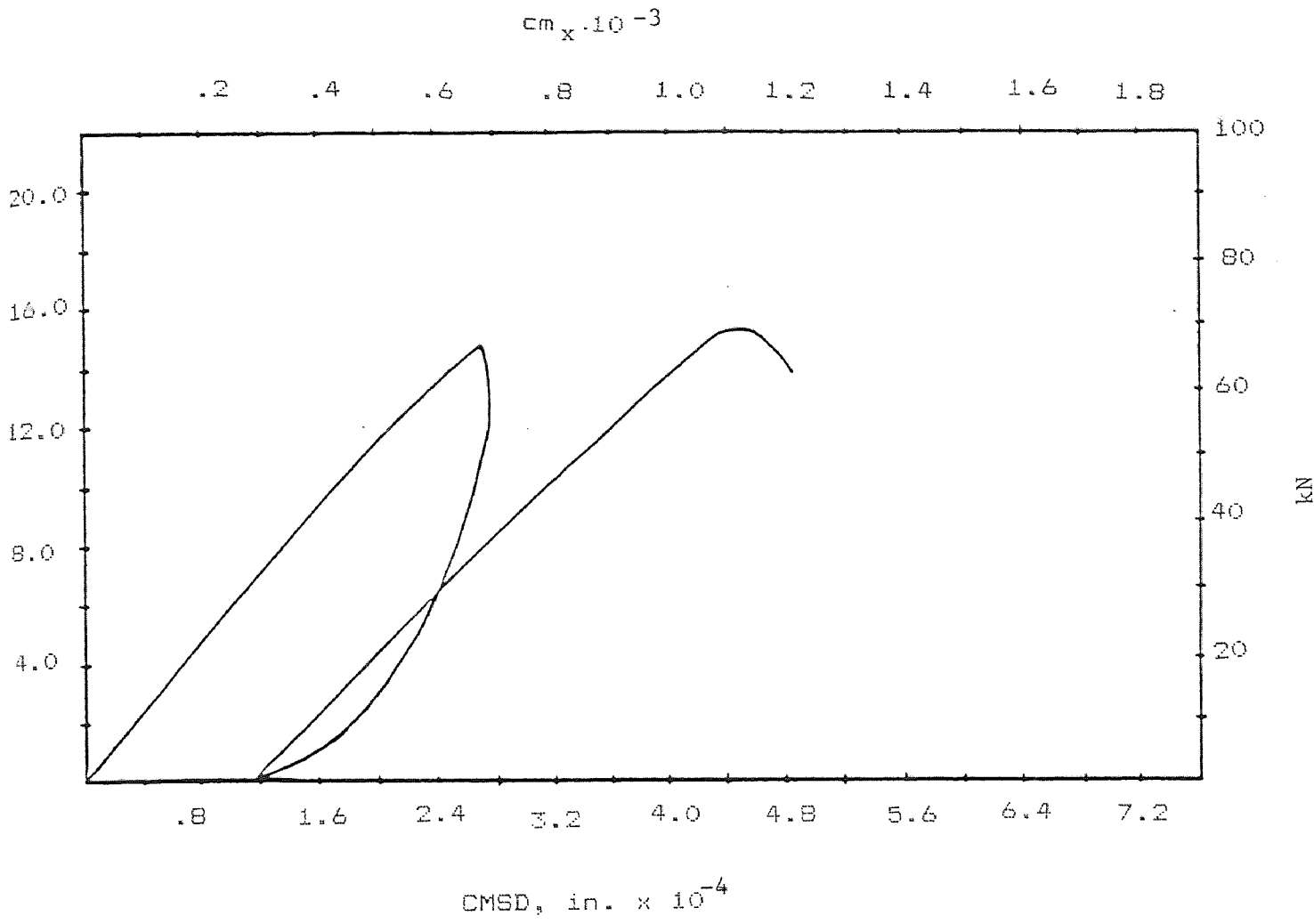


Fig. 2.2 Typical CMSD vs LOAD relationship for Bazant and Pfeiffer test

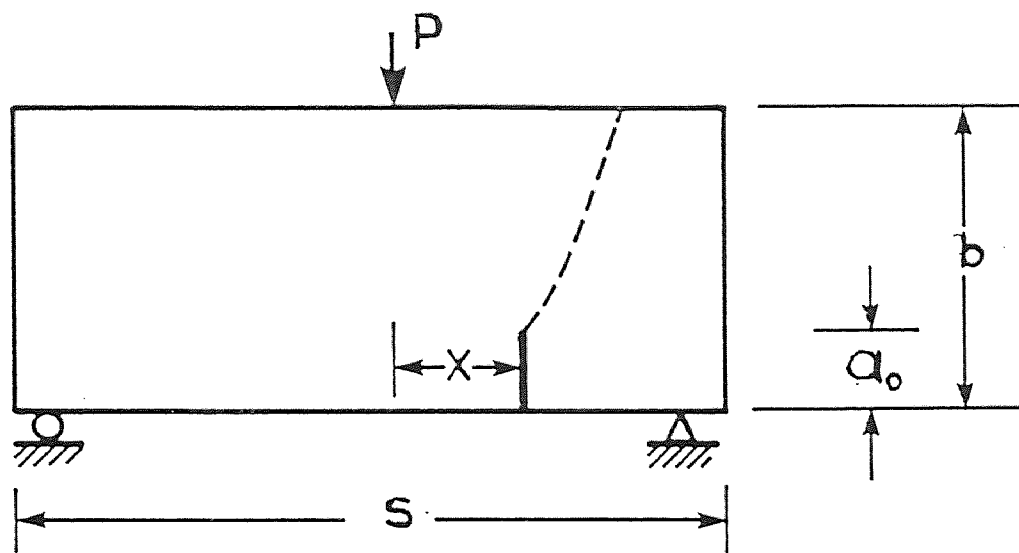
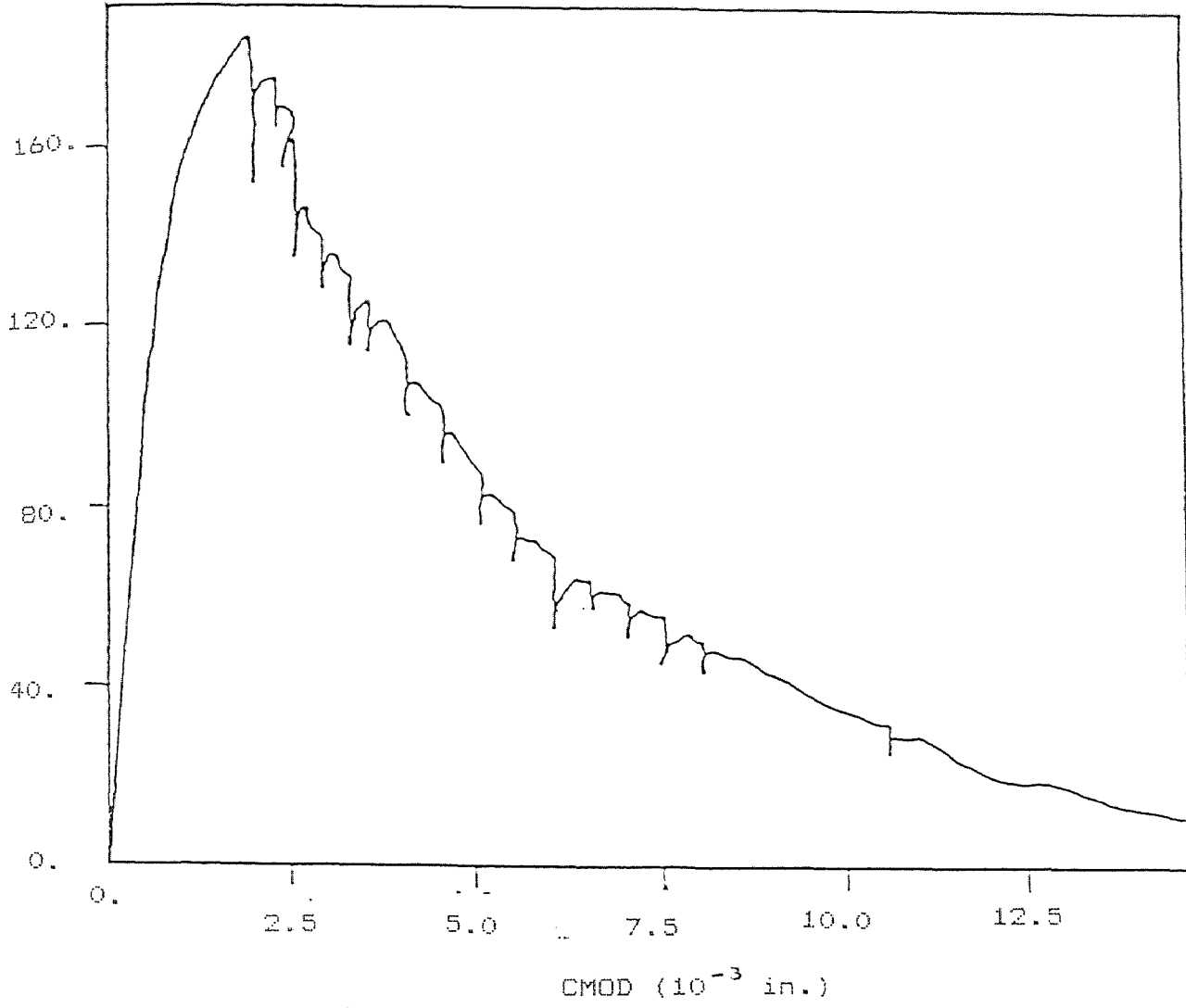


FIG.2.3 – SPECIMEN USED BY JENG AND SHAH (5)



g. 2.4 Typical CMOD vs LOAD relationship for Jeng and Shah's test

CHAPTER 3

RESULTS AND DISCUSSION

3.1 Solution of Beams with Double Notch by FRANC Package

For the double notched beam, the input data given to FRANC were those provided by Bazant and Pfeiffer (3). The dimensions (thickness x depth X span) of the specimens are 3 in. x 8 in. x 21.5 in.. The notches are located at midspan and have a depth of 1.3 inches as shown in Fig. 3.1. The loading and support conditions are shown in Fig. 3.2. The average concrete compressive strength was 6500 psi and the Modulus of Elasticity was 4.6E6 psi. The whole input data given to FRANC is shown on table 2.

Figure 3.3 shows the sliding displacement found by Bazant and Pfeiffer (3) and by the FRANC program. As it can be seen from the graphs the values are very close and show a 97% agreement between FRANC and Bazant and Pfeiffer's experimental results. Figure 3.4 shows the sliding displacement found by Bazant and Pfeiffer (3) and by the FRANC program for different notch depth. The values are still very close with a 95% agreement, which means the depth of the notch does not have any effect on the accuracy of the FRANC program. FRANC cannot provide the unloading part of the load-CMSD curve. Appendix A shows the data and output for double notched beams.

The mesh consists of quadratic elements with 8-nodes and is shown in Fig. 3.5. The deformed specimen under 15.3 kips peak load is shown in Fig. 3.6. The stress distributions along the cross section joining the two notch tips (line 1-1), are shown in Figs. 3.7 to 3.9. In these figures, S_x , S_y , and S_{xy} stand for the tensile, compressive and shearing stresses respectively. As shown in Fig. 3.7, the tensile stress is 670 psi, very close to the assumed tensile strength of the concrete which is taken as 10% of the average concrete compressive strength (650 psi). Also, most of the cross section is under shear stress which is lower than the concrete shear strength (4000 lbs) (Fig. 3.9), which is calculated by the formula $V_c = 2 (\sqrt{f'_c})bd$. For this reason the failure crack is expected to be due to tension at this section.

The stress distributions along a longitudinal section at mid beam height (line 2-2), are shown in Figs. 3.10 and 3.11. Fig 3.10 shows that the tensile stress, S_x is maximum at mid span of the beam where the notches are located. This tensile stress again is 670 psi, very close to the assumed tensile strength of concrete. Fig. 3.11 shows that the shear stress is also maximum at the mid span, but remains below the nominal shear strength of the concrete. Figs 3.12 and 3.13 show the stress distribution for a longitudinal section just at the tip of the top notch (line 3-3). In these figures, again the tensile stress (Fig 3.12) is 600 psi, close to the assumed tensile stress of concrete and the shear stress remains below the nominal strength concrete.

Fig 3.14 indicates that the major principal stress in the region between the notch-tips is tensile. This is evident due to a stress distribution which is nearly perpendicular to a line connecting the two notch tips.

Table 3 summarizes the stress intensity factors calculated by FRANC, for the top crack tip and the bottom crack tip. In both cases, none of the factors is zero which means that the failure is a mixed mode fracture.

3.2 Solution of Beams with Single Notch by FRANC Package

For the single notched beams, the input data given to FRANC were those provided by Jeng and Shah (5). The dimensions (thickness x depth x span) of the specimens are 2.25 in. x 6 in. x 24 in.. The notch has depth of 2 inches as shown in Fig. 3.15. Three different offsets (x) of 3, 6 and 9 inches are being used for this analysis. The load is applied on the middle of the beams and its peak value is equal to 1.8, 1.2 and 0.8 kips for 9, 6 and 3 inches offsets respectively. The average concrete compressive strength was 5245 psi and the Modulus of Elasticity was 3.8 E6 psi. The whole input data given to FRANC is shown on table 2.

Figure 3.16 shows the crack mouth opening displacement found by Jeng and Shah (5) and by the FRANC program. The dimensions of the beam are the same as above (2.25 in. x 6 in. x 24 in.) and

the offset is 2 in. As it can be seen from the graphs the values are very close and show a 92% agreement between FRANC and Jeng and Shah's experimental results. Figure 3.17 shows the crack mouth opening displacement for a smaller beam. The dimensions (thickness x depth x span) are 1.125 in. x 3 in. x 12 in. and the offset is 2 in. The graphs show an agreement of 83% between FRANC and Jeng and Shah's experimental results which means that the size of the beam has some effect on the accuracy of the FRANC program. Figure 3.18 shows the crack mouth opening displacement for the same beam as Figure 3.17 but a difference in offset of 1 in. The graphs show that the agreement between FRANC's results and Jeng and Shah's experimental results was only 76%. This means that the offset of the notch from the center of the beam has some effect on the accuracy of the FRANC program.

Another important observation was that FRANC does not stop increasing the value of the load after the peak load found by experiments which means that the FRANC does not read the failure of the beam. All the data and outputs for the single notched beams are shown in Appendix B.

After considering the effects of specimen size, notch depth, and the offset of the notch, an overall accuracy of 89% can be concluded for the FRANC program.

The mesh consists of quadratic elements with 8-nodes and is shown in Figs 3.19 to 3.21. The deformed specimen for each offset is shown in Figs. 3.22 to 3.24.

The stress distributions along the notch tip cross section (line 1-1) are shown in Figs. 3.25 to 3.33 where S_x , S_y , and S_{xy} , are the tensile, compressive, and shear stresses respectively. As shown in Figs. 3.25 to 3.27 the tensile stress is very high at the crack tip location and this gives a proof that at this point the failure crack is due to tensile failure.

Figs. 3.31 to 3.33 show that the shear force is lower than the nominal concrete shear strength (2000 psi) and for this reason shear failure is not expected at this section. The same results are shown on the stress distribution along a longitudinal section just at the tip of the notch (line 2-2). The tensile and shear stress distributions are shown in Figs. 3.34 to 3.36 and Figs, 3.37 to 3.39 respectively. The maximum tensile stress is at the point of the crack and has a very high value. This indicates that the failure at this point is due to tension. The shear stress is maximum at the point of the crack but does not exceed that of concrete. Figs. 3.40 to 3.42 indicate that the major principal stress in the region along the notch-tip is tensile and that the direction of the stress is nearly perpendicular to a line

connecting the notch tips. Figures 3.43 to 3.48 show plots of normal and shear stresses along line 1-1.

Table 4 summarizes the stress intensity factors, K_I and K_{II} , calculated by FRANC on the single notch beam with different offsets. The value of K_{II} is very small and the value of zero is reached when the notch is in the middle of the beam. The tensile intensity factor, K_I , starts from a low value and increases when the notch is closer to the center of the beam.

3.3 Comparison of results with other studies

The results of the analysis of beams with a single notch indicate a Mixed-Mode Fracture. Arrea and Ingraffea (1) who first studied this model of fracture concluded that shear failure does not exist and the fracture is mostly due to tension. The same results were obtained by Jeng and Shah (5). This analysis shows that the shear intensity factor (K_{II}) is very small, but not exactly zero. This means that even though the tensile stresses are the major cause of the fracture a mixed mode fracture actually occurs.

The results of the computer analysis of beams with double notch agree with Swartz and Taha (8) which showed that the failure was also a mixed mode fracture. These results disagree with Bazant and Pfeiffer (3) who concluded that the fracture was due to

pure shear, as well as, with Ingraffea and Panthaki (4) who summarized that the fracture was due to pure tension. The present study does not reveal the existance of a pure Mode II fracture for the double notch beams; nor does it support the assertion that beams always fracture in Mode I. Rather it concludes a mixed mode failure occures.

TABLE 1: INPUT DATA GIVEN TO FRANC FOR
SINGLE AND DOUBLE NOTCHED BEAMS

	SINGLE NOTCHED BEAMS	DOUBLE NOTCHED BEAMS
THICKNESS	2.25 in.	3 in.
DEPTH	6 in.	8 in.
SPAN	24 in.	21.5 in.
NOTCH DEPTH	2 in.	1.3 in.
MODULUS OF ELASTICITY	3.8E6 psi	4.6E6 psi
CONCRETE COMPRESSIVE STRENGTH	5245 psi	6500 psi
NUMBER OF MATERIAL TYPES	1	1
ANALYSIS TYPE	Plane stress	Plane stress
MATERIAL TYPE	Linear elastic isotropic	Linear elastic isotropic
NUMBER OF NODES	333	333
NUMBER OF ELEMENTS	96	96
ELEMENTS TYPE	Quadratic 8-nodes & triangular 6-nodes	Quadratic 8-nodes & triangular 6-nodes
LOADS	Values between 120 lbs & 500 lbs	Values between 4,000 lbs & 15,000 lbs

TABLE 2: STRESS INTENSITY FACTORS FOR
THE DOUBLE NOTCHED BEAMS

	K_I (kips/in $3/2$)	K_{II} (kips/in $3/2$)
Top Tip	-1.53	5.60
Bottom Tip	-2.07	5.92

TABLE 3: STRESS INTENSITY FACTORS FOR
THE SINGLE NOTCHED BEAMS

	K_I (kips/in $3/2$)	K_{II} (kips/in $3/2$)
Offset $x=9$	1.01	-0.30
Offset $x=6$	1.44	-0.28
Offset $x=3$	1.53	-0.17

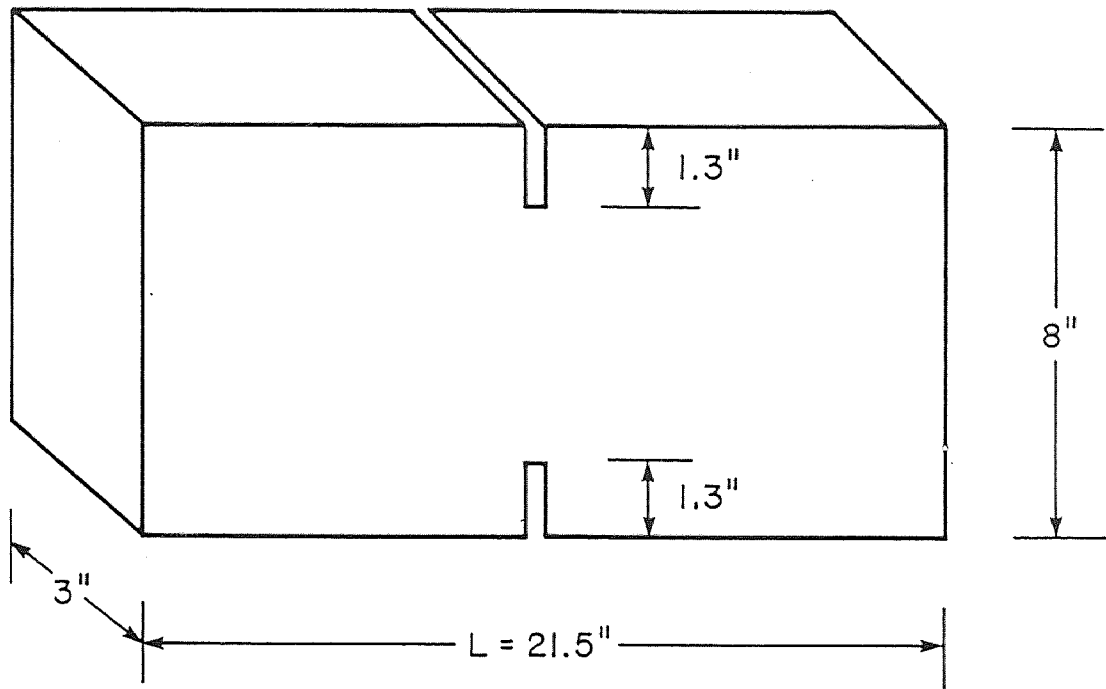


FIG. 3.1 – DIMENSIONS OF DOUBLE NOTCH SPECIMEN

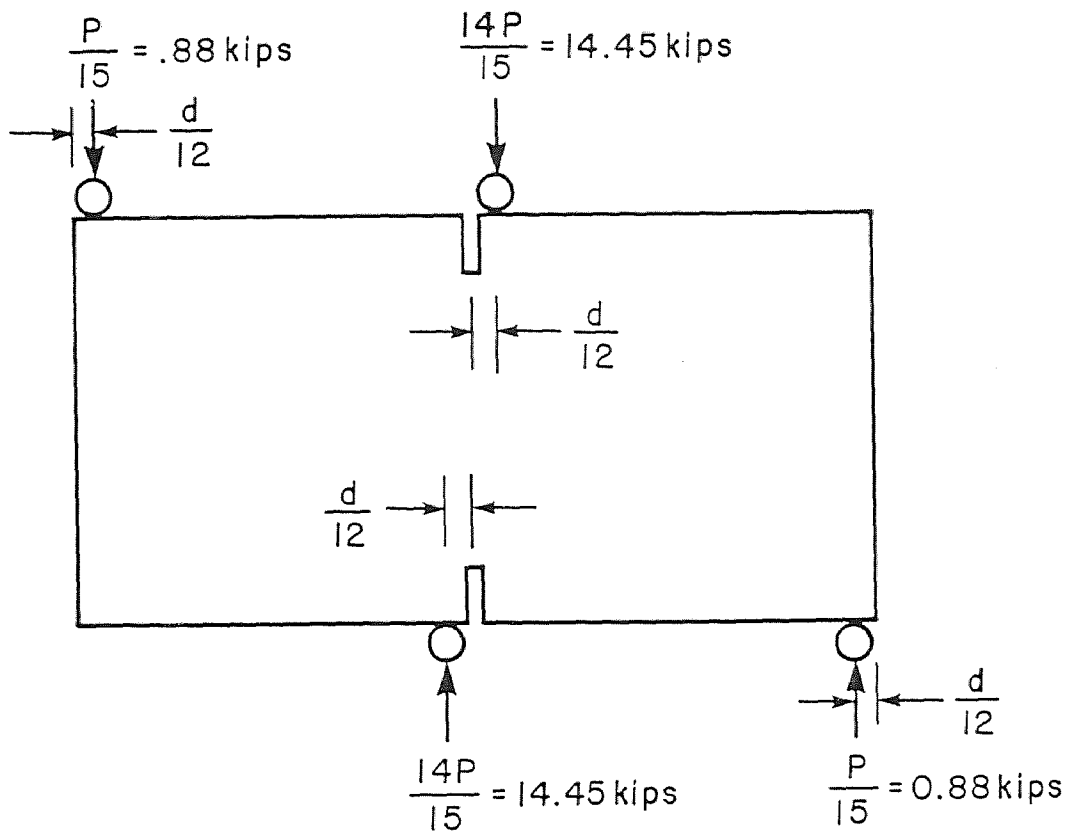


FIG.3.2 – LOADING AND SUPPORT CONDITIONS

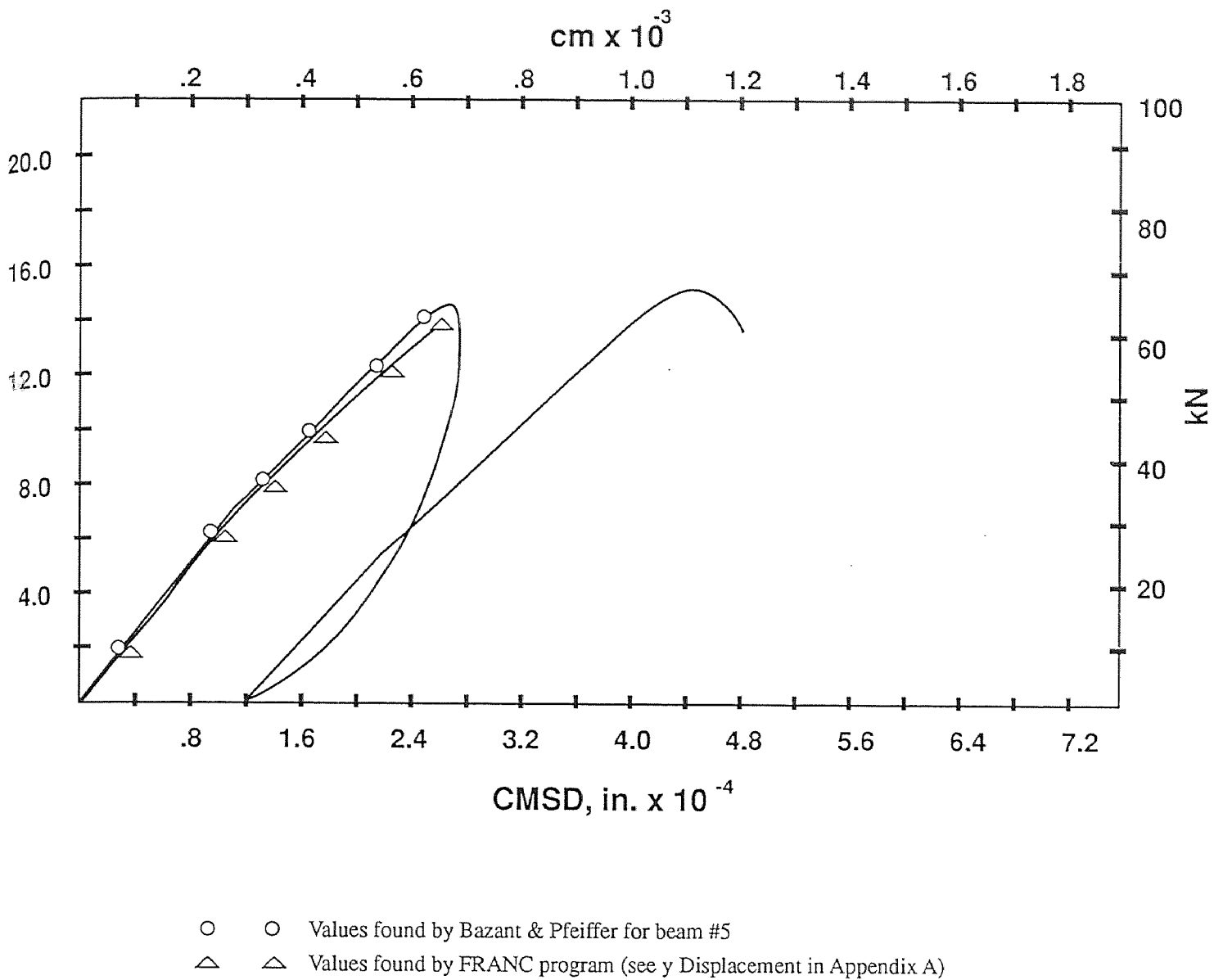


Fig 3.3 Sliding Displacement for the double notched beam #5 Bazant & Pfeiffer (3)

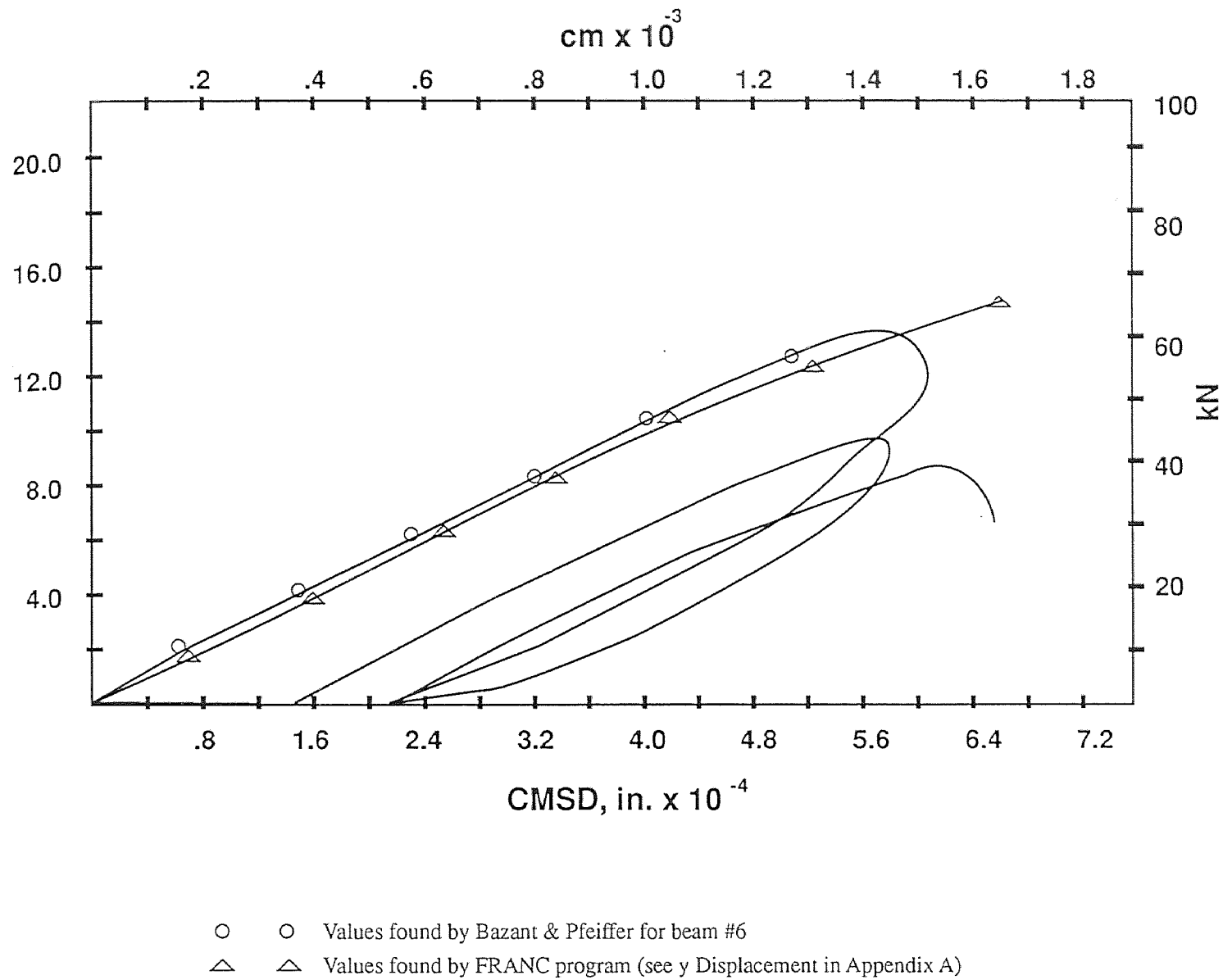


Fig 3.4 Sliding Displacement for the double notched beam #6 Bazant & Pfeiffer (3)

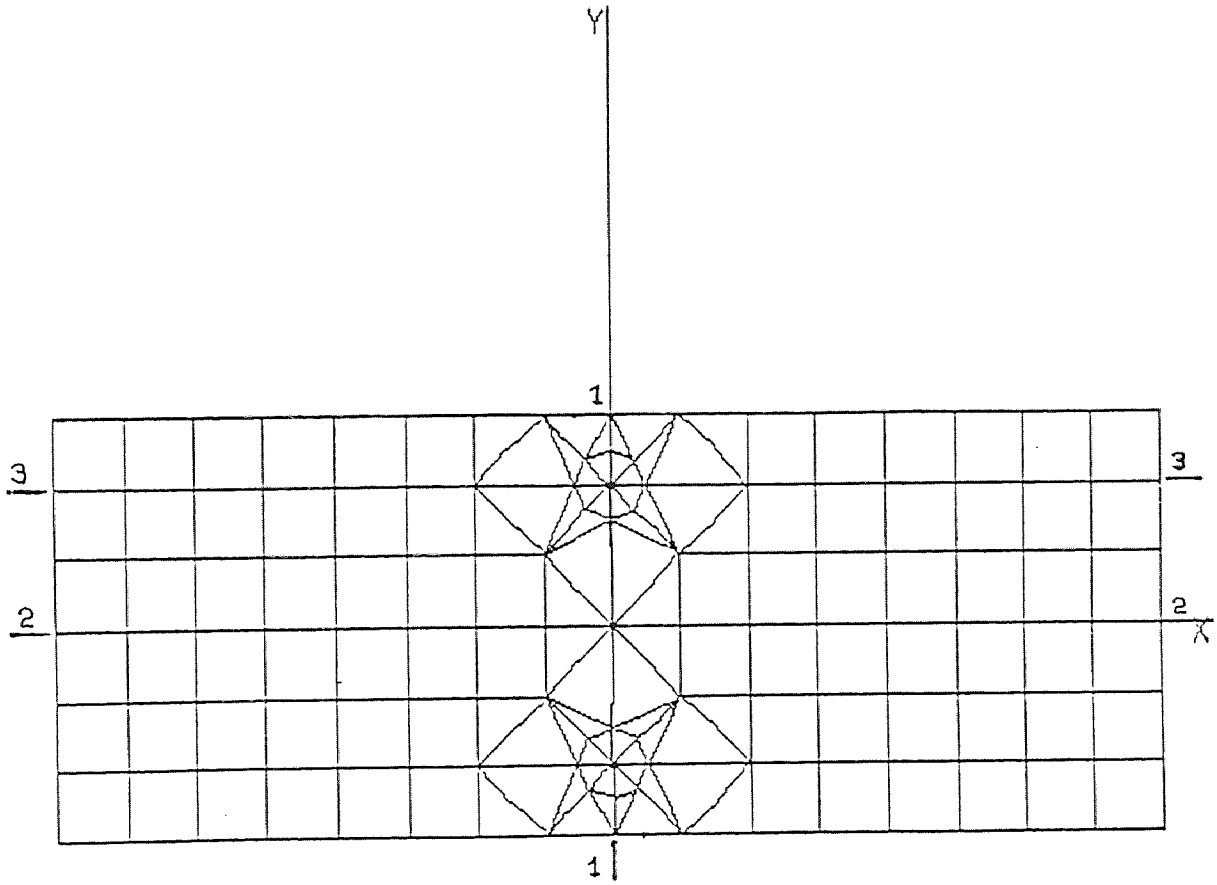


Fig. 3.5 Mesh Configuration

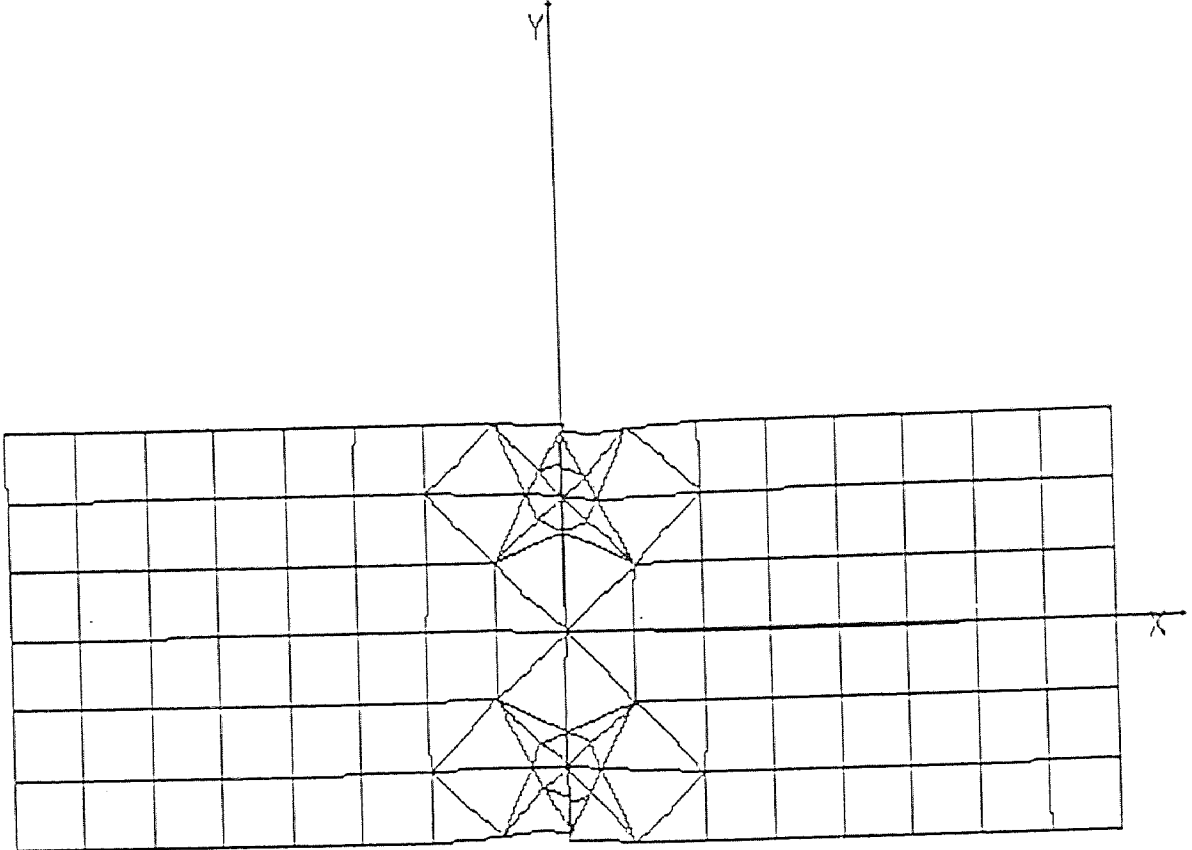


Fig. 3.6 Deformed Mesh

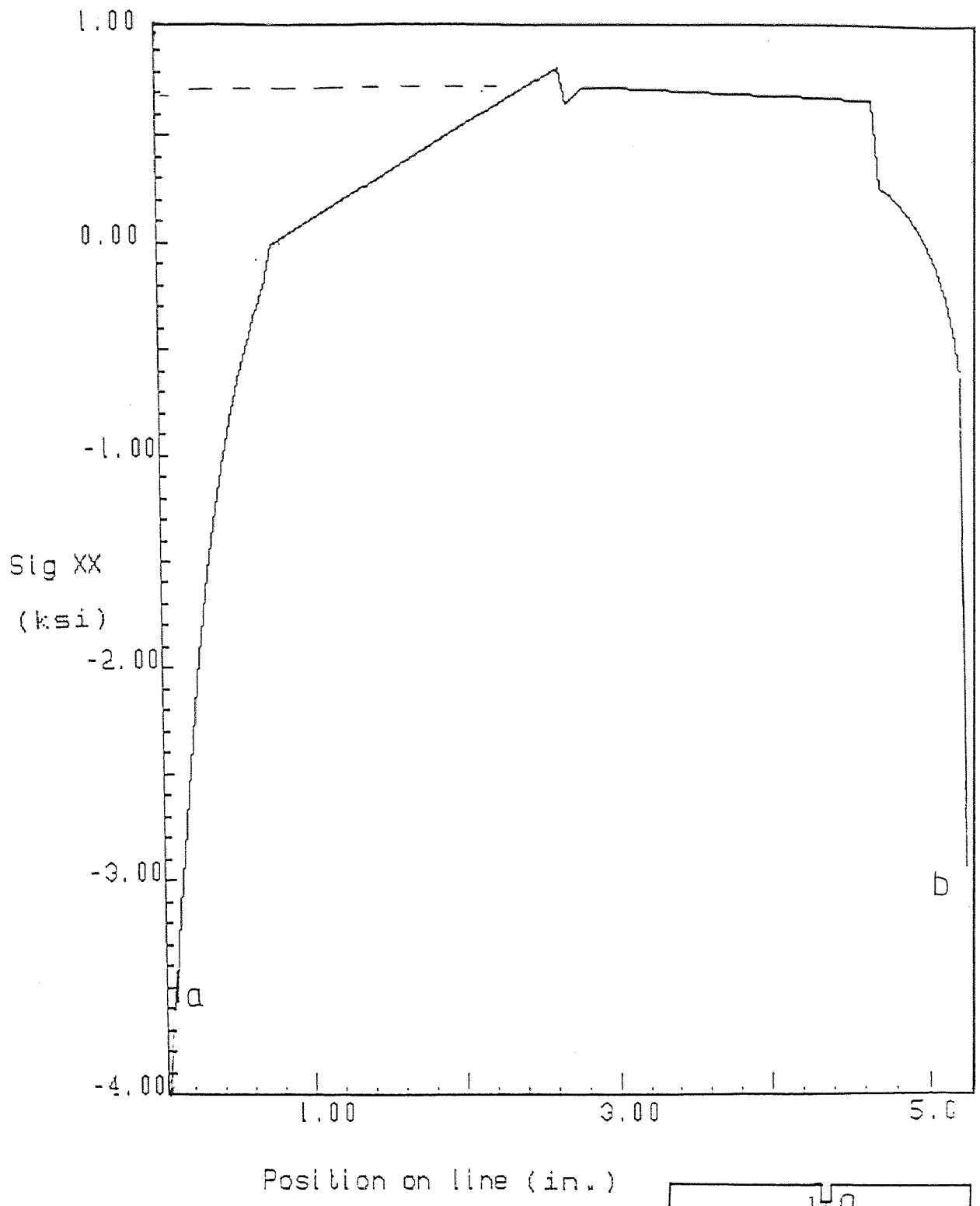


Fig. 3.7 Sx on Section 1-1 Line 1-1

Sig YY vs Position

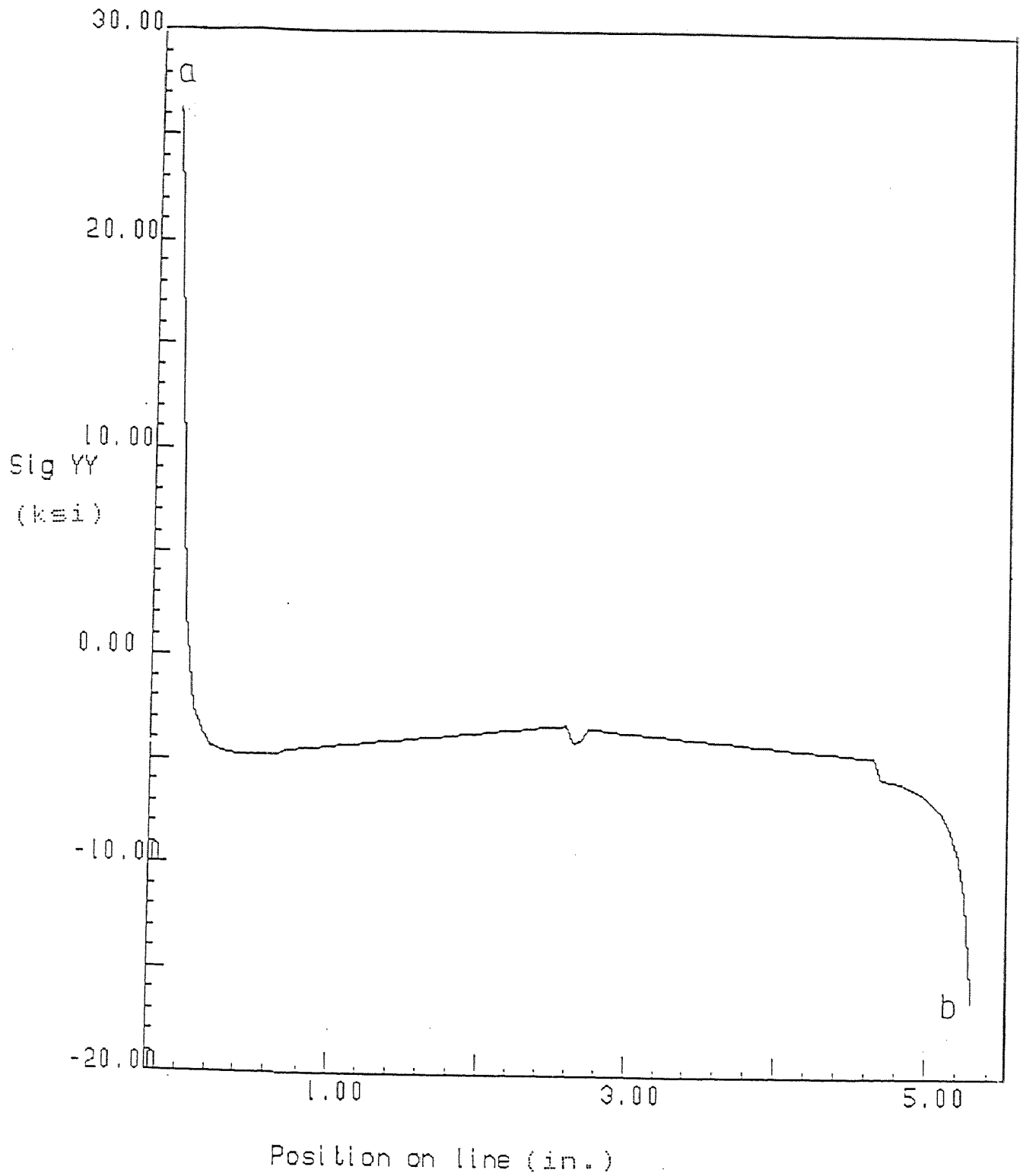


Fig. 3.8 σ_y on Section 1-1

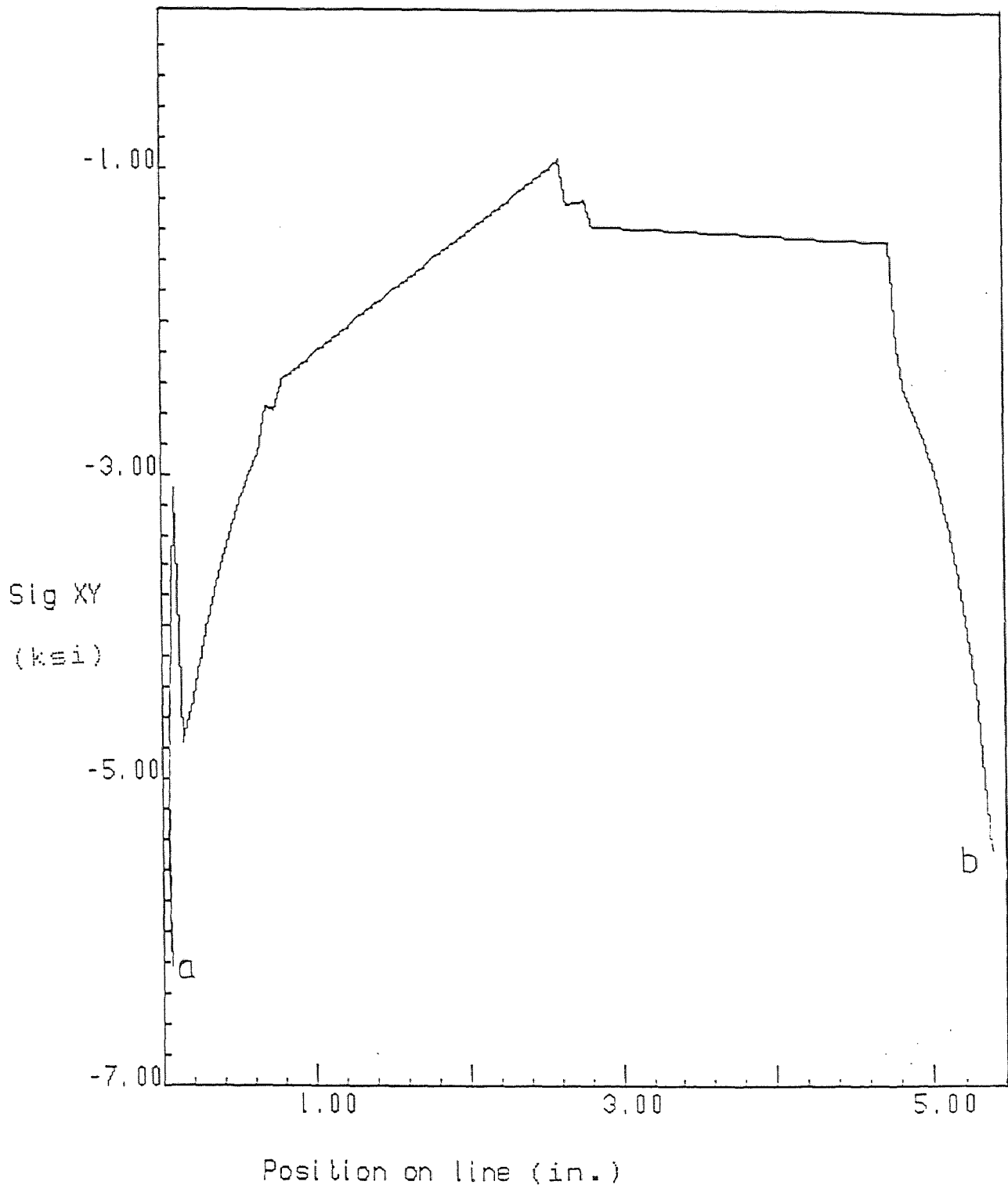


Fig. 3.9 τ_{xy} on Section 1-1

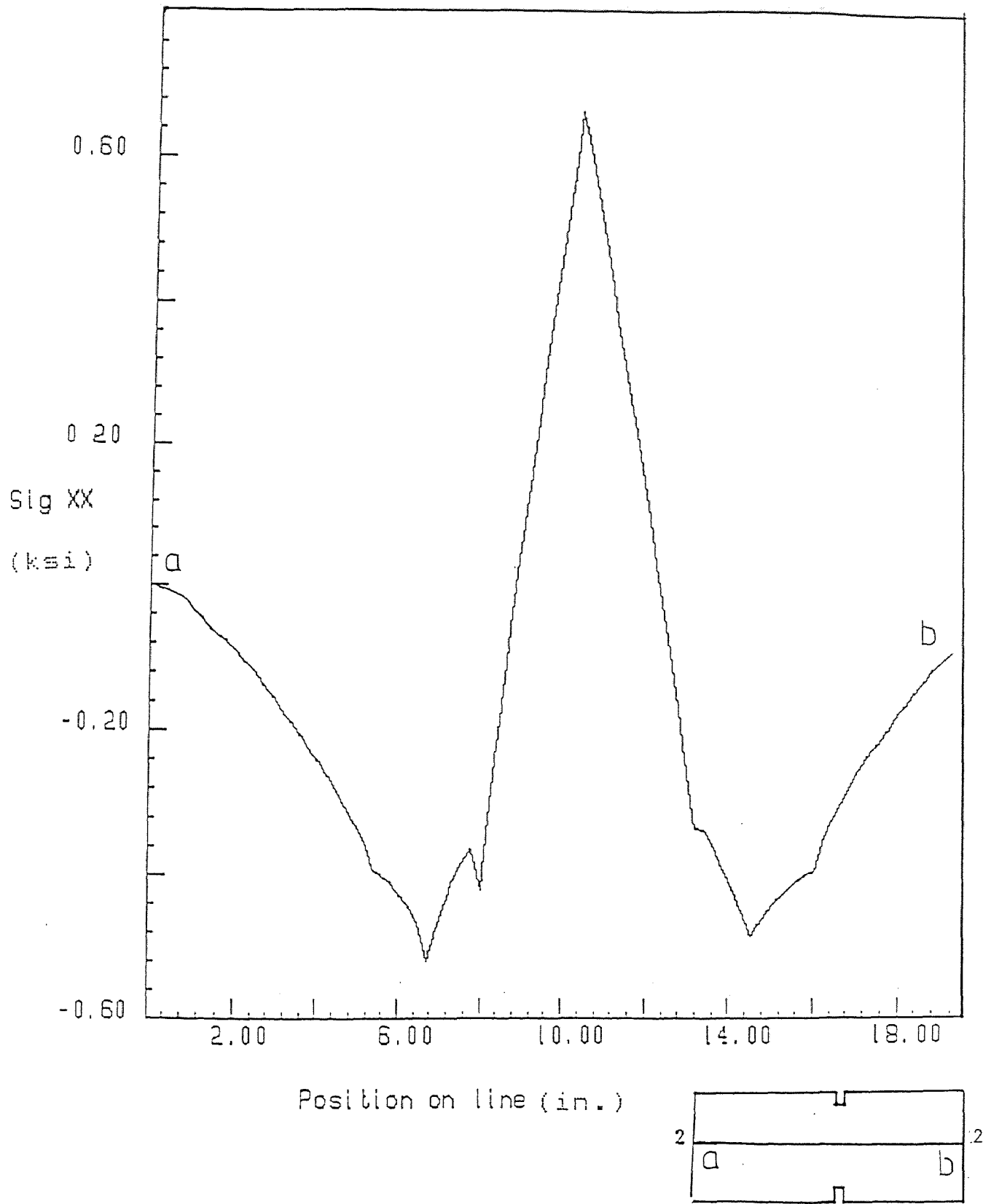


Fig. 3.10 σ_x on Section 2-2

Line 2-2

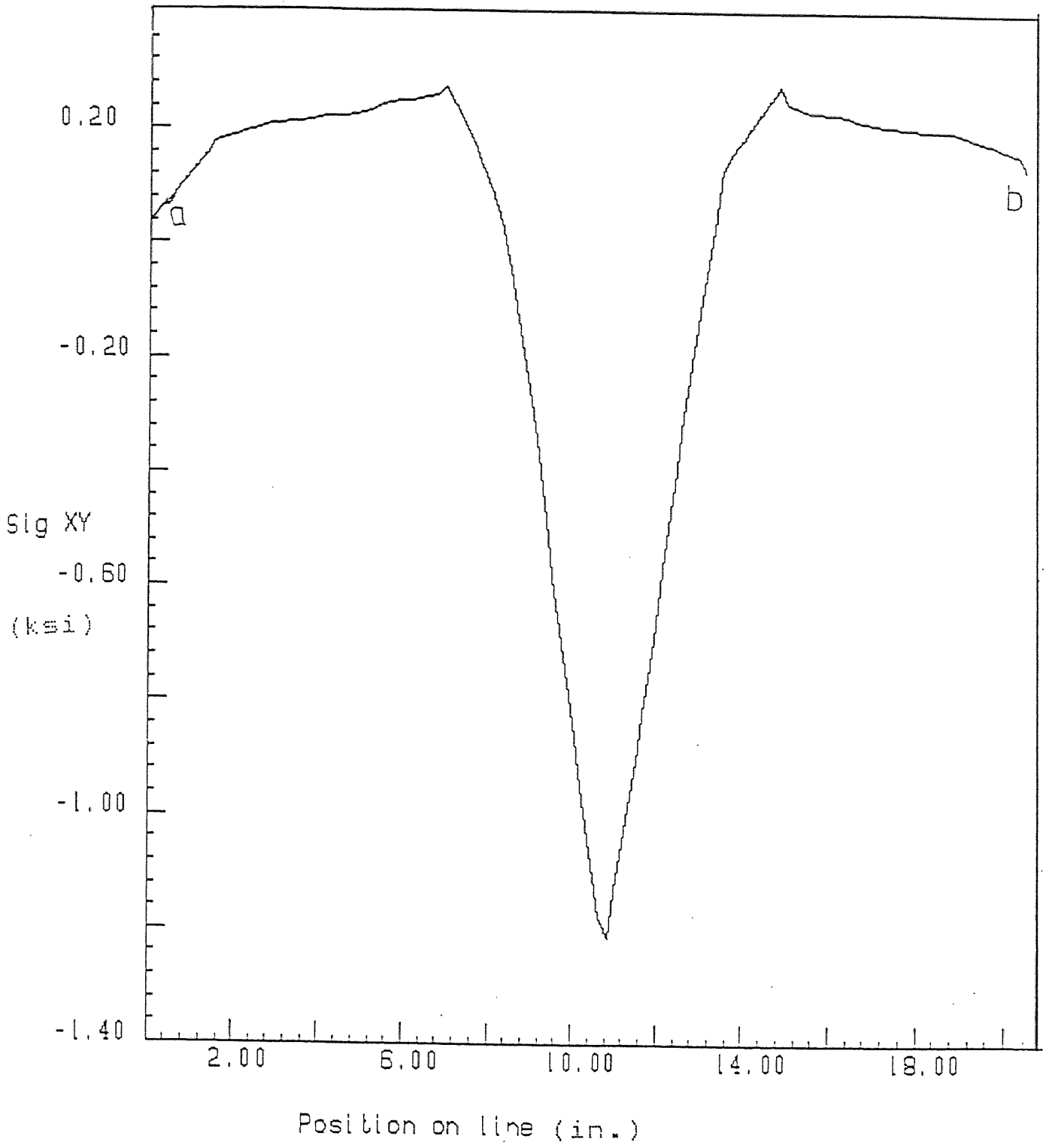


Fig. 3.11 σ_{xy} on Section 2-2

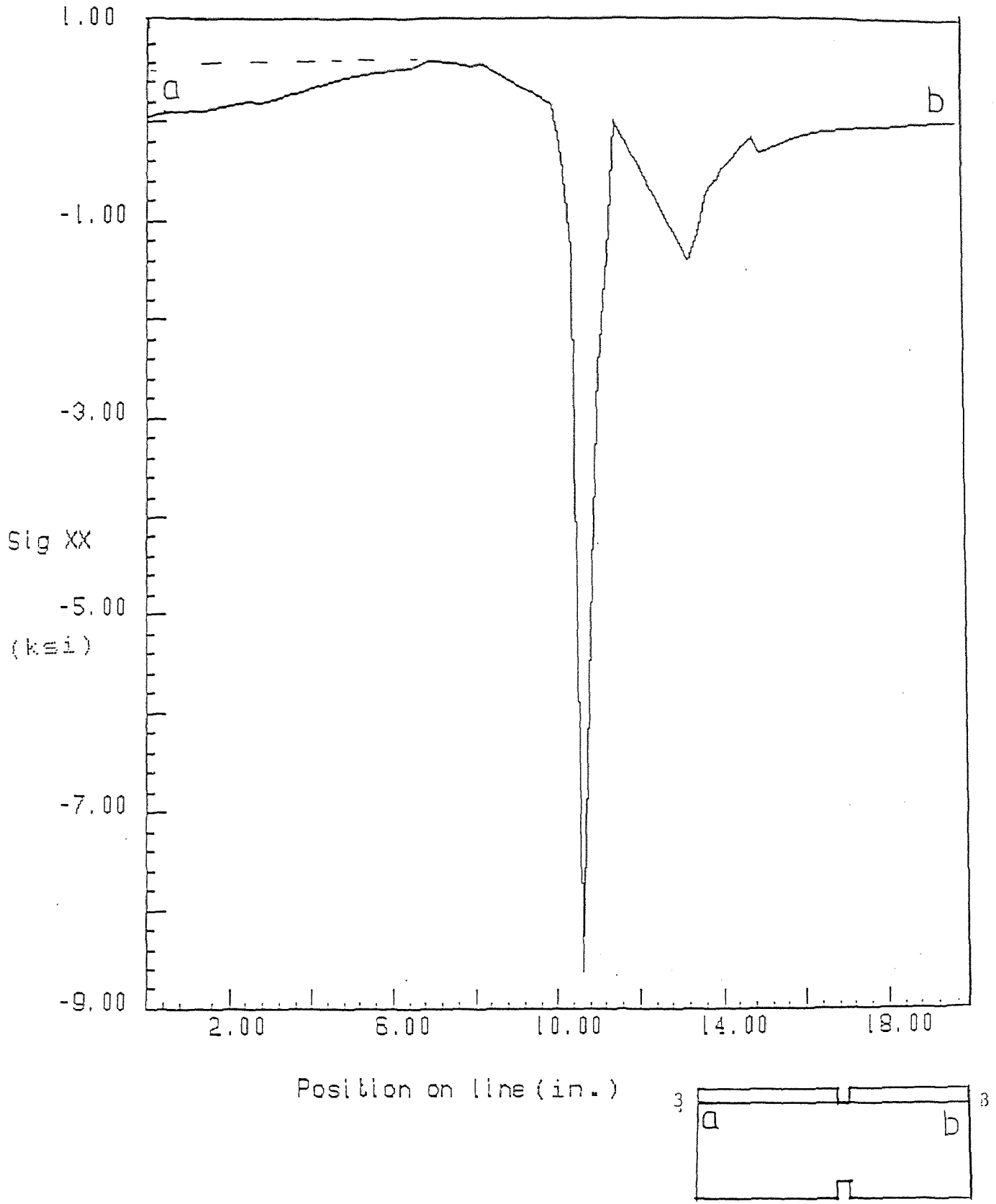


Fig. 3.12 Sx on Section 3-3

Line 3-3

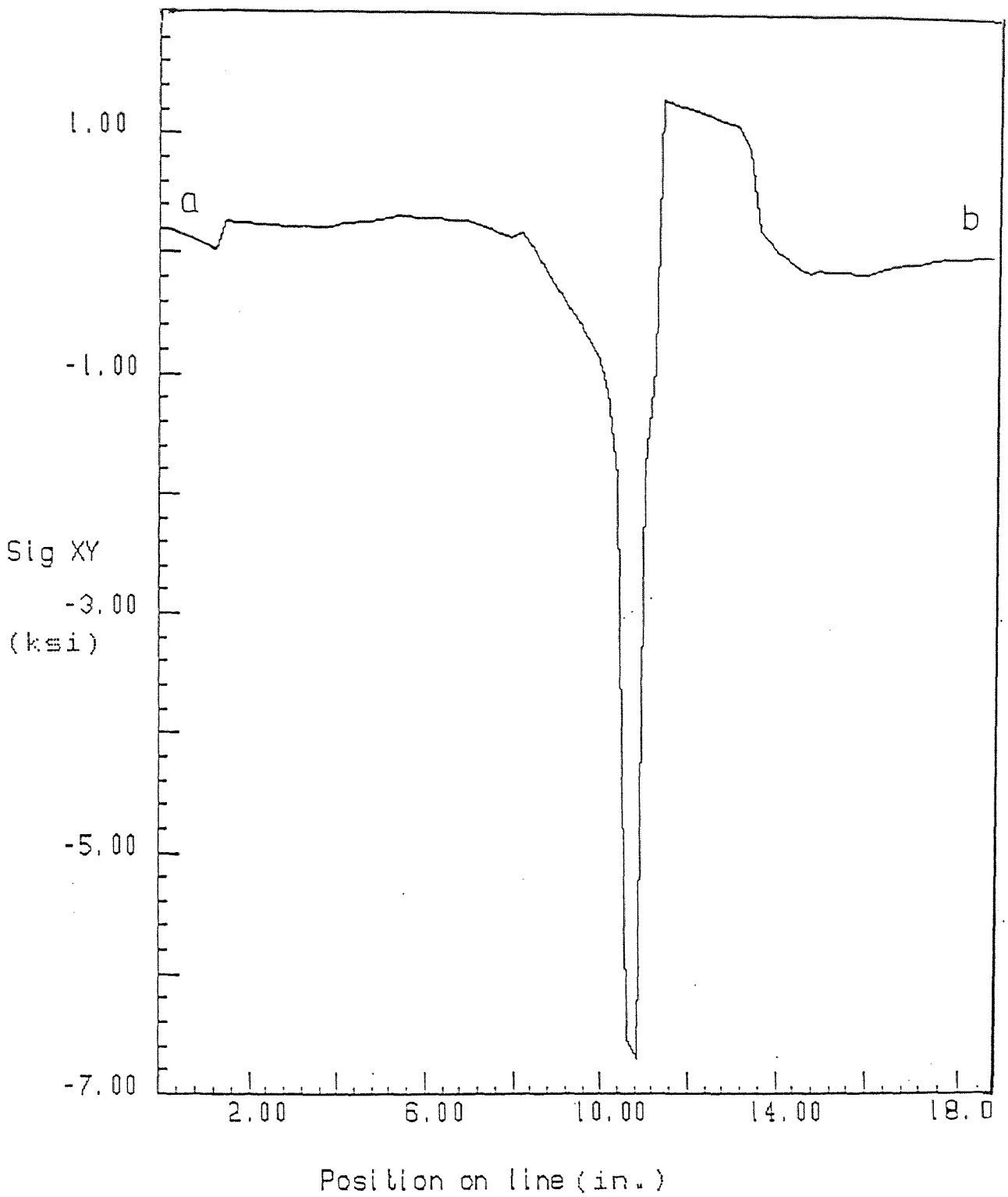


Fig. 3.13 Sxy on Section 3-3

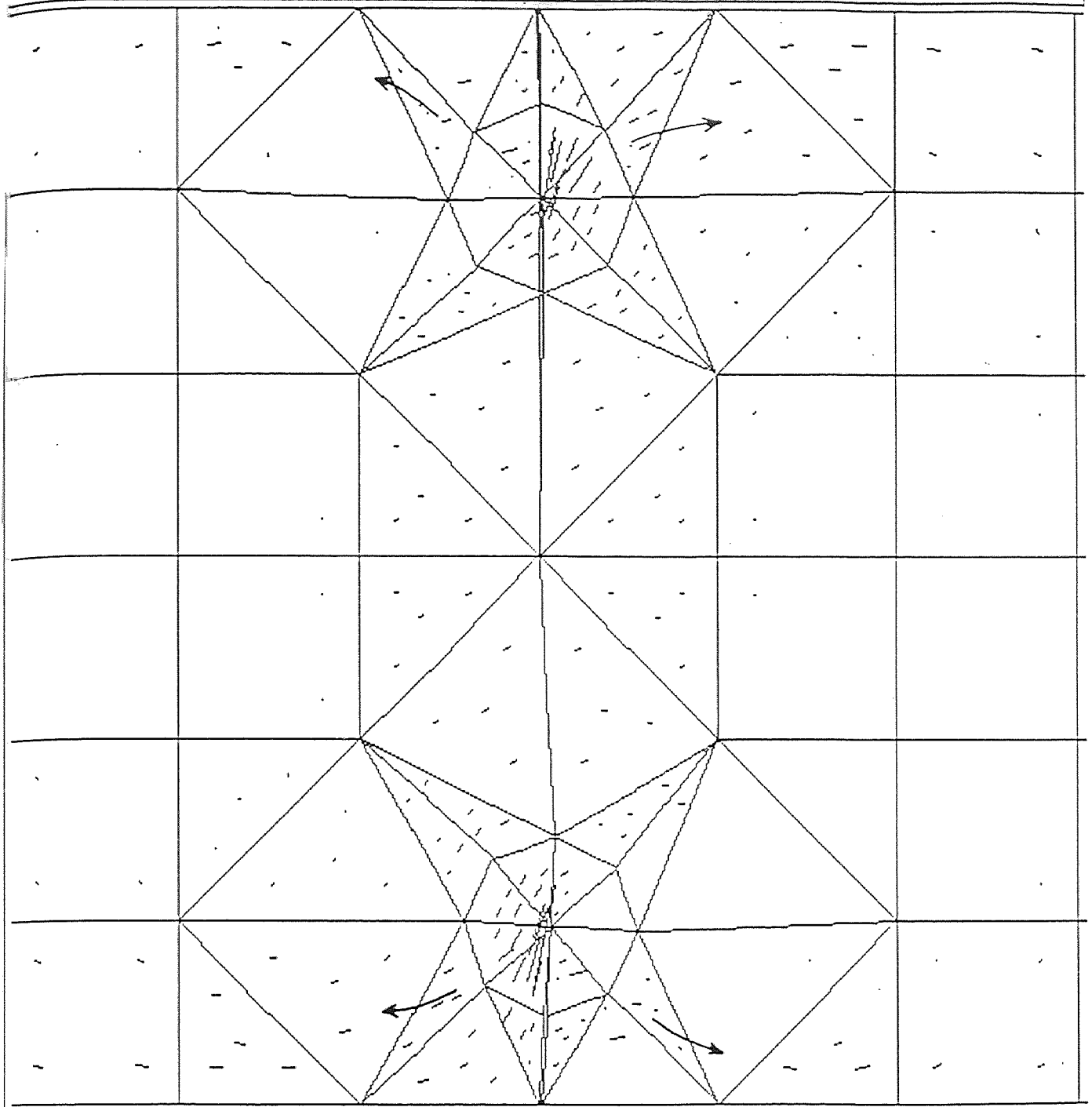


Fig. 3.14 Tensile Principal Stress Vectors

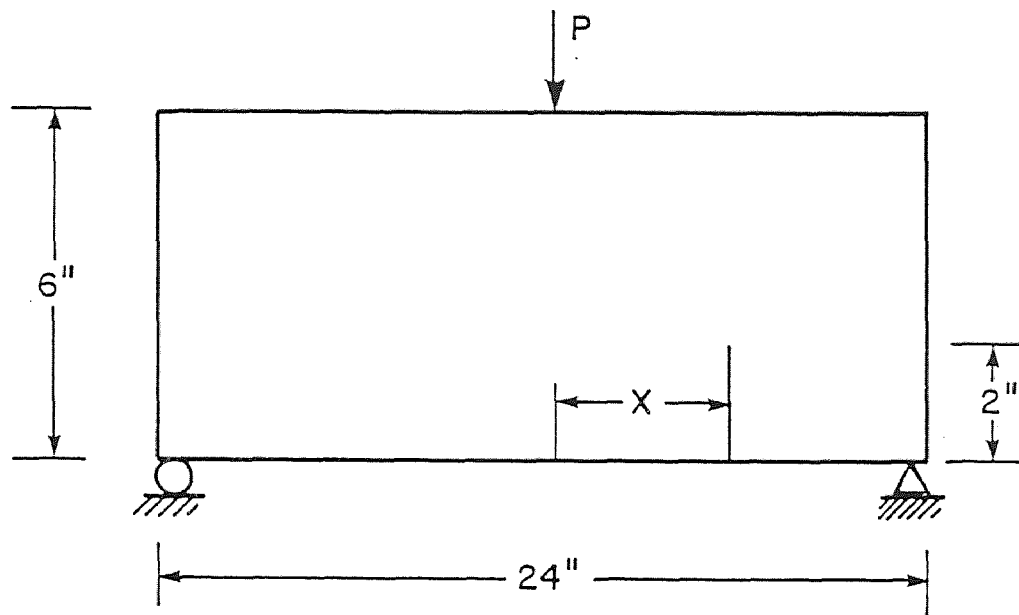
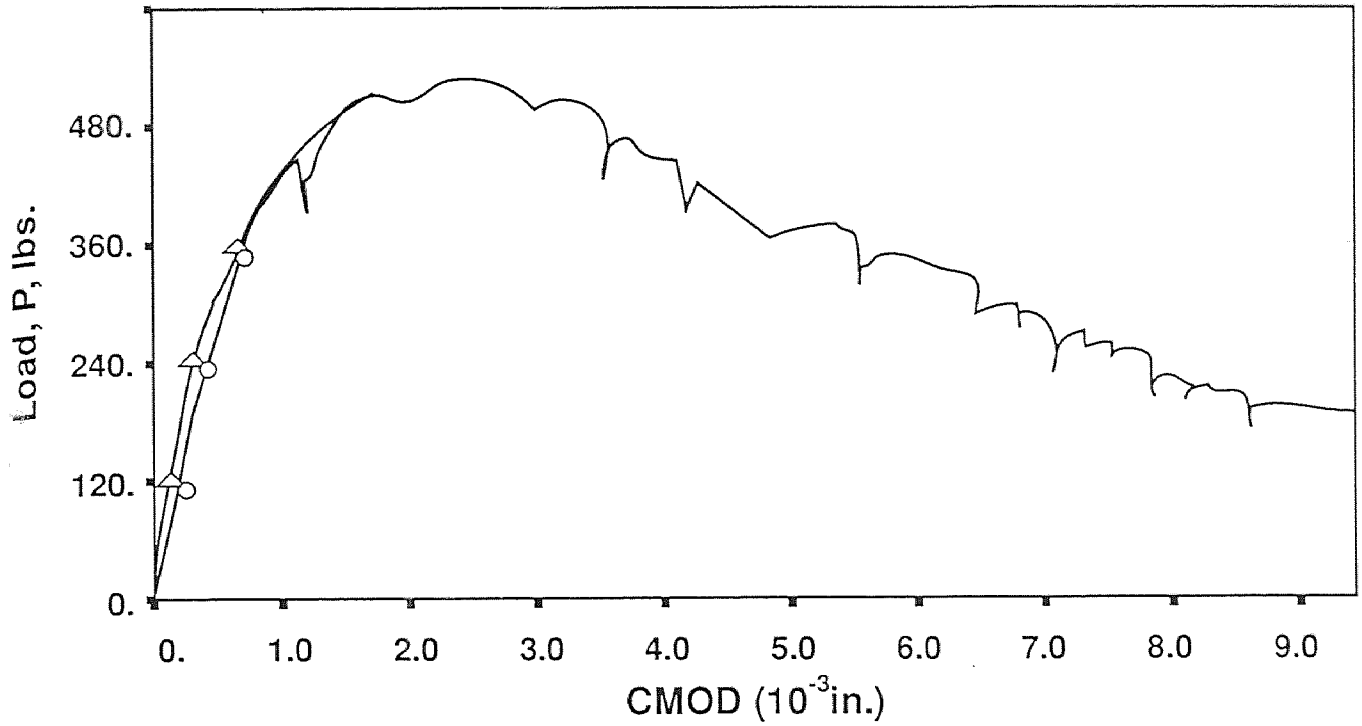
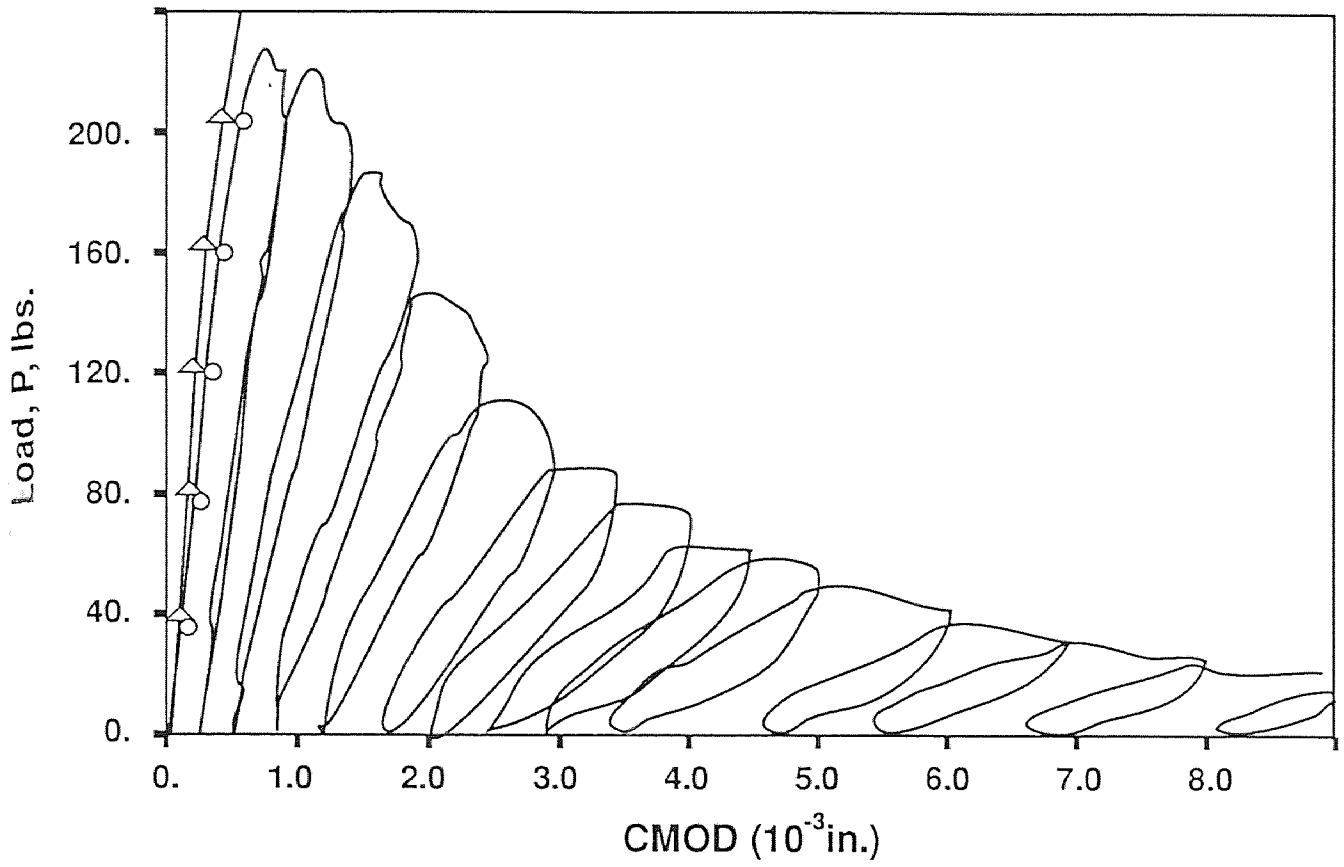


FIG. 3.15 - DIMENSIONS OF SINGLE NOTCH SPECIMEN (5)



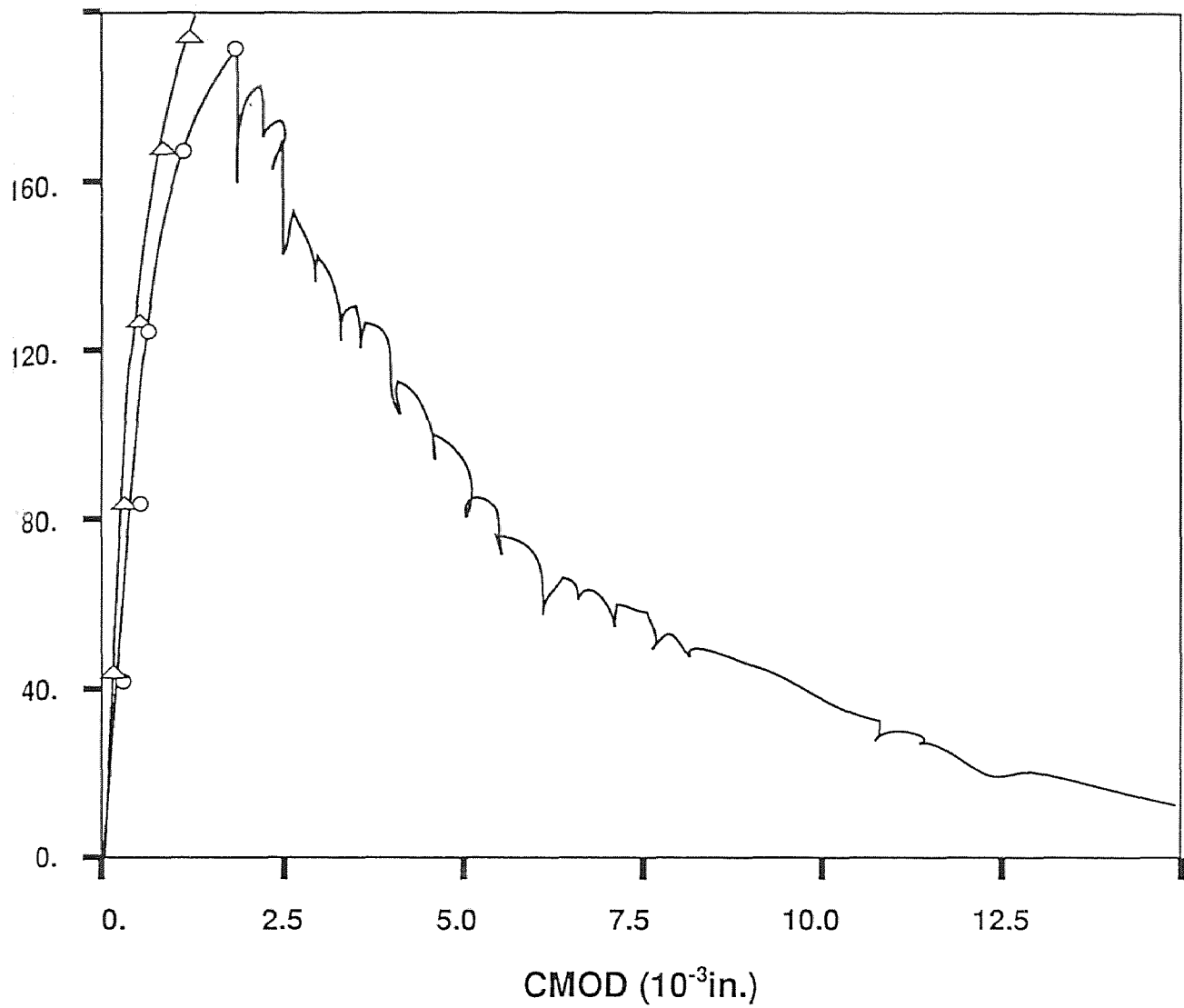
- ○ Values found by Jeng and Shah for beam #C1M2
- △ △ Values found by FRANC program (see x displacement in Appendix B)

Fig 3.16 Crack mouth opening displacement for the single notched beam #C1M2, Jeng and Shah (5)



- ○ Values found by Jeng and Shah for beam #M2S6
- △ △ Values found by FRANC program (see x Displacement in Appendix B)

Fig 3.17 Crack mouth opening displacement for the single notched beam #M2S6, Jeng and Shah (5)



- ○ Values found by Jeng and Shah for beam #C1S3
- △ △ Values found by FRANC program (see x displacement in Appendix B)

Fig 3.18 Crack mouth opening displacement for the single notched beam #C1S3, Jeng and Shah (5)

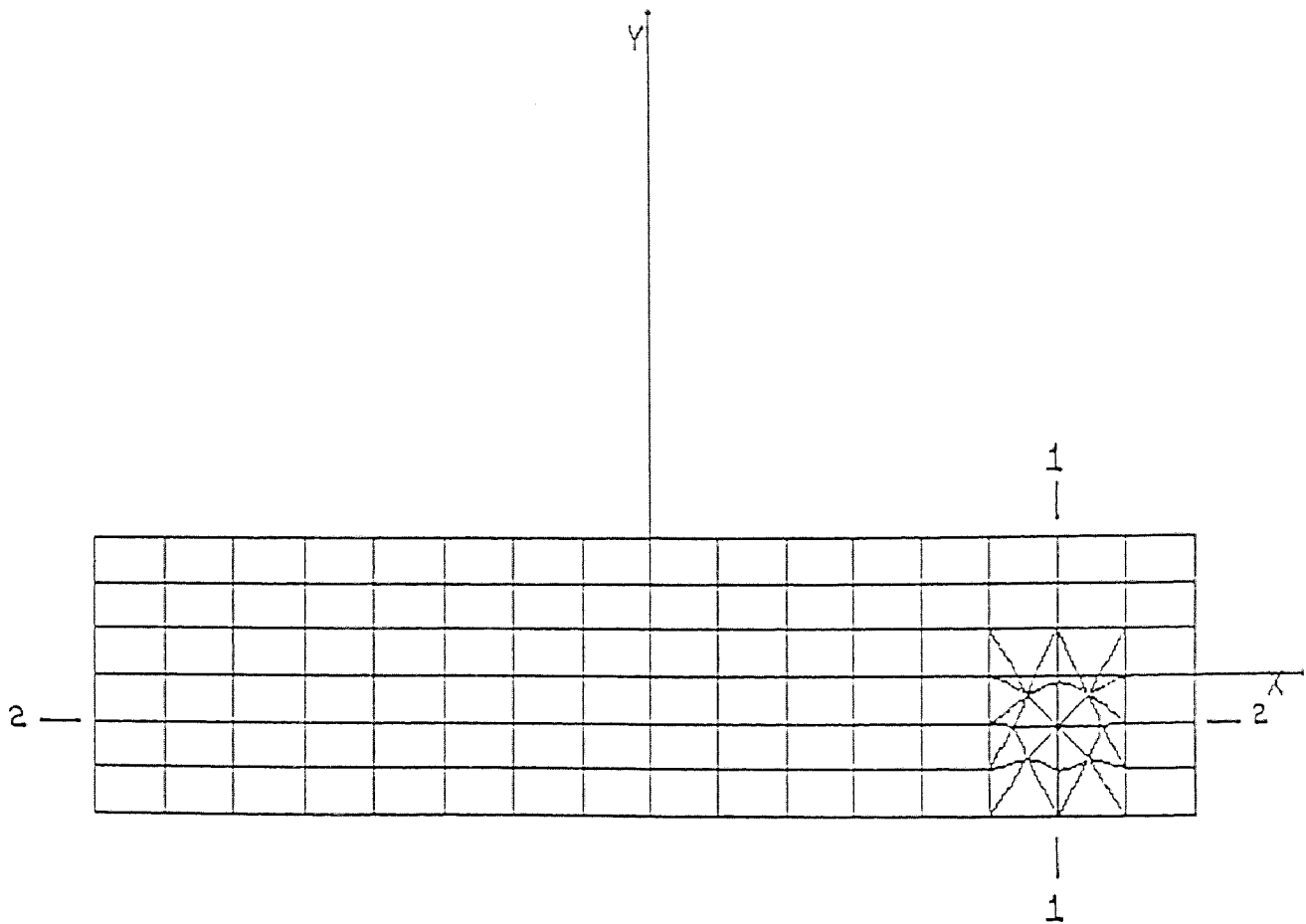


Fig. 3.19 Mesh Configuration for $x=9$

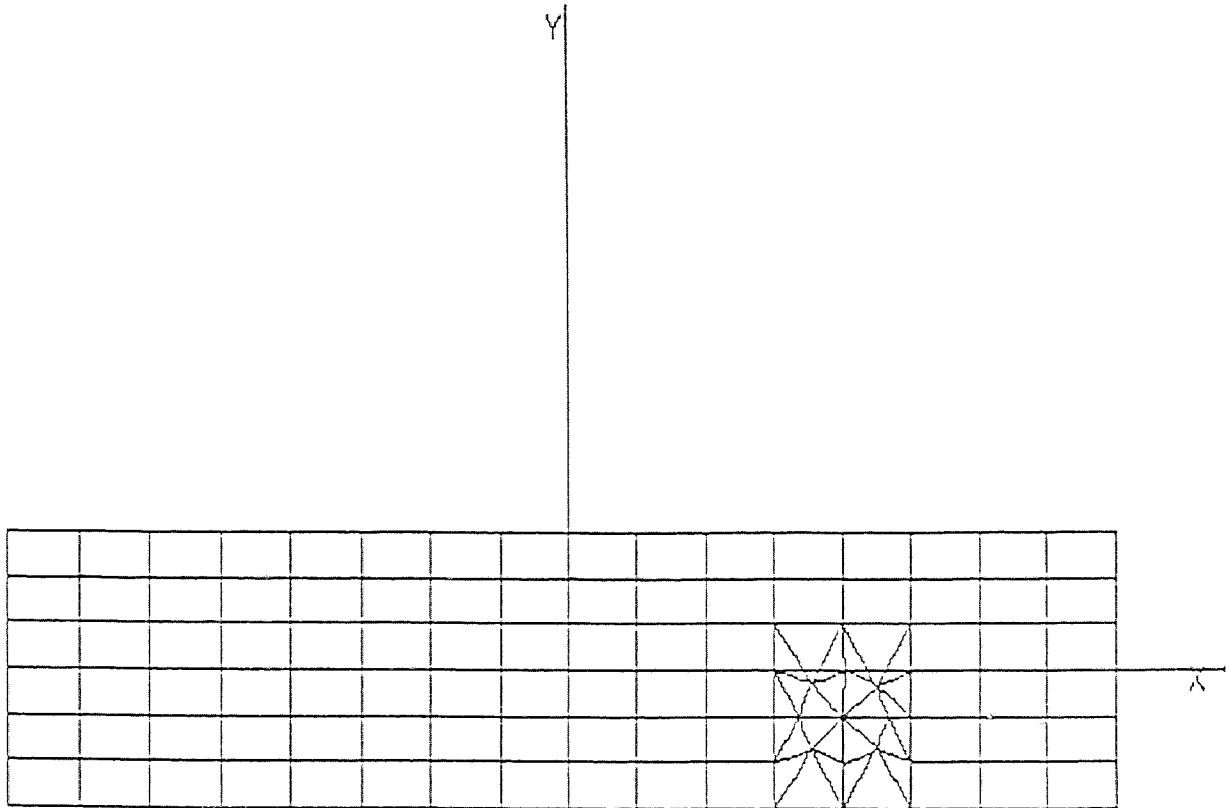


Fig. 3.20 Mesh Configuration for $x=6$

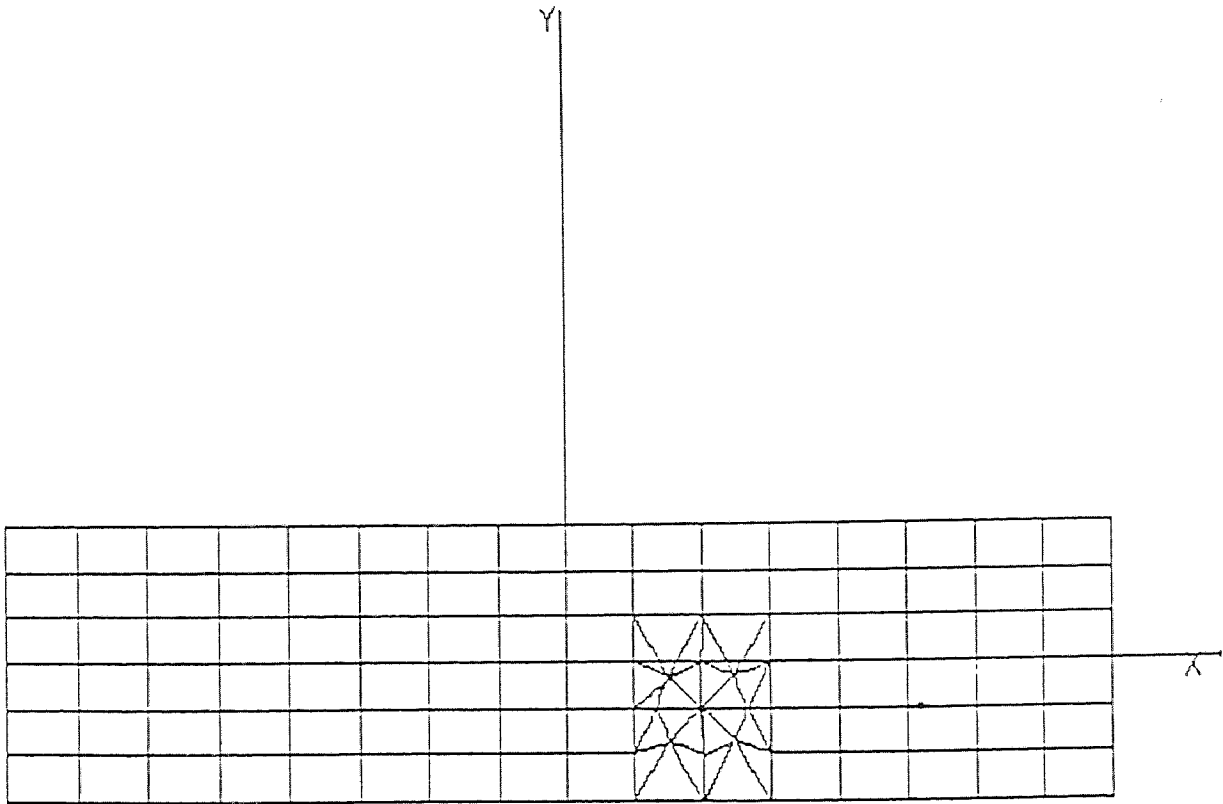


Fig. 3.21 Mesh Configuration for $x=3$

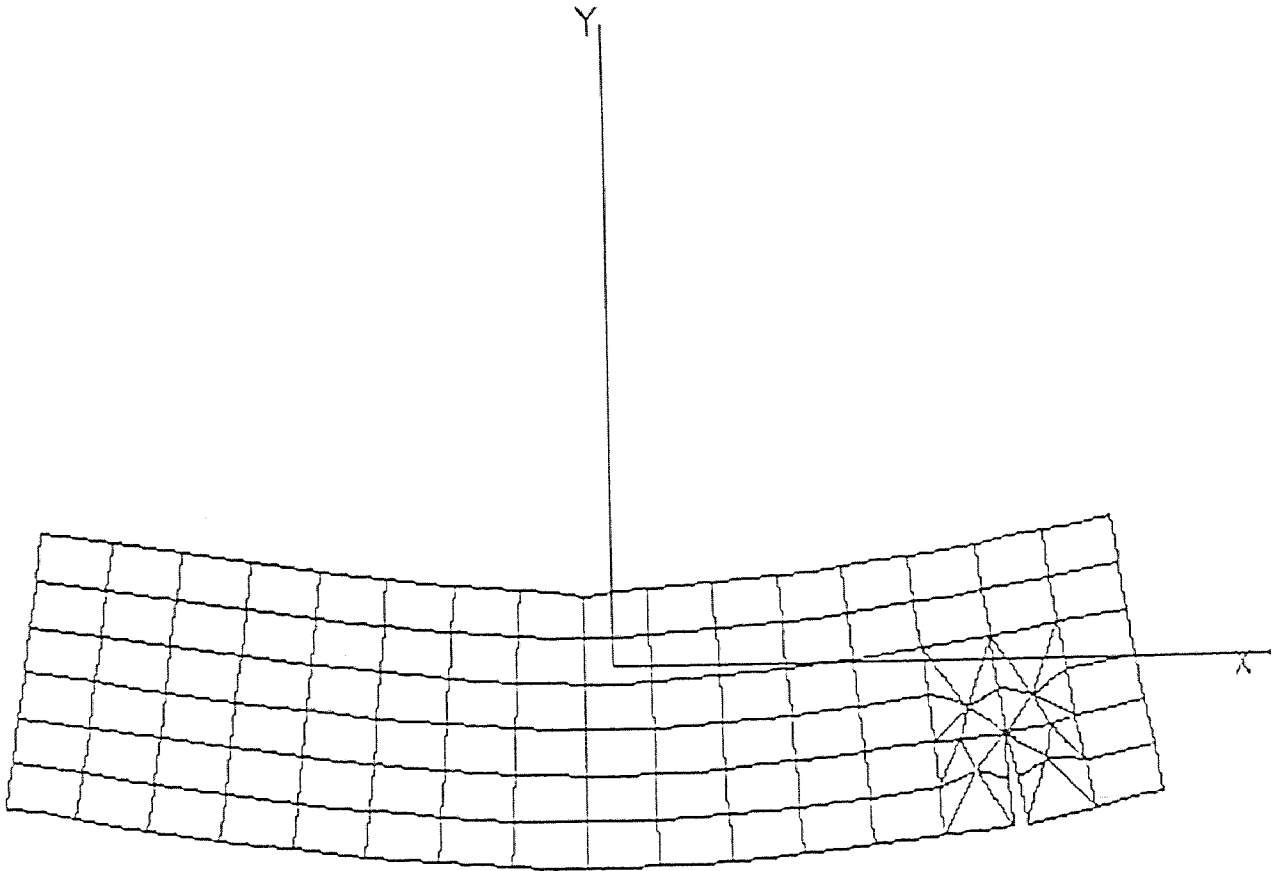


Fig. 3.22 Deformed Mesh ($x=9$)

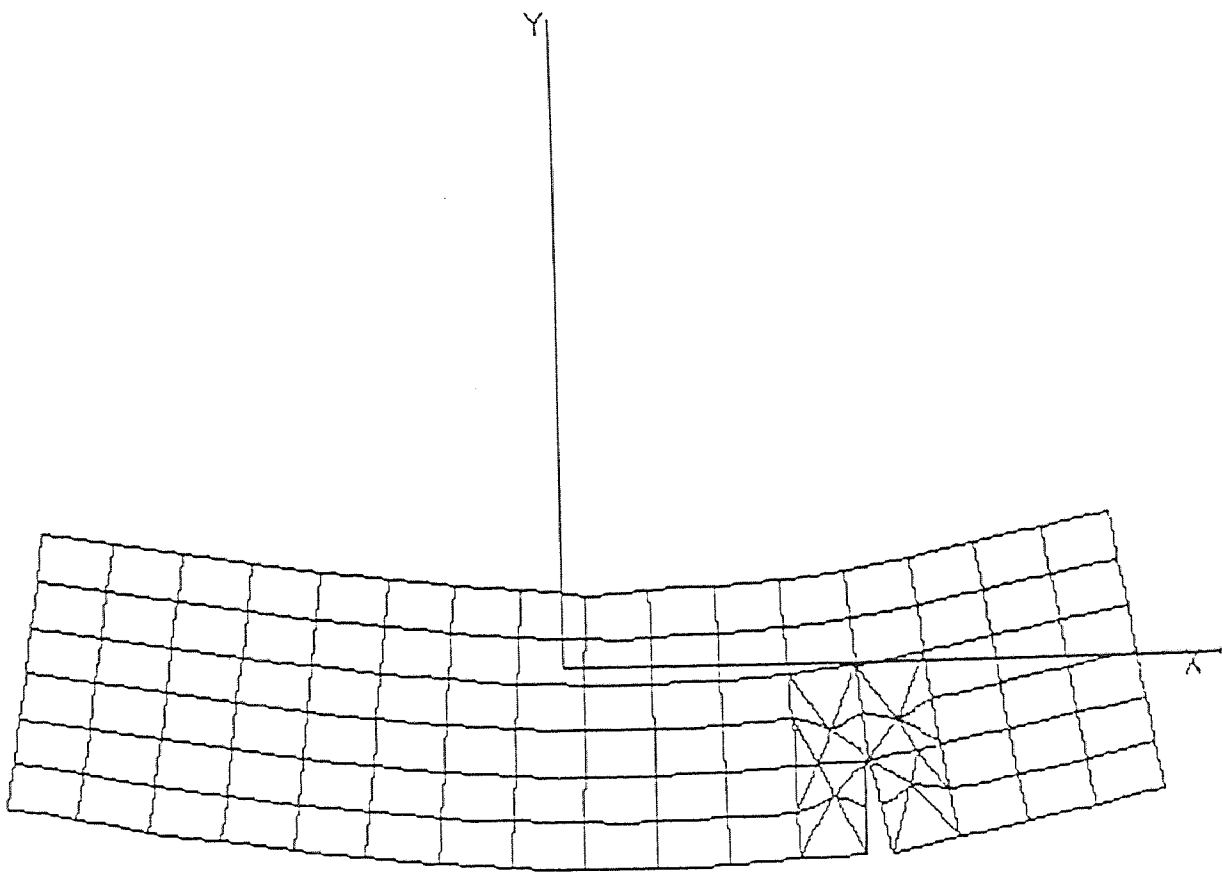


Fig. 3.23 Deformed Mesh ($x=6$)

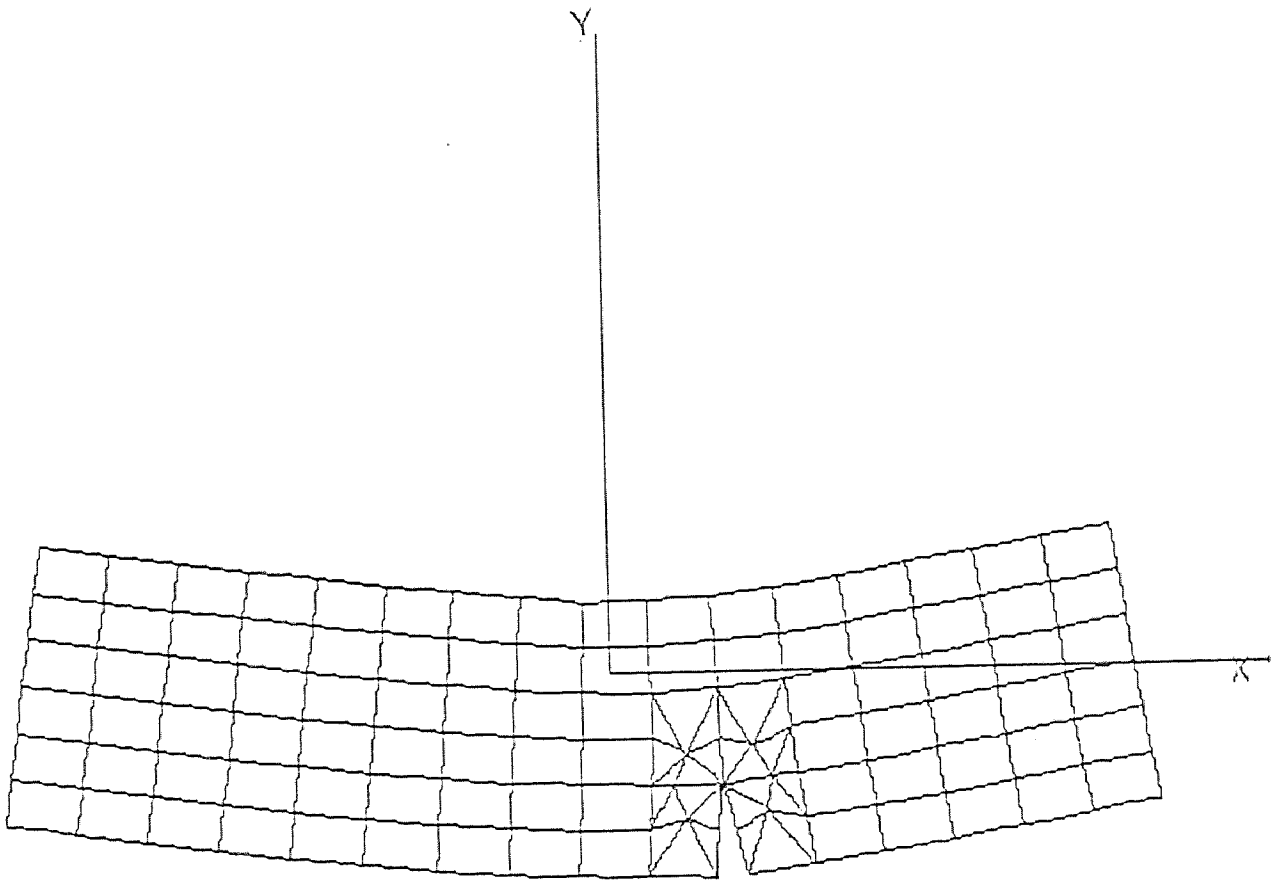
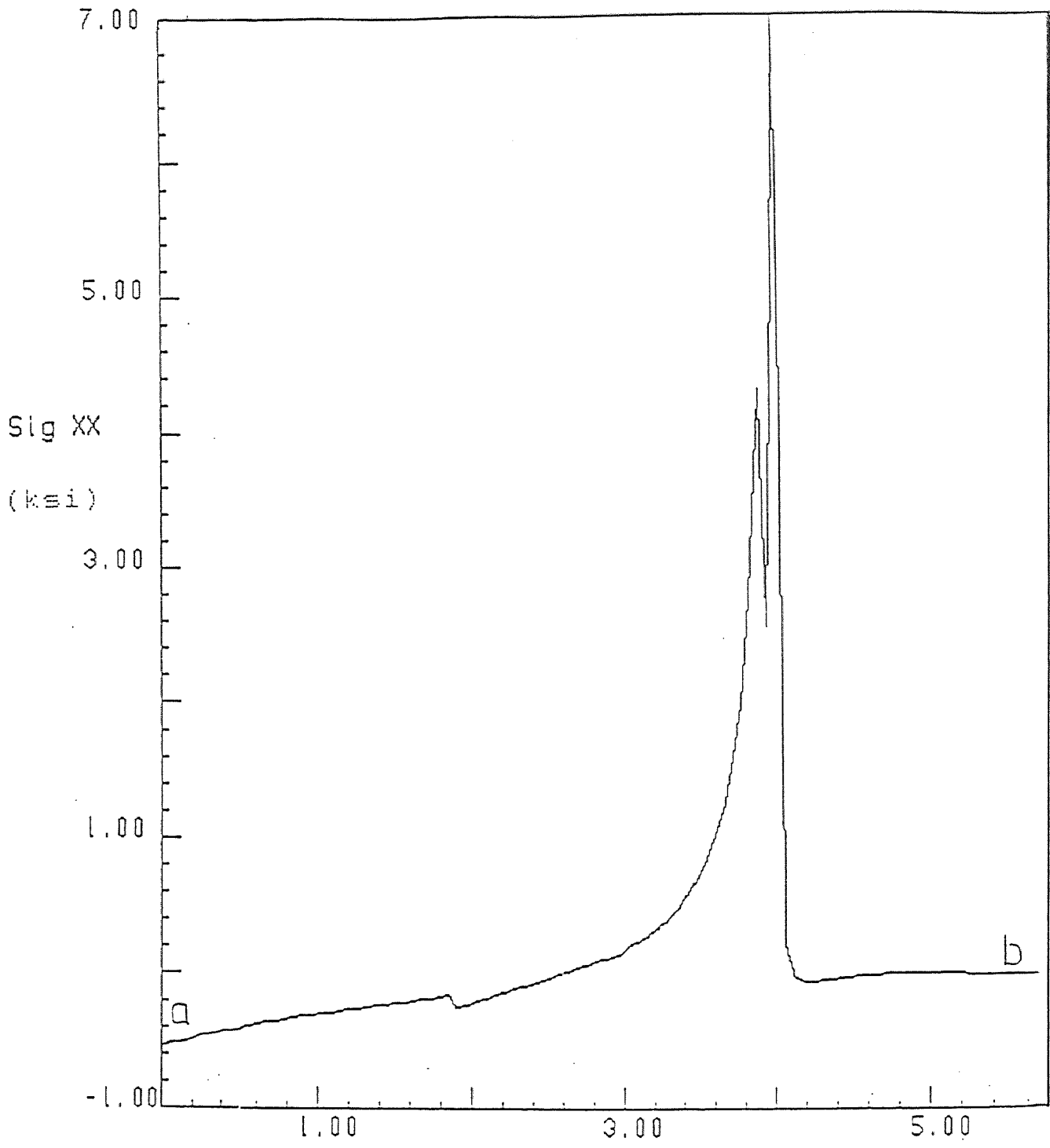
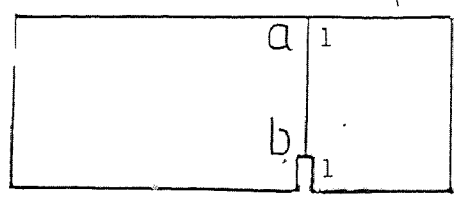


Fig. 3.24 Deformed Mesh ($x=3$)



Position on line (in.)



Line 1-1

Fig. 3.25 S_x on Section 1-1 ($x=9$)

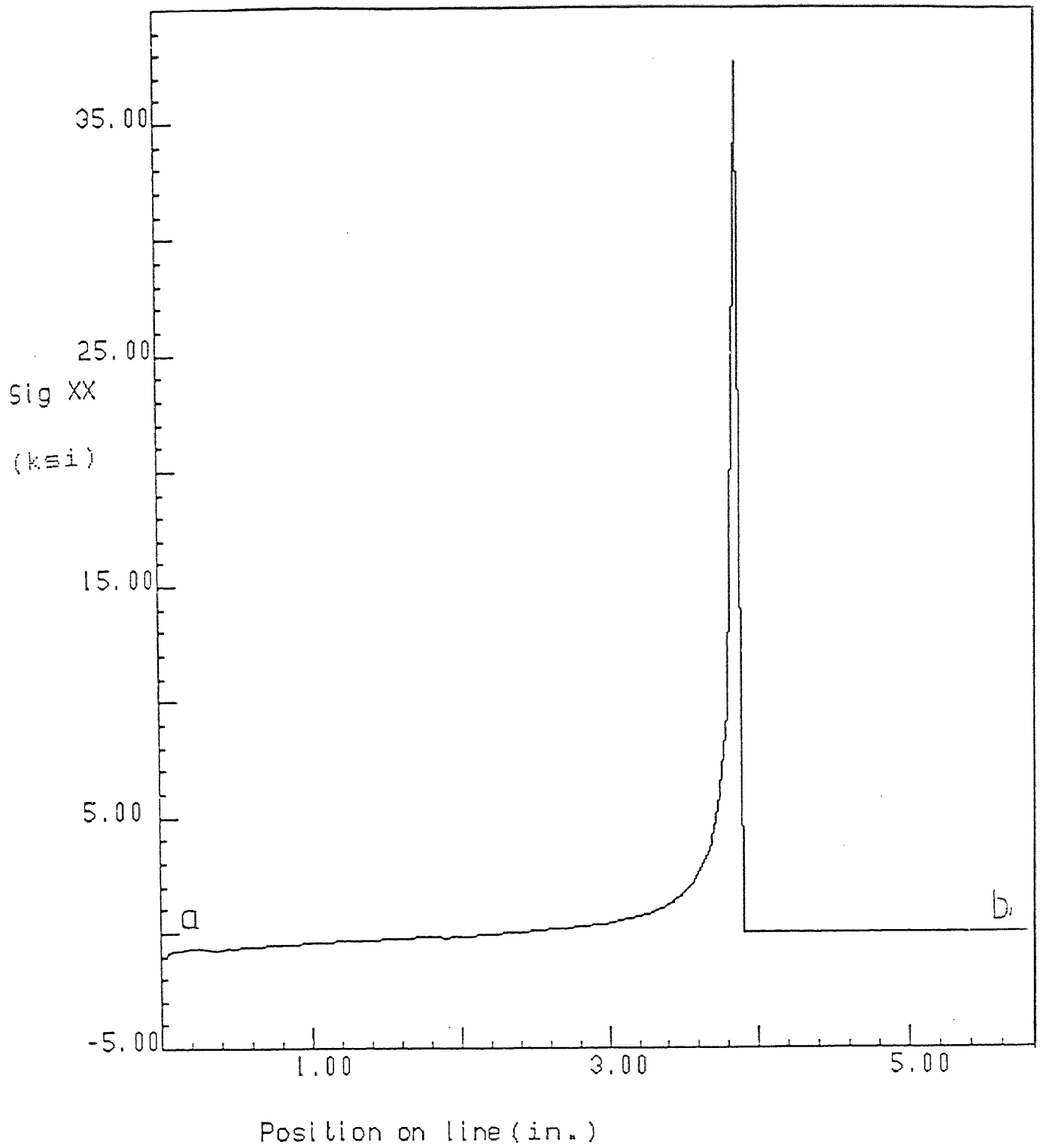


Fig. 3.26 S_x on Section 1-1 ($x=6$)

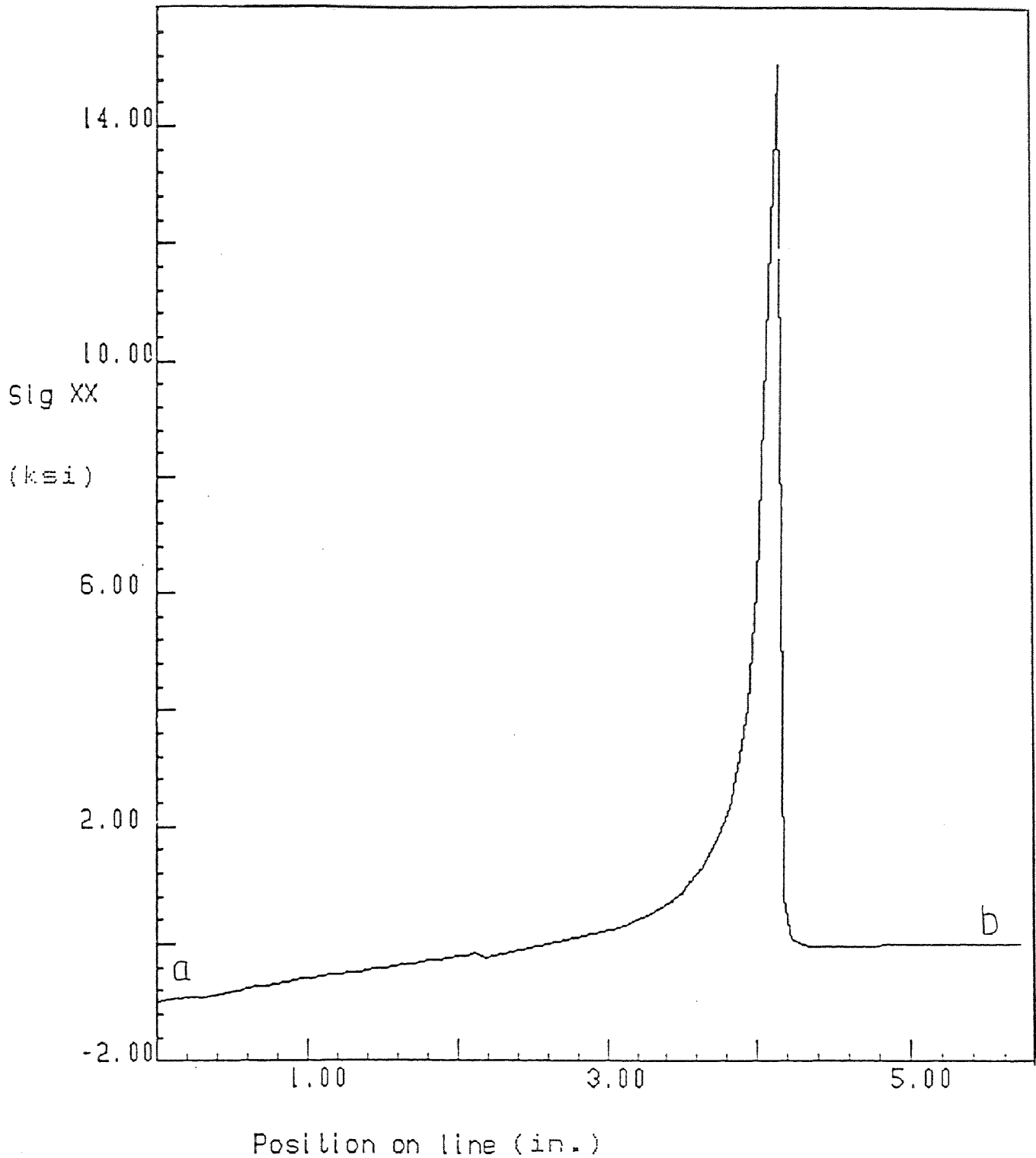


Fig. 3.27 Sx on Section 1-1 (x=3)

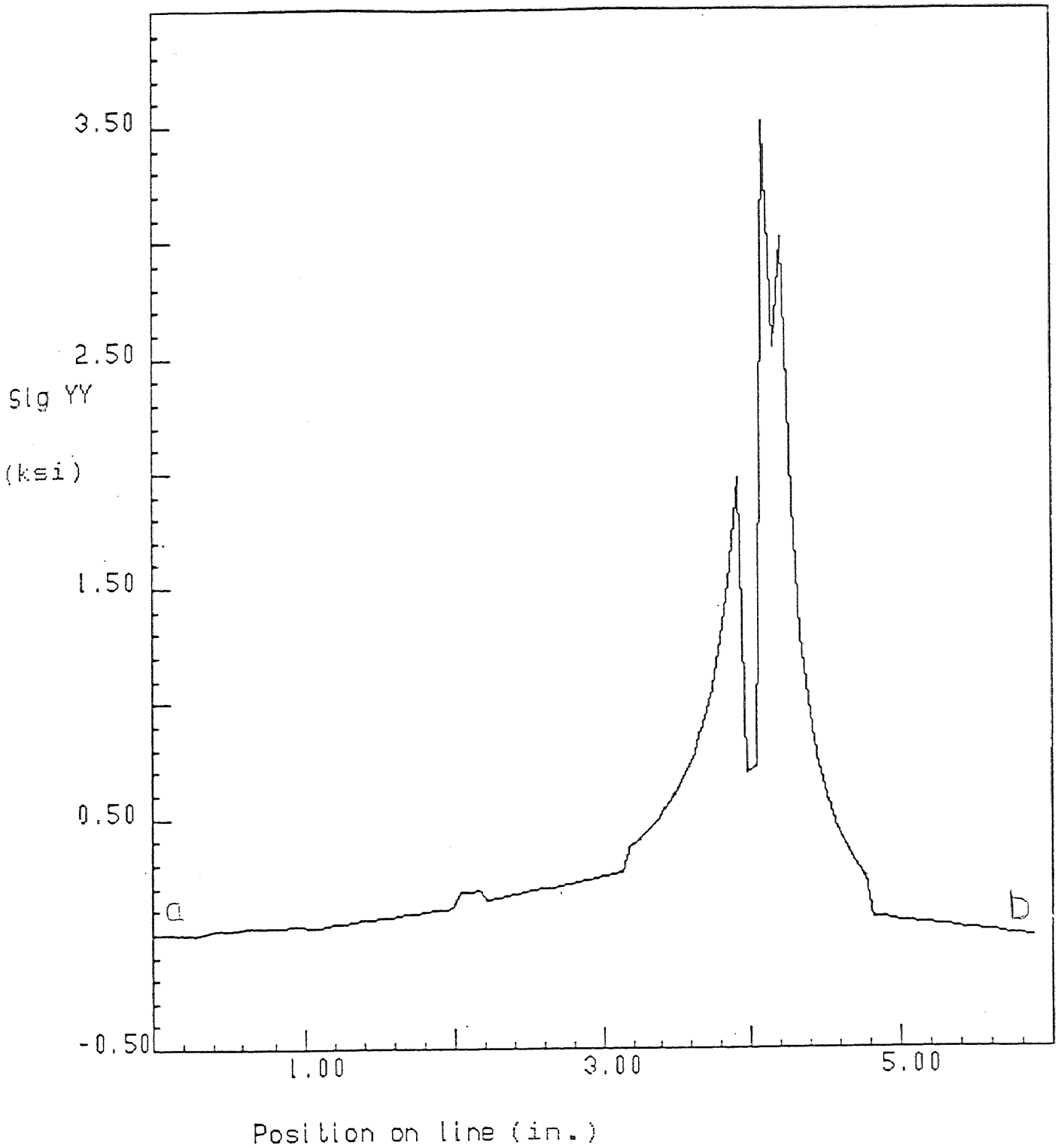


Fig. 3.28 S_y on Section 1-1 ($x=9$)

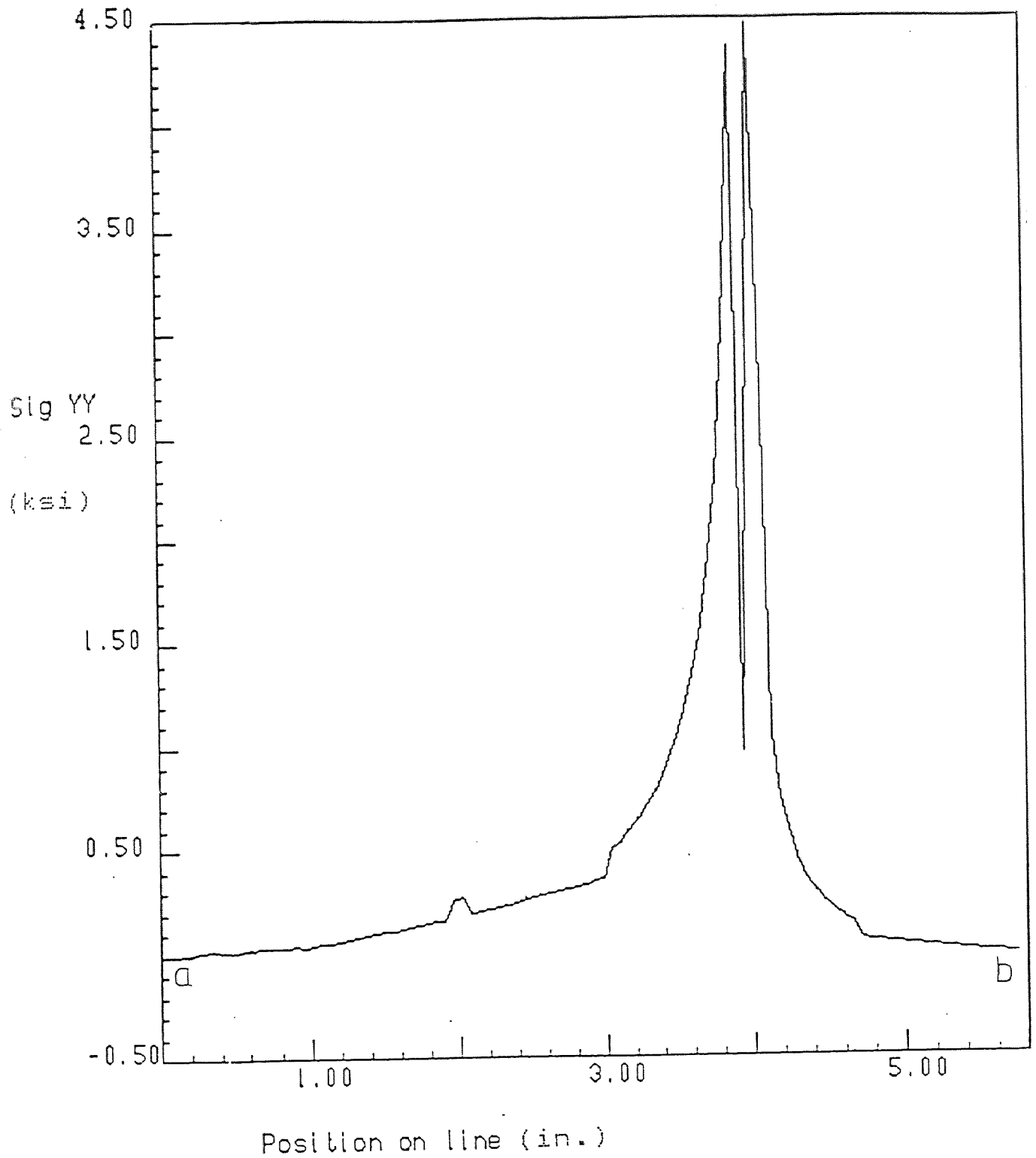


Fig. 3.29 S_y on Section 1-1 ($x=6$)

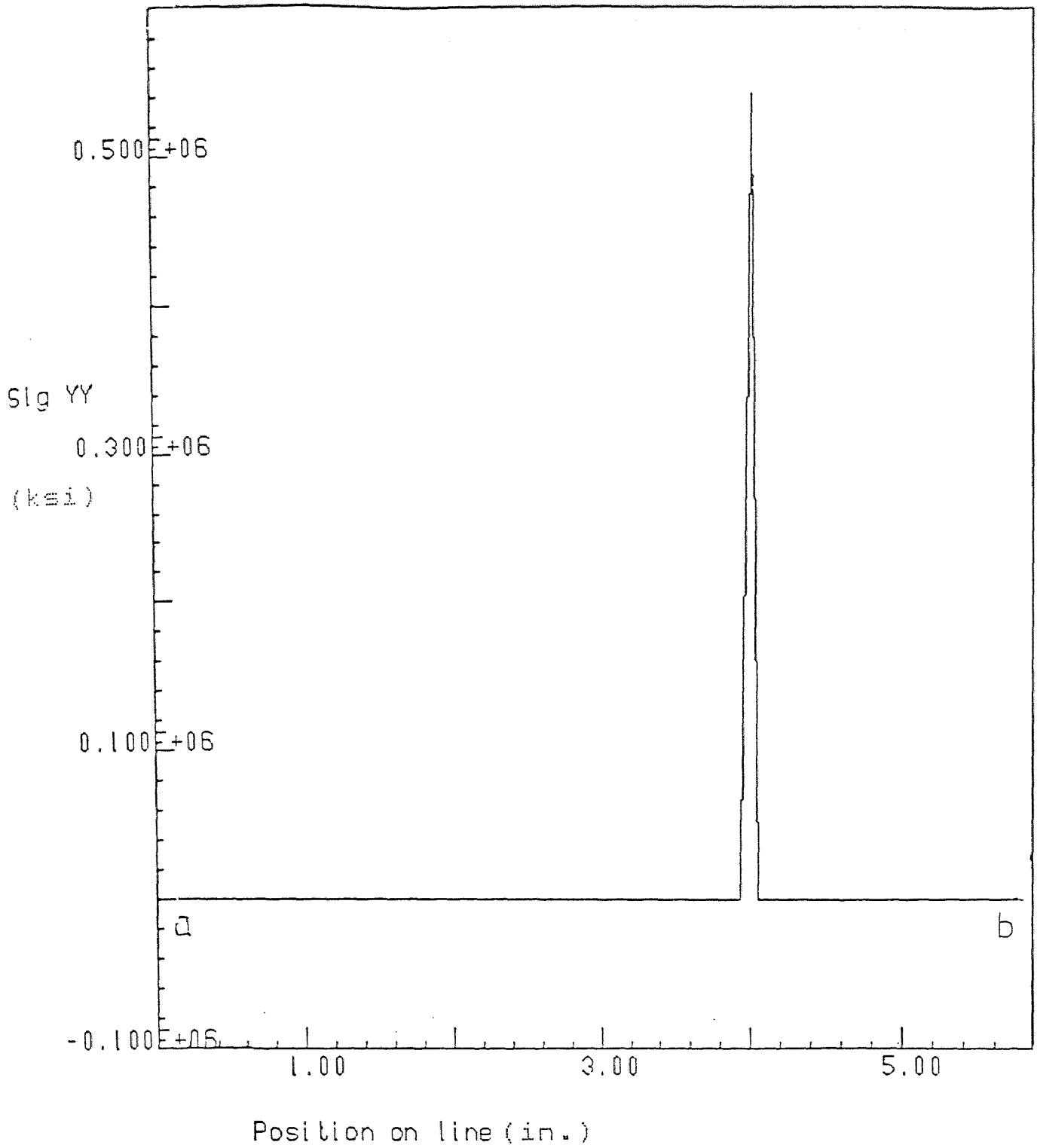


Fig. 3.30 S_y on Section 1-1 ($x=3$)

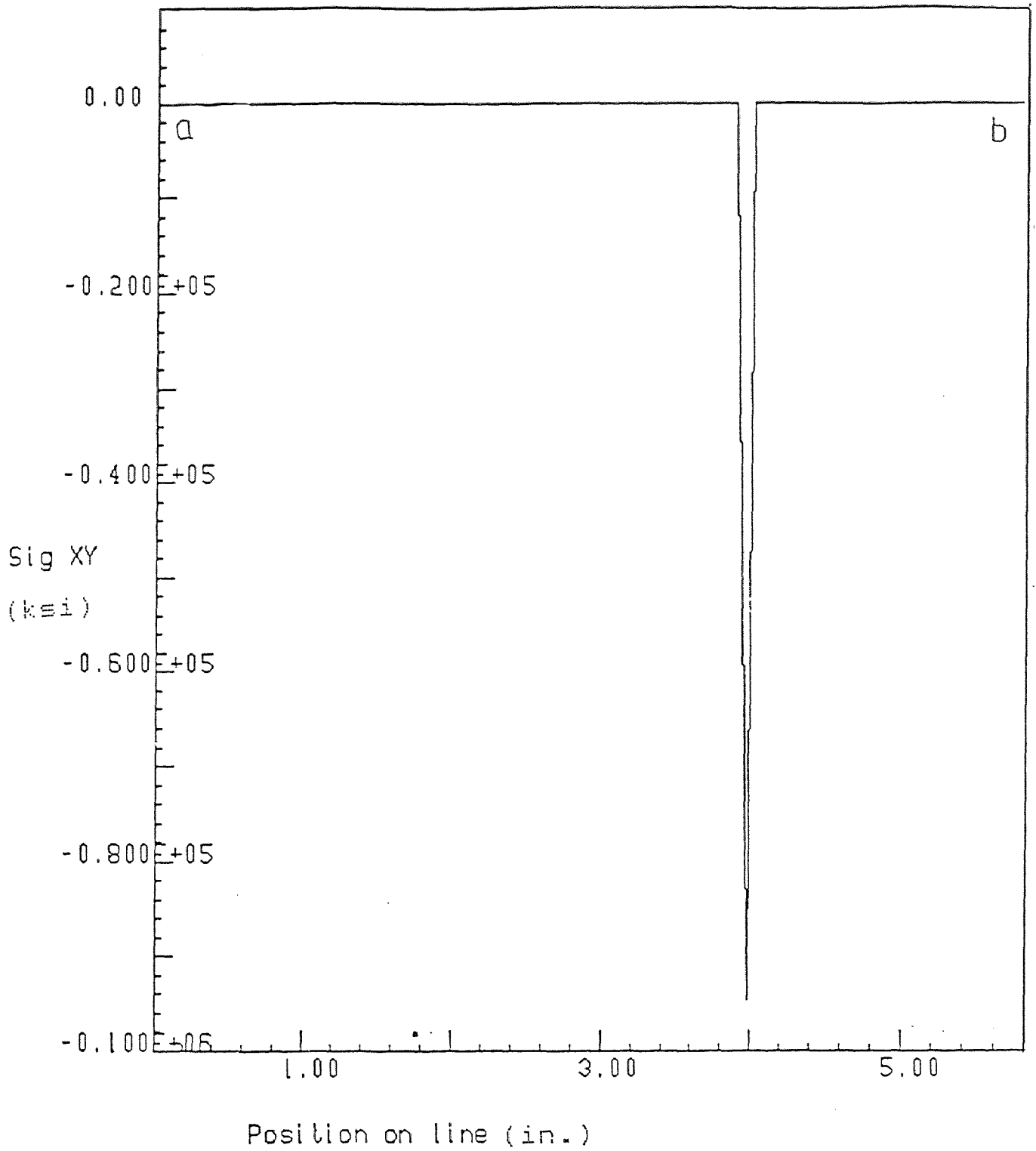


Fig. 3.31 Sxy on Section 1-1 (x=9)

Sig XY vs Position

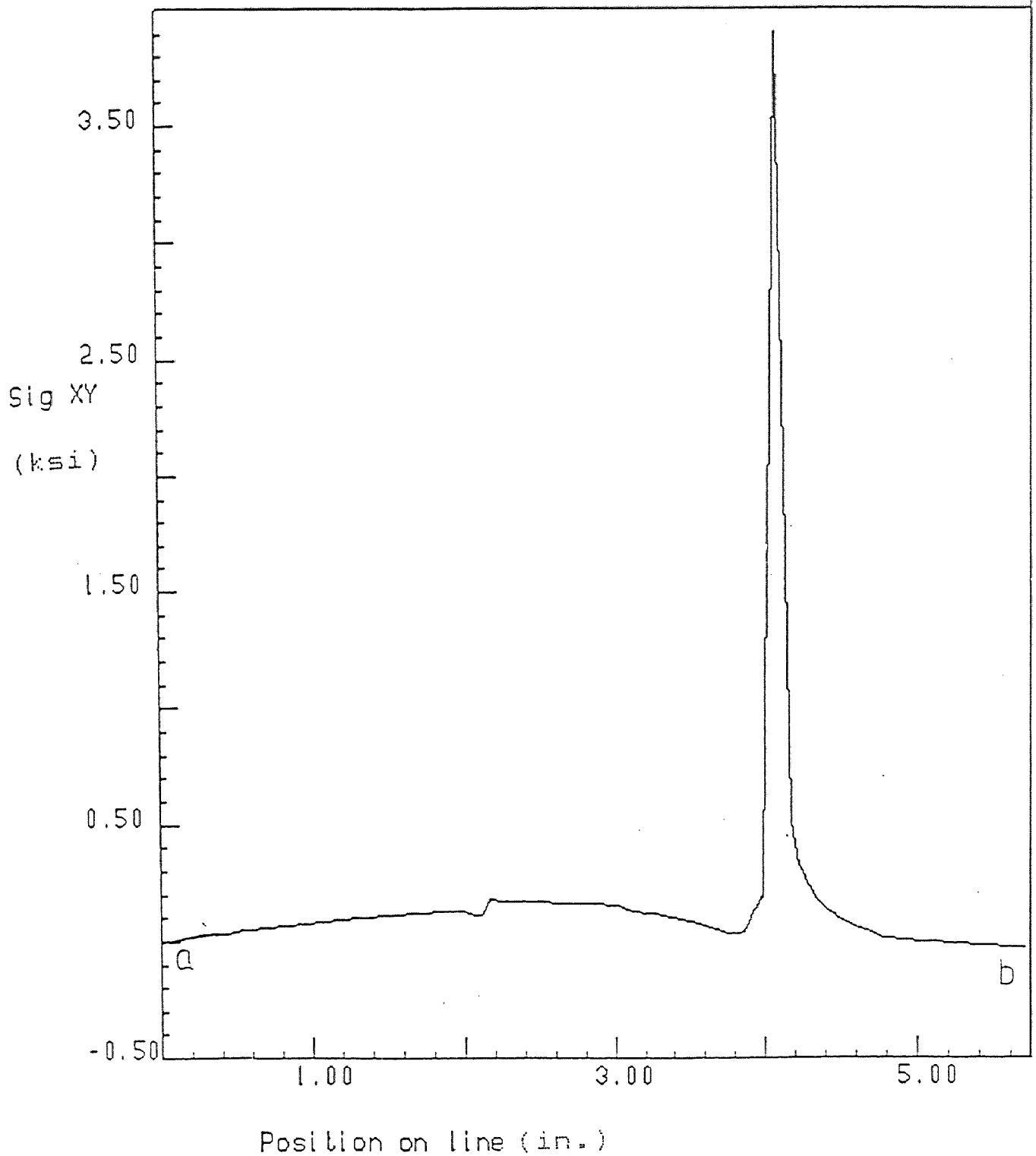


Fig. 3.32 Sxy on Section 1-1 (x=6)

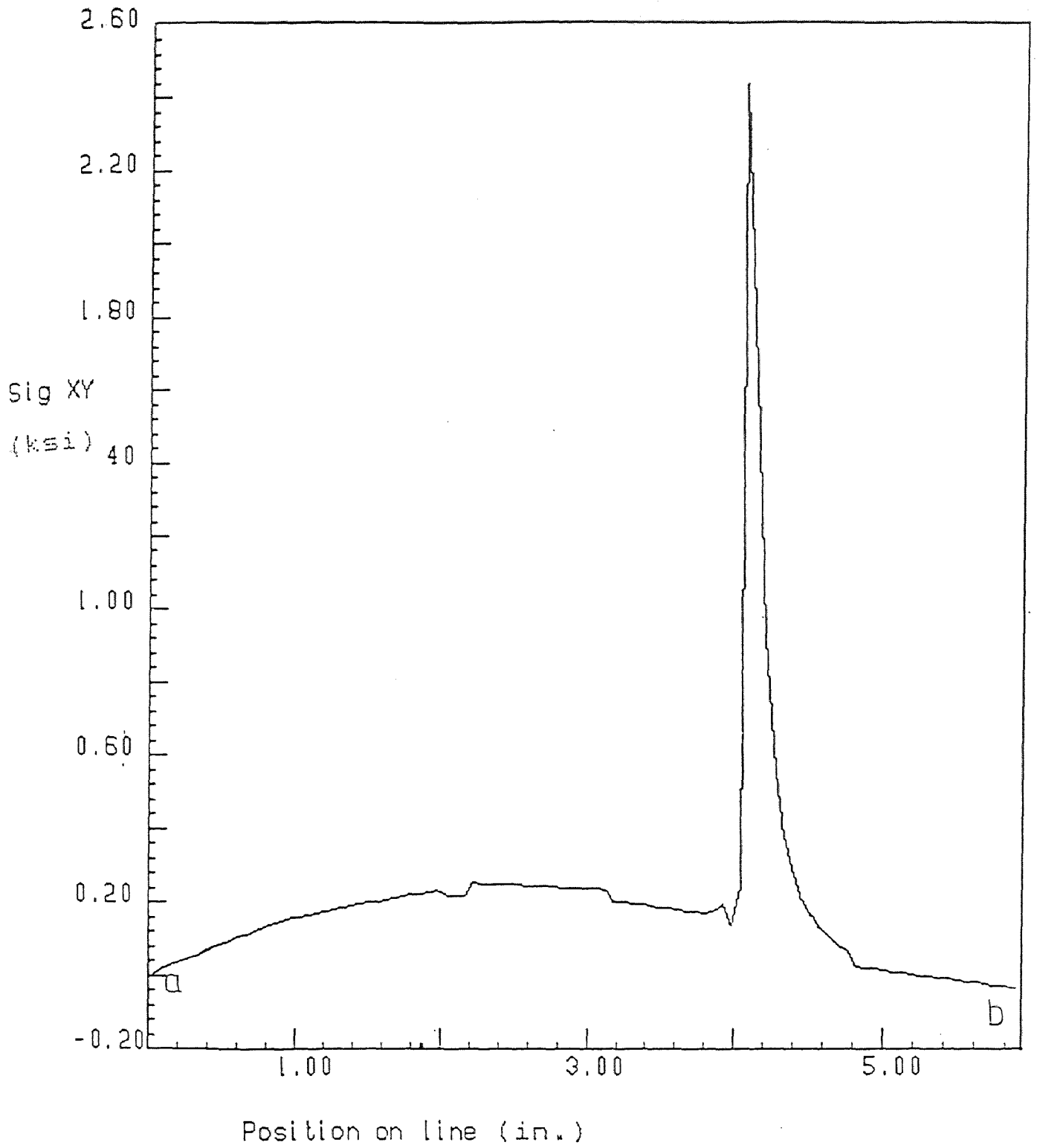
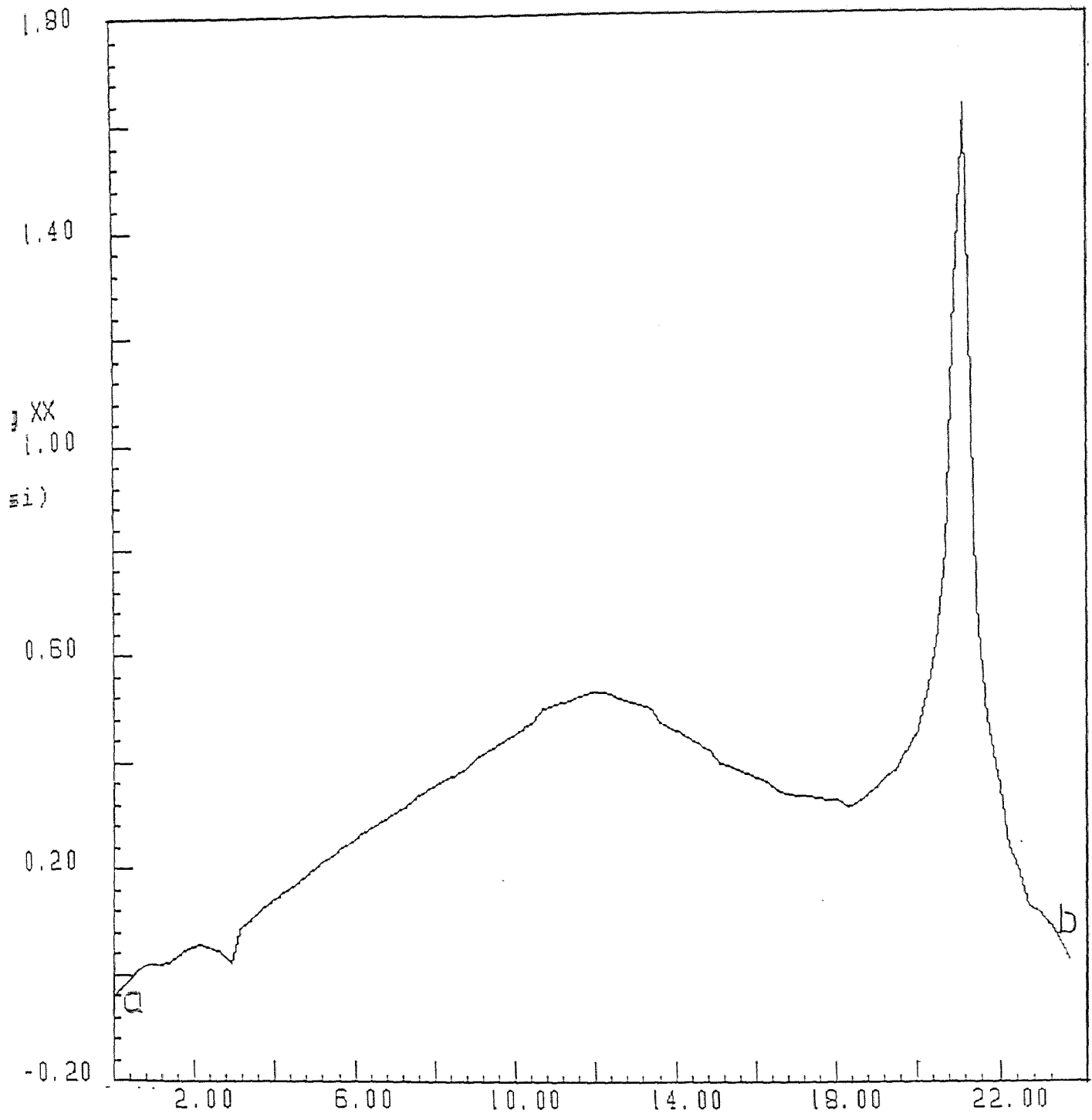
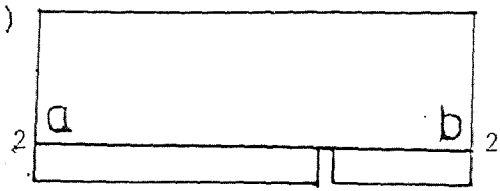


Fig. 3.33 Sxy on Section 1-1 (x=3)



Position on line (in.)



Line 2-2

Fig. 3.34 Sx on Section 2-2 (x=9)

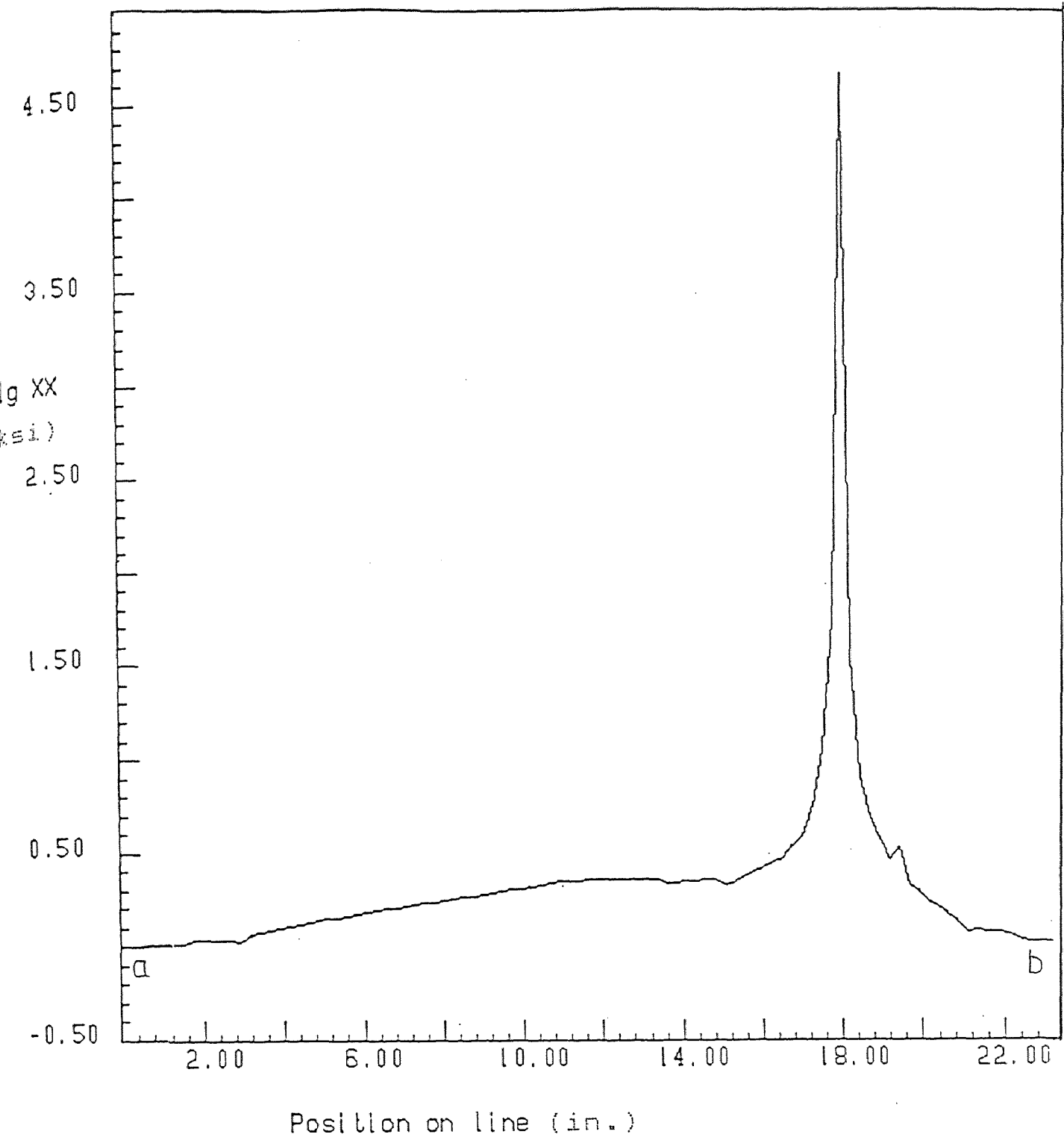


Fig. 3.35 Sx on Section 2-2 (x=6)

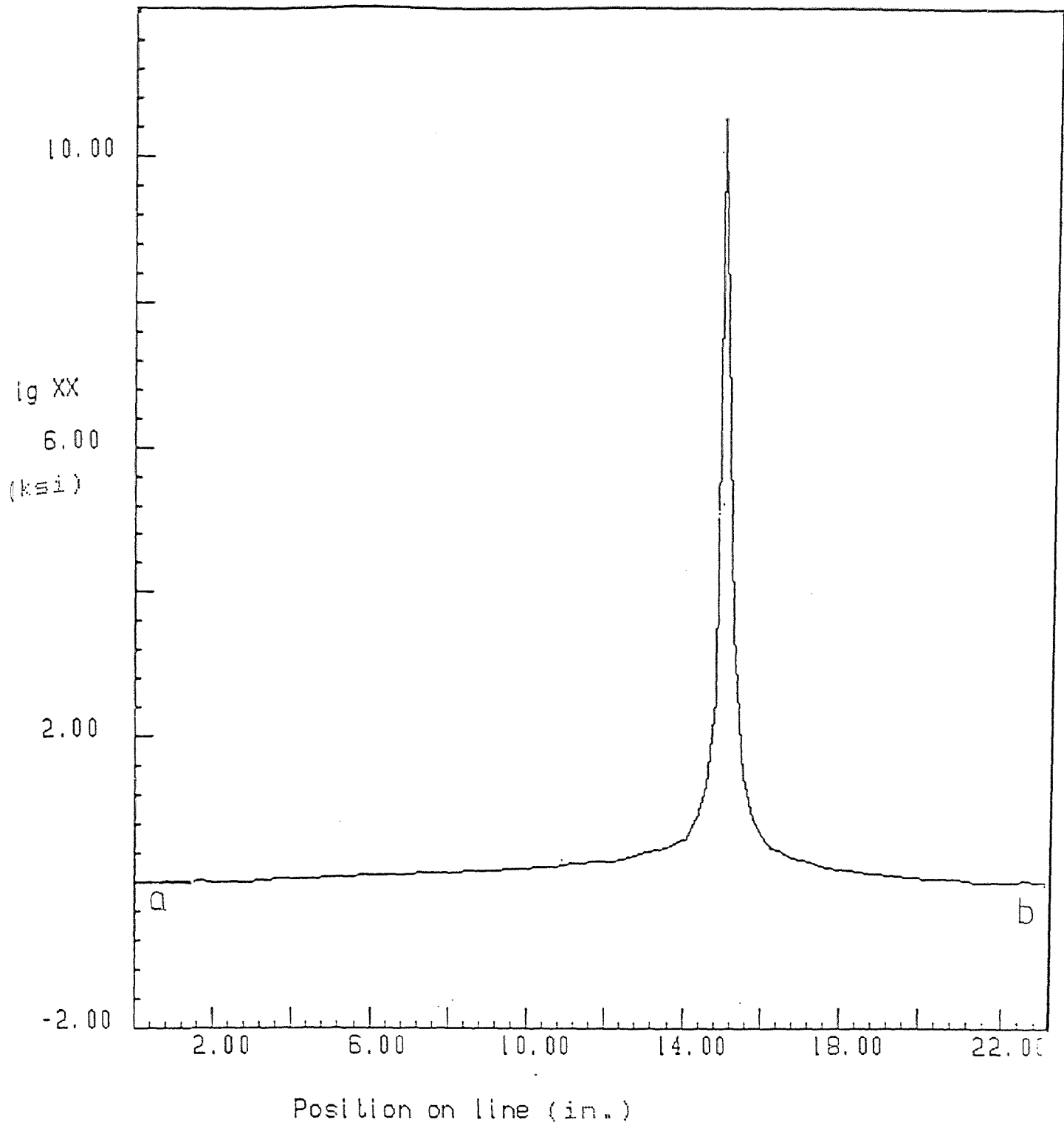


Fig. 3.36 S_x on Section 2-2 ($x=3$)

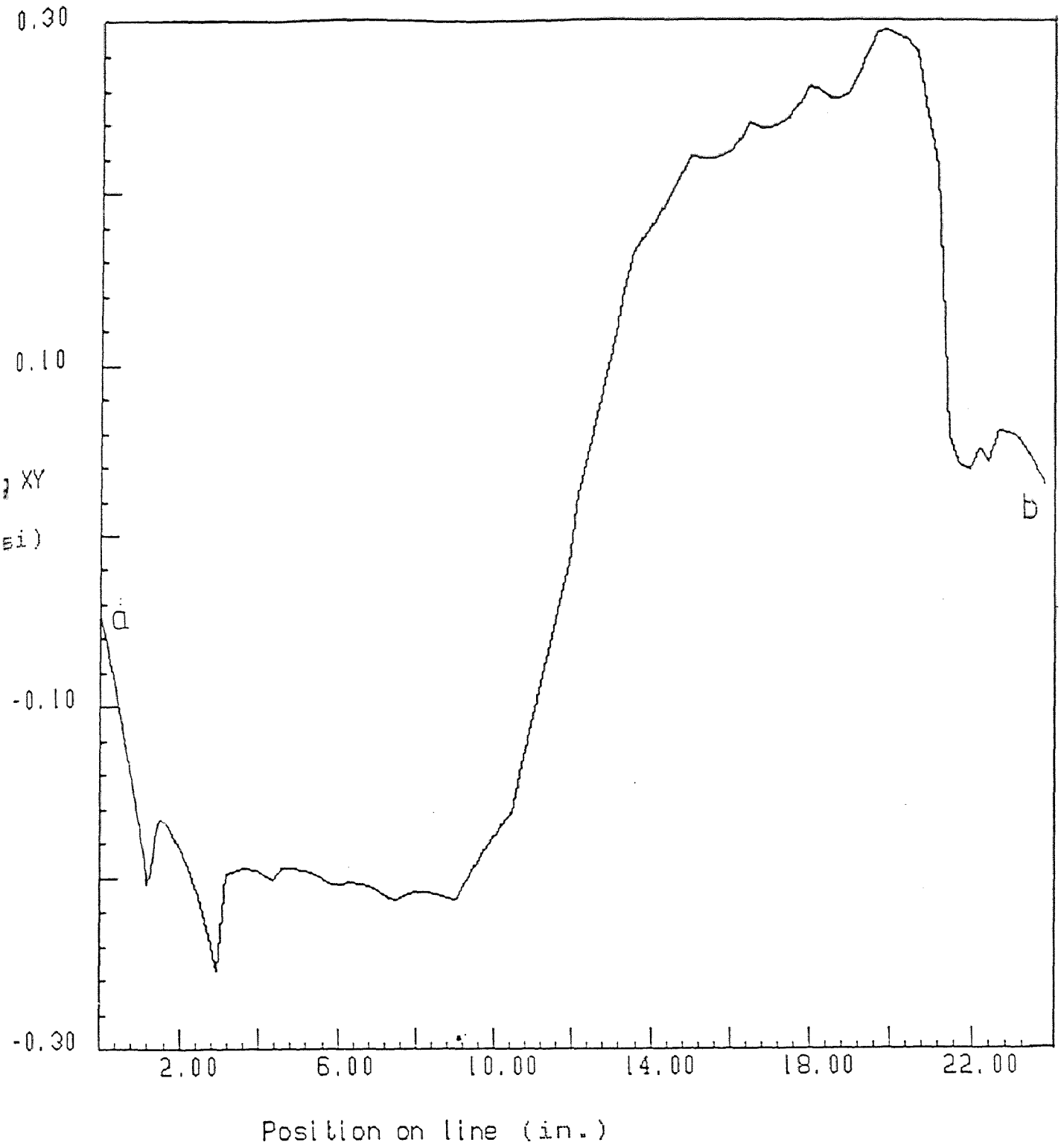


Fig. 3.37 S_{xy} on section 2-2 ($x=9$)

Slg XY vs Position

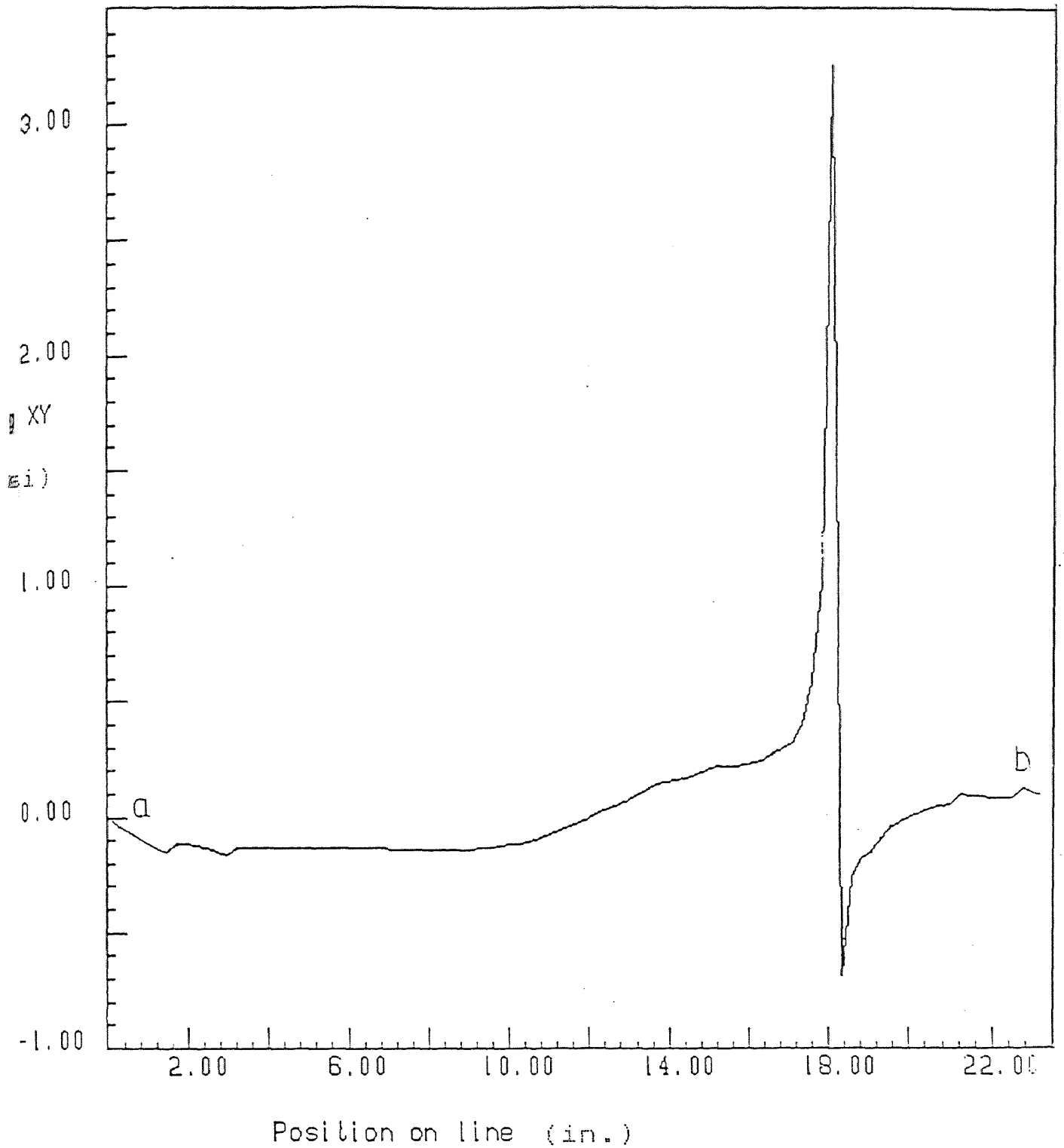


Fig. 3.38 Sxy on Section 2-2 (x=6)

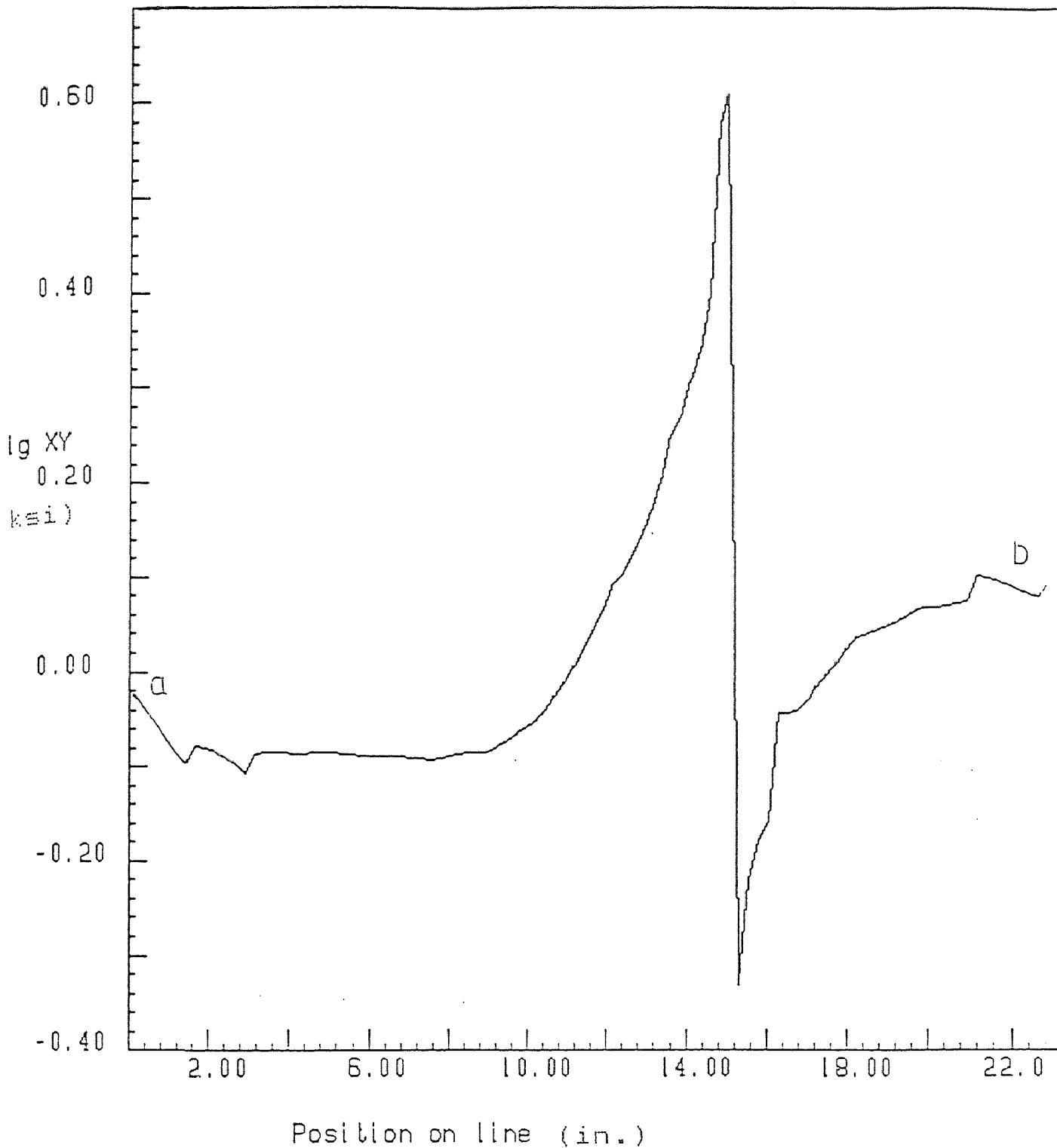


Fig. 3.39 Sxy on Section 2-2 (x=3)

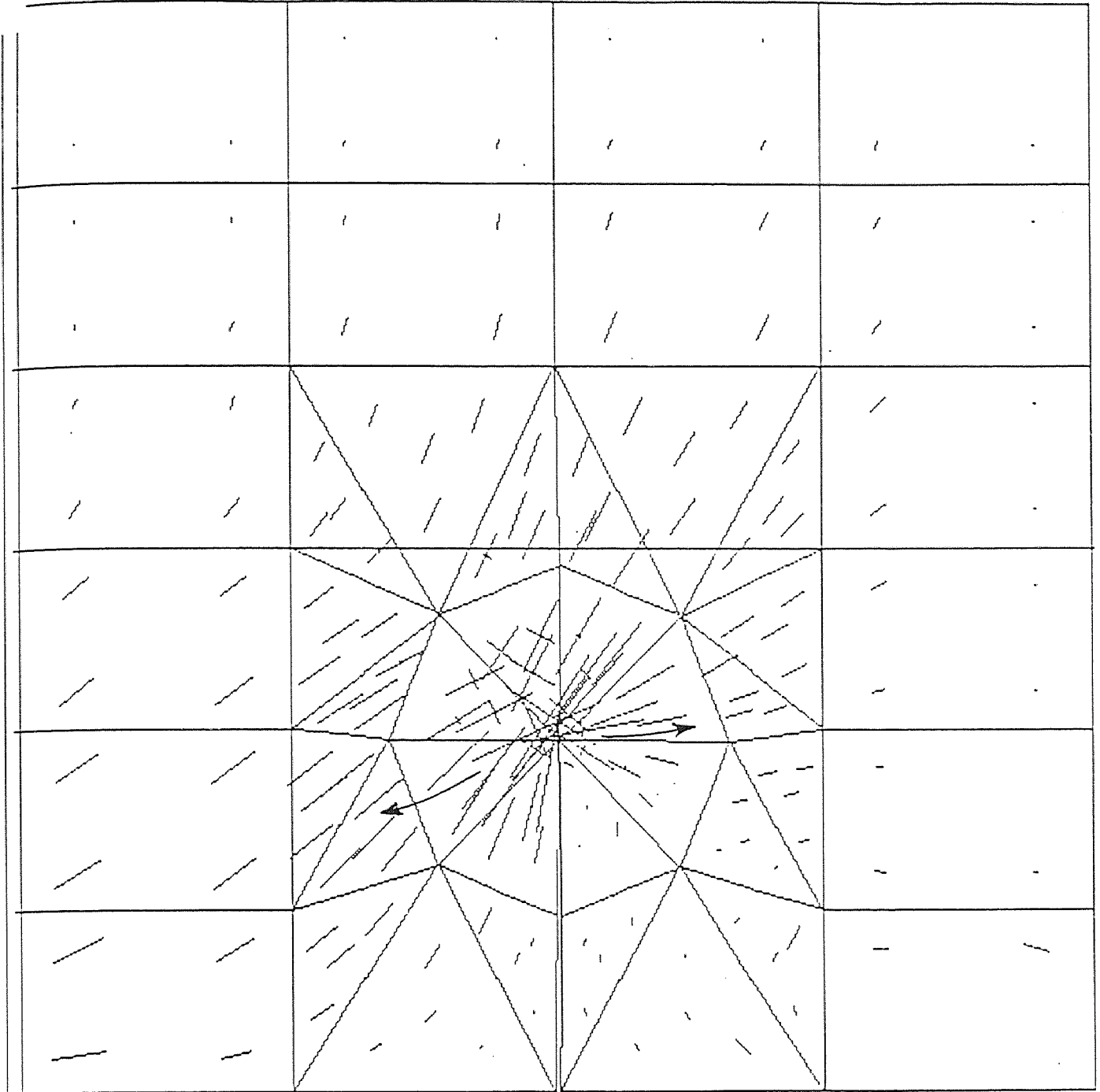


Fig. 3.40 Tensile Principal Stress Vectors (x=9)

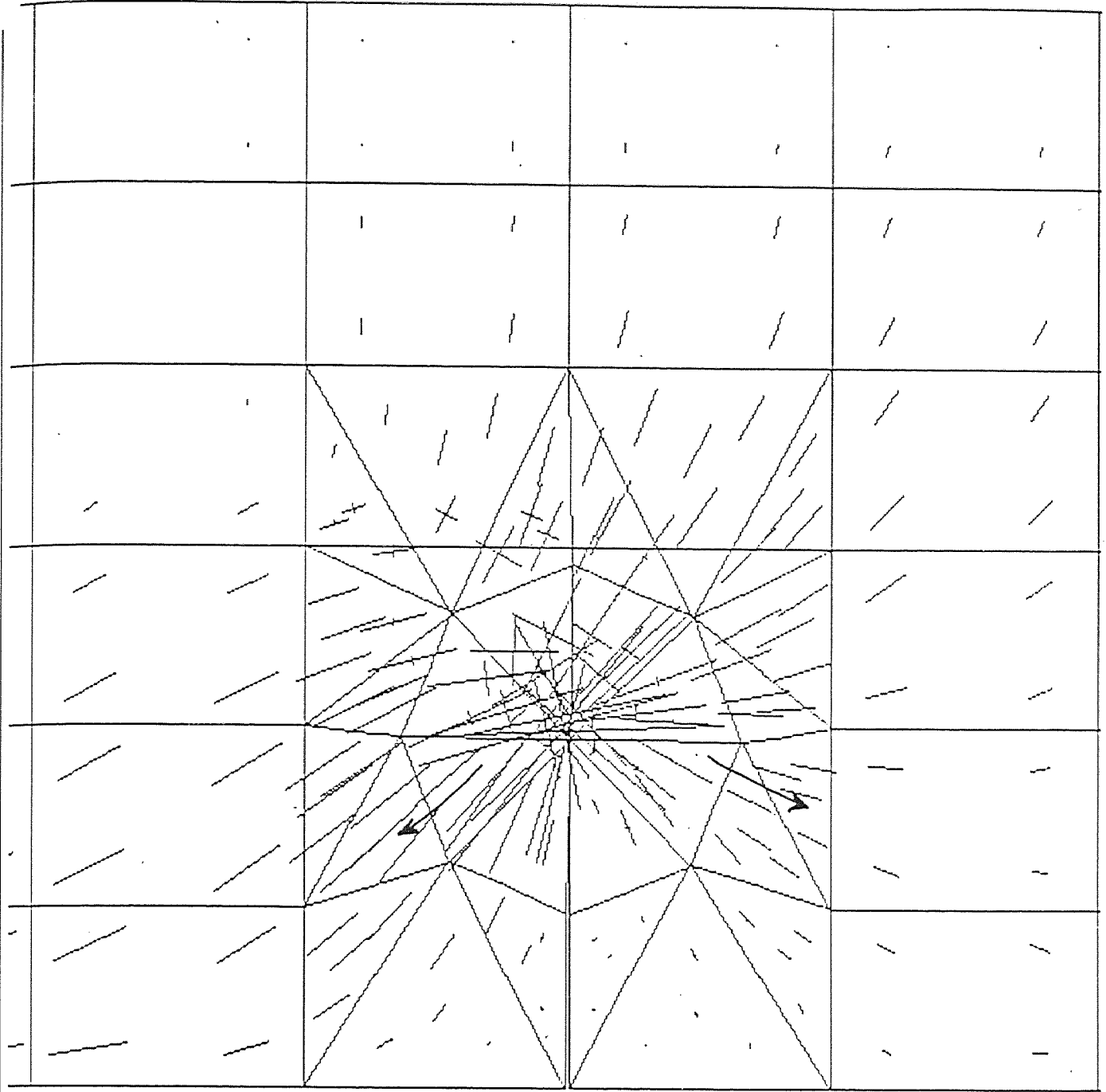


Fig. 3.41 Tensile Principal Stress Vectors (x=6)

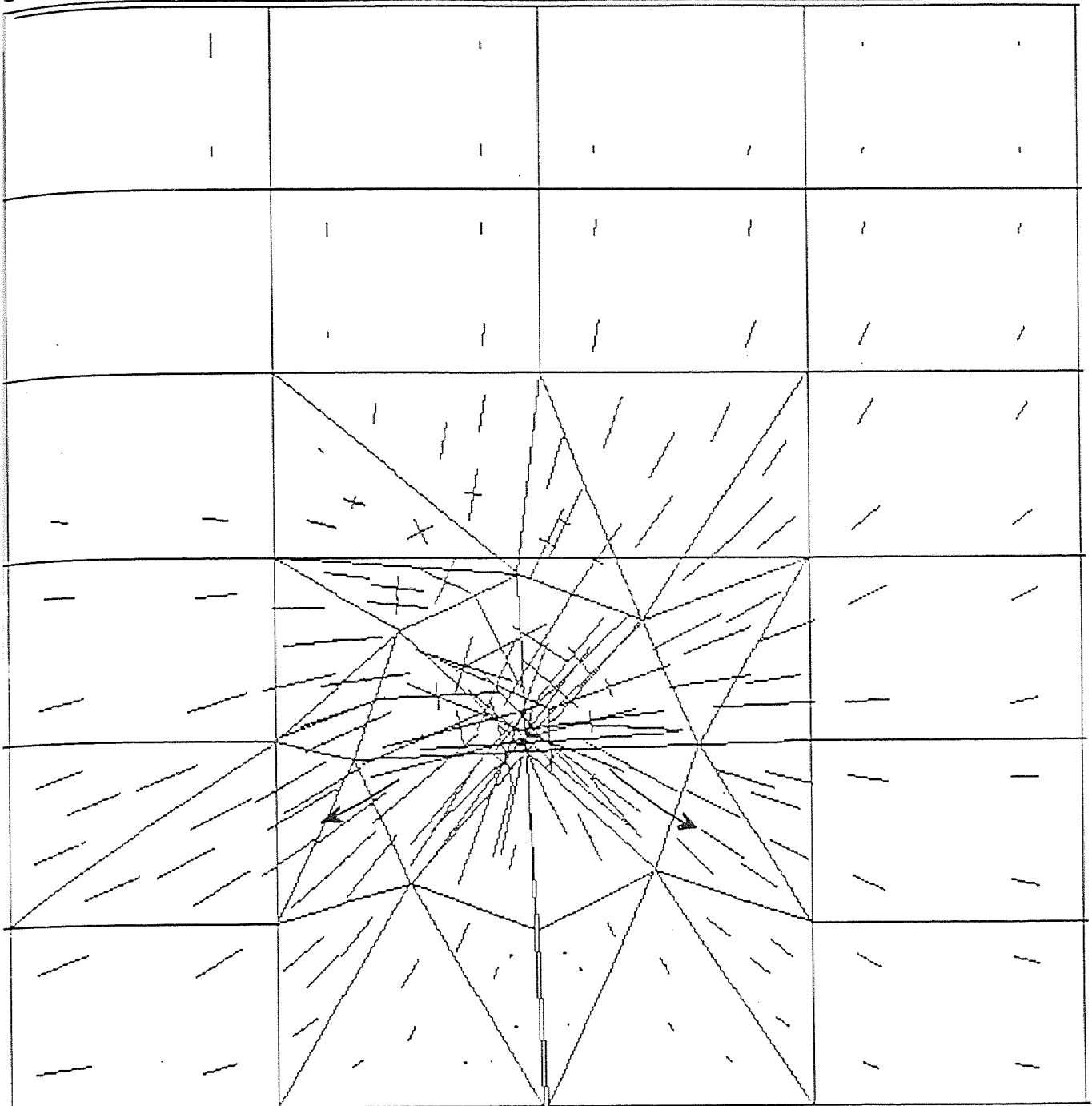


Fig. 3.42 Tensile Principal Stress Vectors (x=3)

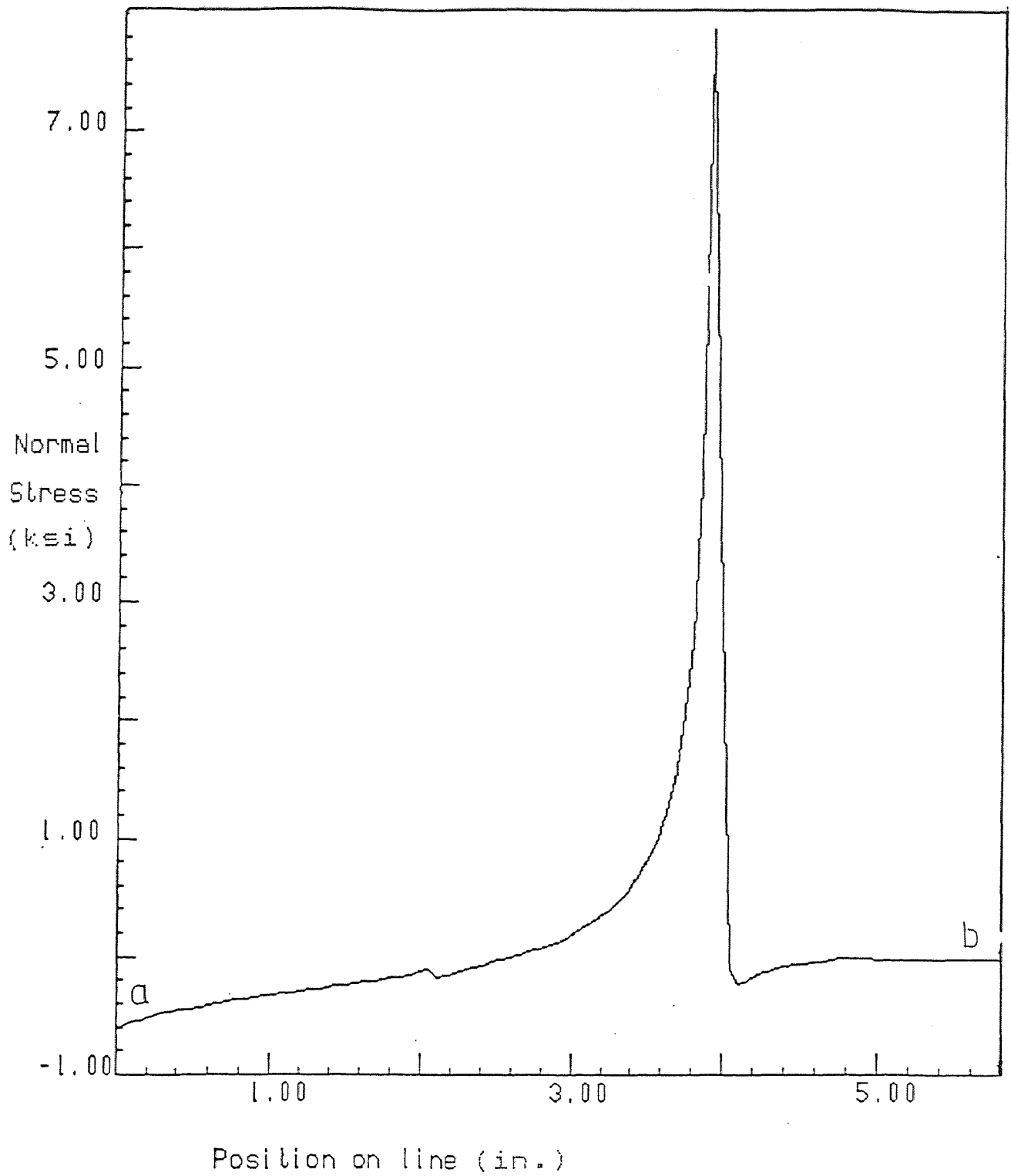


Fig. 3.43 Stress Normal to Line 1-1 (x=9)

Normal Stress vs Position

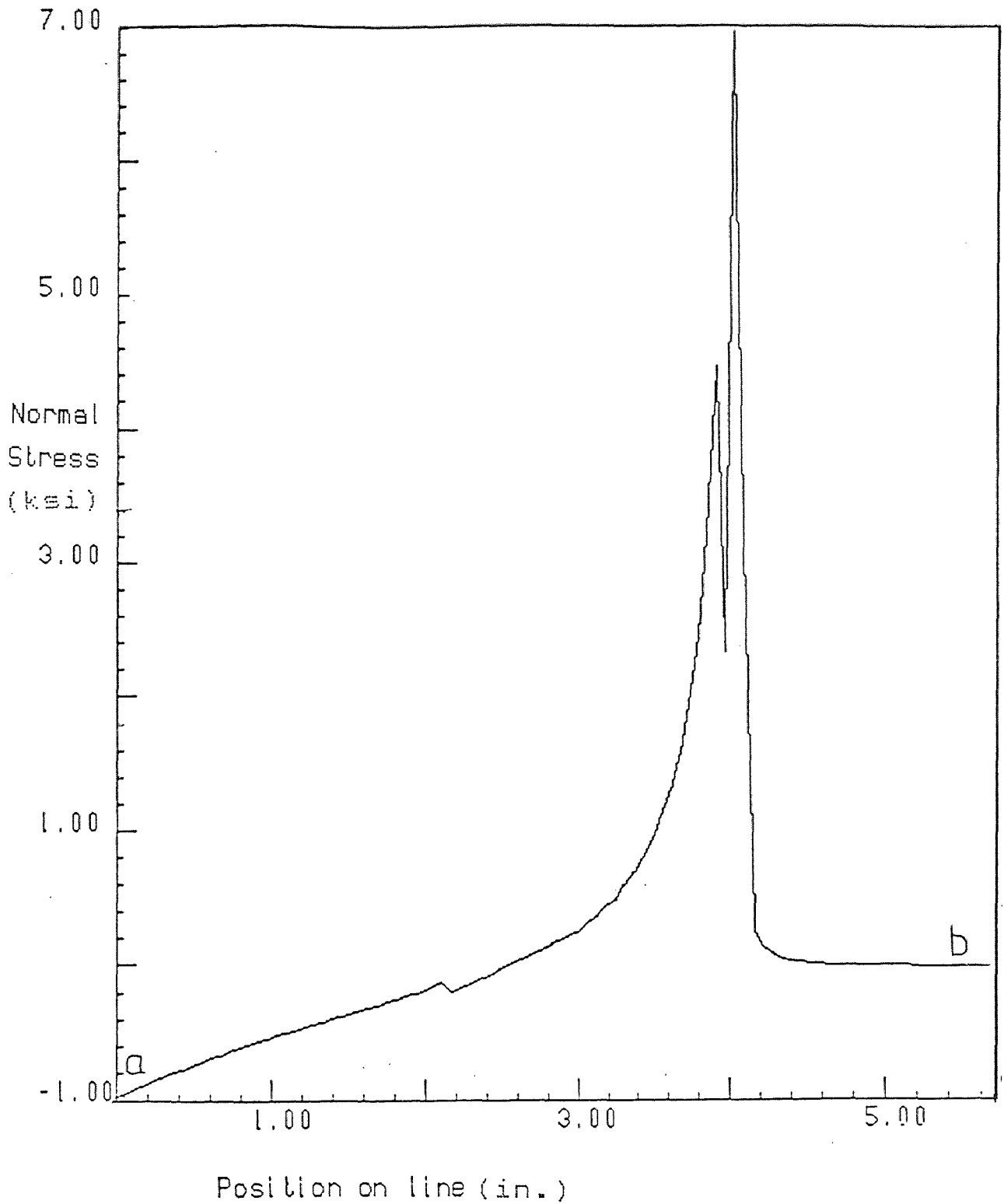


Fig. 3.44 Stress Normal to Line 1-1 ($x=6$)

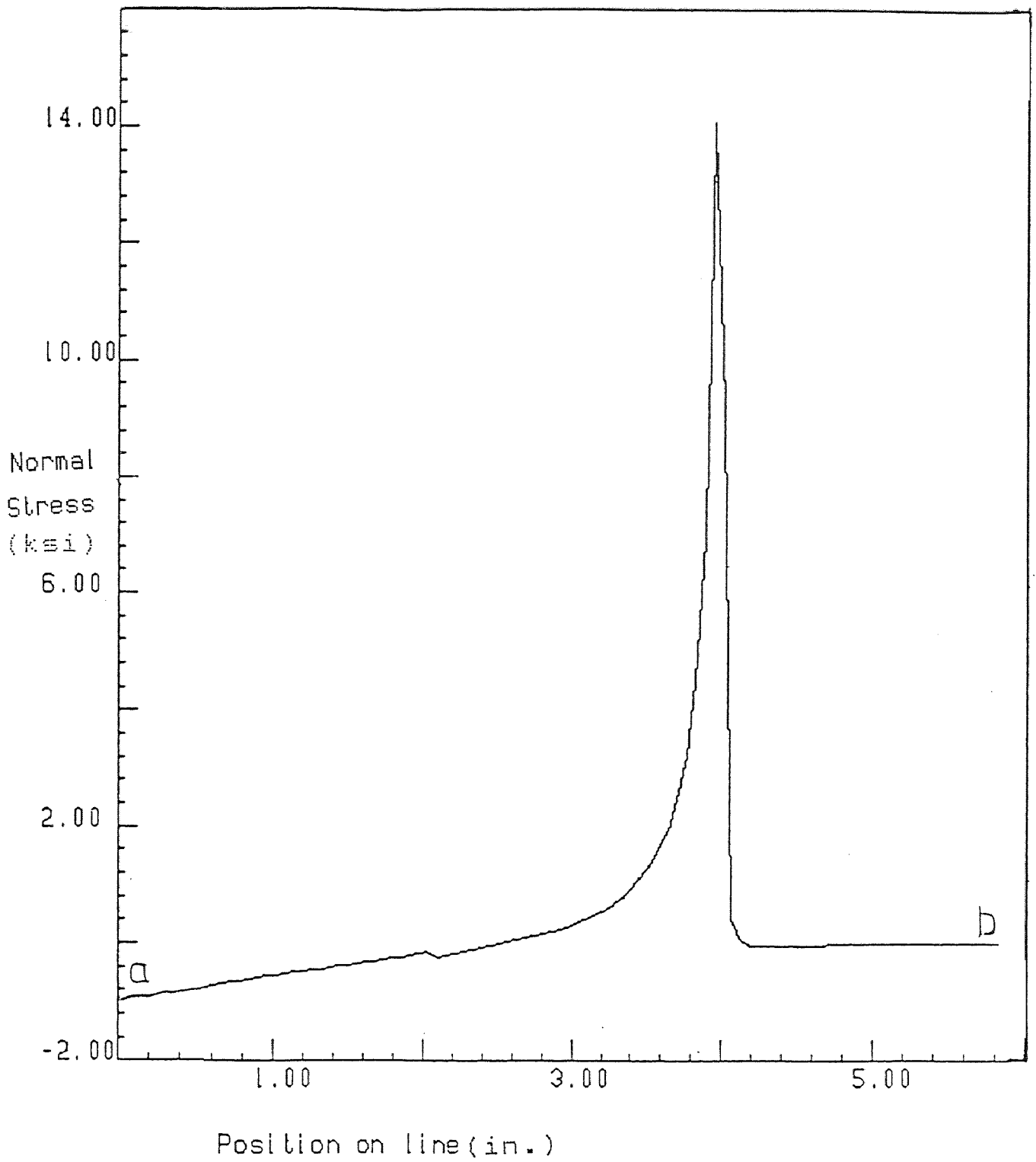


Fig. 3.45 Stress Normal to Line 1-1.(x=3)

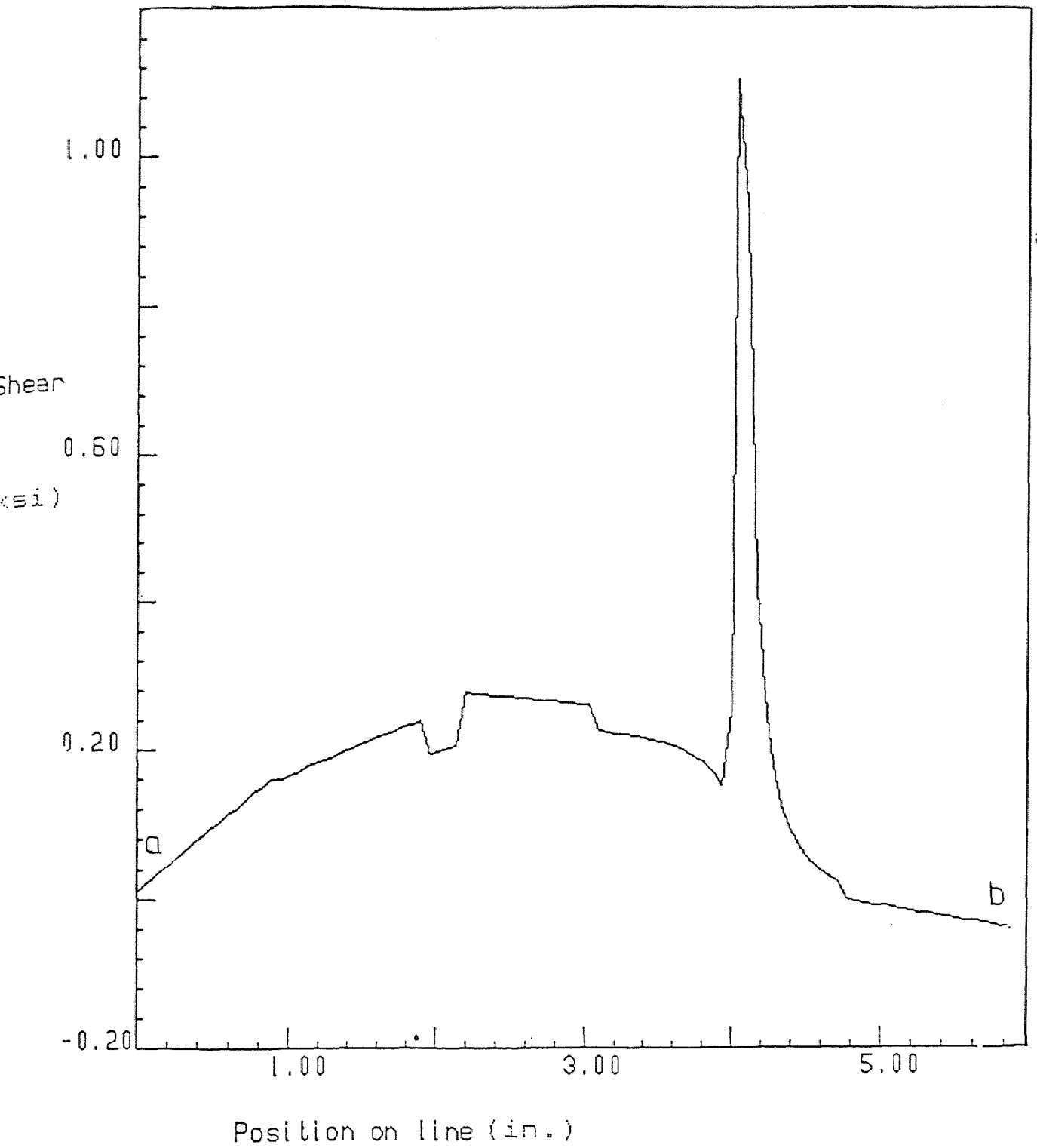


Fig. 3.46 Shear Stress Along Line 1-1 (x=9)

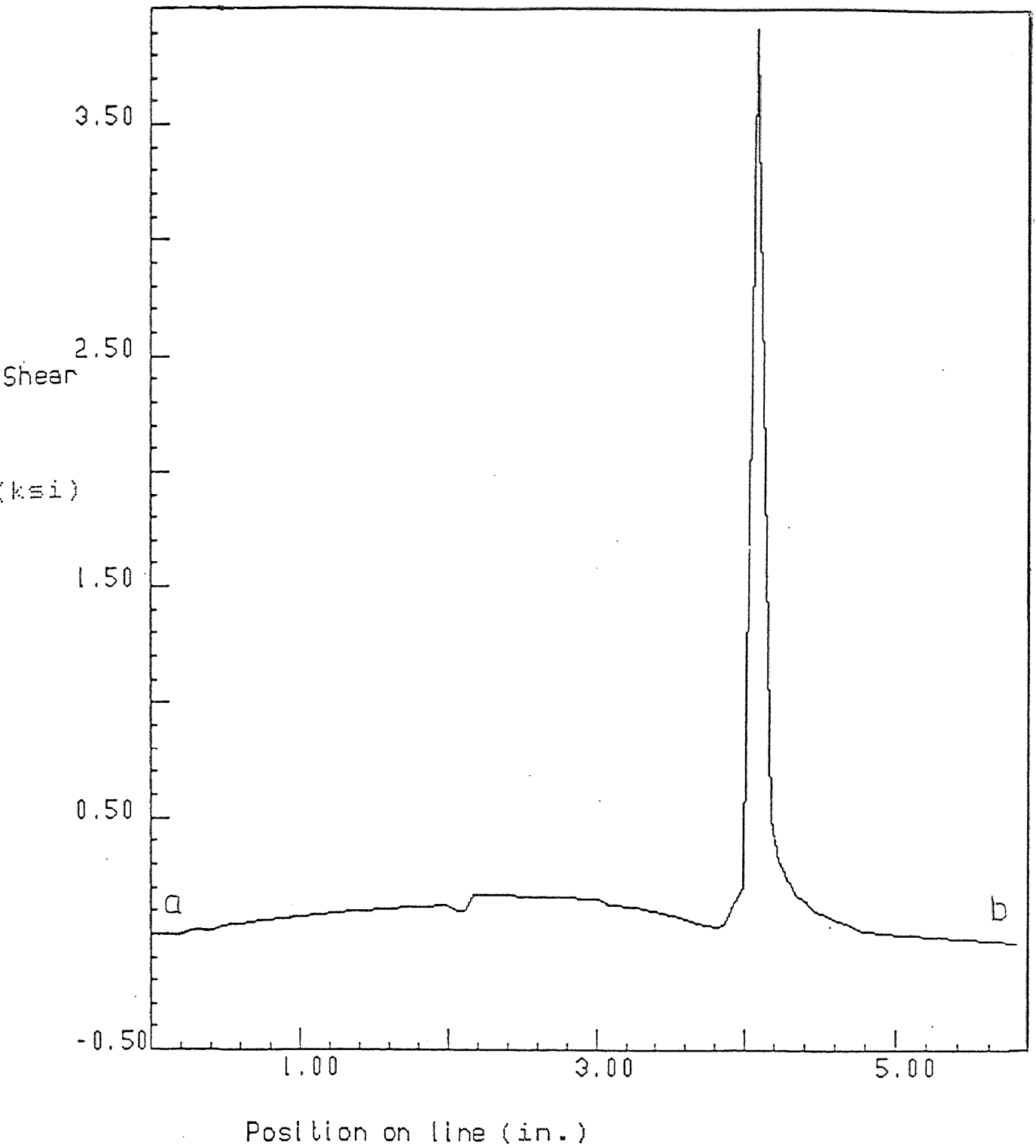


Fig. 3.47 Shear Stress Along Line 1-1 (x=6)

Missing Page

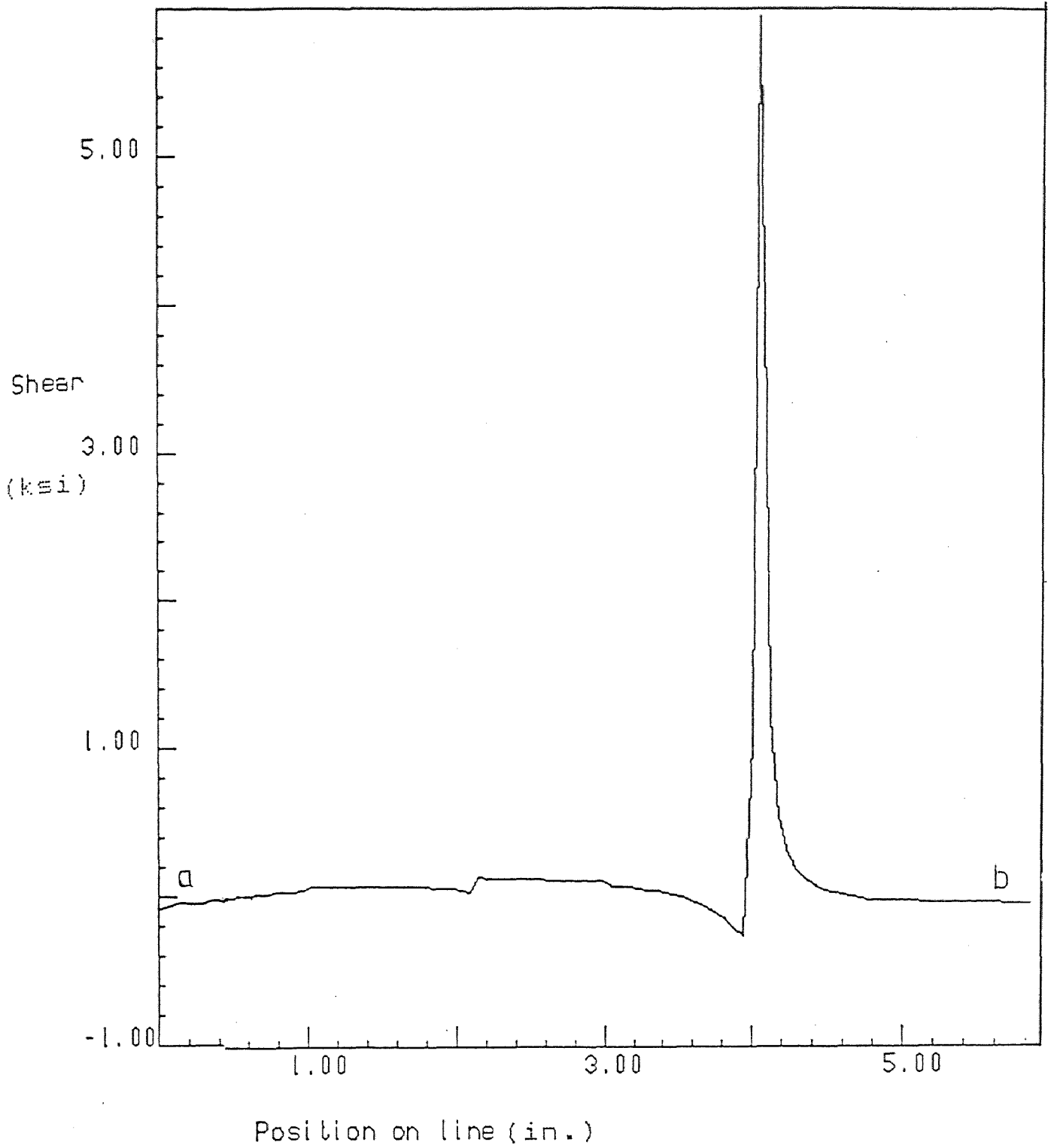


Fig. 3.48 Shear Stress Along Line 1-1 (x=3)

CHAPTER 4

CONCLUSIONS

The computer study of the fracture mechanics of single and double notch beams using the FRANC package gave the following results.

1. For beams with double notches, the tensile stress for the cross section connecting the two notch tips is very close to the assumed tensile strength of concrete whereas the shear stress is below the nominal shearing strength of concrete. For beams with a single notch the tensile stress has a very high value at the notch tip, whereas the shear stress is still below the nominal shearing strength of concrete.
2. The major principal stress in the plane of the notch tips is tensile and its direction is horizontal.
3. The shear stress in the plane of the notch tips does not show parabolic distribution one expects from elementary beam bending theory.
4. None of the stress intensity factors is zero.
5. The average accuracy of FRANC is 89%. For the double notched beam there is no effect of the accuracy on the size. For the single notched beam the effect on size and geometry is more pronounced.

From this study it is clear that tensile fracture as well as shear fracture exists. So, the fracture is a Mixed-Mode fracture.

APPENDIX A
DATA & OUTPUT OF BAZANT & PFEIFFER
(DOUBLE-NOTCHED BEAM)

SPECIMEN DIMENSIONS

Span	:	21.5	in.
Depth	:	8	in.
Thickness	:	3	in.
Notch Depth	:	1.5	in.
Beam Number	:	5	

NODAL INFORMATION

Node number : 394

Coordinates (X,Y): 0.00 0.00

Equation numbers : 418 419

Displacements:

Load Case	X-Disp	Y-Disp
1	0.17E-01	-0.42E-01
2	-0.16E-01	0.41E-01

Total displacement

X-disp: 0.855E-03

Y-disp: -0.262E-03

Input load used: 14 Kips

NODAL INFORMATION

Node number : 394

Coordinates (X,Y): 0.00 0.00

Equation numbers : 418 419

Displacements:

Load Case	X-Disp	Y-Disp
1	0.14E-01	-0.35E-01
2	-0.14E-01	0.35E-01

Total displacement

X-disp: 0.720E-03

Y-disp: -0.220E-03

Input load used: 12 Kips

NODAL INFORMATION

Node number : 394

Coordinates (X,Y): 0.00 0.00

Equation numbers : 418 419

Displacements:

Load Case	X-Disp	Y-Disp
1	0.11E-01	-0.26E-01
2	-0.10E-01	0.26E-01

Total displacement

X-disp: 0.540E-03

Y-disp: -0.165E-03

Input load used: 10 Kips

NODAL INFORMATION

Node number : 394

Coordinates (X,Y): 0.00 0.00

Equation numbers : 418 419

Displacements:

Load Case	X-Disp	Y-Disp
1	0.89E-02	-0.22E-01
2	-0.85E-02	0.22E-01

Total displacement

X-disp: 0.450E-03

Y-disp: -0.138E-03

Input load used: 8 Kips

NODAL INFORMATION

Node number : 394

Coordinates (X,Y): 0.00 0.00

Equation numbers : 418 419

Displacements:

Load Case	X-Disp	Y-Disp
1	0.71E-02	-0.18E-01
2	-0.68E-02	0.17E-01

Total displacement

X-disp: 0.360E-03

Y-disp: -0.110E-03

Input load used: 6 Kips

NODAL INFORMATION

Node number : 394

Coordinates (X,Y): 0.00 0.00

Equation numbers : 417 418

Displacements:

Load Case	X-Disp	Y-Disp
1	0.34E-02	-0.84E-02
2	-0.34E-02	0.83E-02

Total displacement

X-disp: 0.122E-04

Y-disp: -0.292E-04

Input load used: 2 Kips

SPECIMEN DIMENSIONS

Span : 21.5 in.
Depth : 8 in.
Thickness : 3 in.
Notch Depth : 1.75 in.
Beam Number : 6

NODAL INFORMATION

Node number : 396

Coordinates (X,Y): -0.67 0.00

Equation numbers : 465 466

Displacements:

Load Case	X-Disp	Y-Disp
1	-0.14E-01	-0.33E-01
2	0.14E-01	0.34E-01

Total displacement

X-disp: -0.712E-03

Y-disp: 0.620E-03

Input load used: 14 Kips

NODAL INFORMATION

Node number : 396

Coordinates (X,Y): -0.67 0.00

Equation numbers : 465 466

Displacements:

Load Case	X-Disp	Y-Disp
1	-0.11E-01	-0.26E-01
2	0.10E-01	0.26E-01

Total displacement

X-disp: -0.548E-03

Y-disp: 0.477E-03

Input load used: 12 Kips

NODAL INFORMATION

Node number : 396

Coordinates (X,Y): -0.67 0.00

Equation numbers : 465 466

Displacements:

Load Case	X-Disp	Y-Disp
1	-0.88E-02	-0.20E-01
2	0.83E-02	0.21E-01

Total displacement

X-disp: -0.438E-03

Y-disp: 0.382E-03

Input load used: 10 Kips

NODAL INFORMATION

Node number : 396

Coordinates (X,Y): -0.67 0.00

Equation numbers : 465 466

Displacements:

Load Case	X-Disp	Y-Disp
1	-0.71E-02	-0.17E-01
2	0.68E-02	0.17E-01

Total displacement

X-disp: -0.356E-03

Y-disp: 0.310E-03

Input load used: 8 Kips

NODAL INFORMATION

Node number : 404

Coordinates (X,Y): 0.67 0.00

Equation numbers : 367 368

Displacements:

Load Case	X-Disp	Y-Disp
1	-0.11E-01	-0.26E-01
2	0.11E-01	0.26E-01

Total displacement

X-disp: -0.189E-03

Y-disp: -0.237E-03

Input load used: 6 Kips

NODAL INFORMATION

Node number : 396

Coordinates (X,Y): -0.67 0.00

Equation numbers : 465 466

Displacements:

Load Case	X-Disp	Y-Disp
1	-0.33E-02	-0.77E-02
2	0.31E-02	0.78E-02

Total displacement

X-disp: -0.164E-03

Y-disp: 0.143E-03

Input load used: 4 Kips

NODAL INFORMATION

Node number : 396

Coordinates (X,Y): -0.67 0.00

Equation numbers : 465 466

Displacements:

Load Case	X-Disp	Y-Disp
1	-0.14E-02	-0.33E-02
2	0.14E-02	0.34E-02

Total displacement

X-disp: -0.712E-04

Y-disp: 0.620E-04

Input load used: 2 Kips

APPENDIX B
DATA & OUTPUT OF JENG & SHAH
(SINGLE-NOTCHED BEAM)

SPECIMEN DIMENSIONS

Span	:	24	in.
Depth	:	6	in.
Thickness	:	2.25	in.
Notch Depth	:	1.94	in.
Offset	:	2	in.
Beam Number	:	C1M2	

NODAL INFORMATION

Node number : 437

Coordinates (X,Y): 5.99 -3.00

Equation numbers : 261 262

Displacements:

Load Case	X-Disp	Y-Disp
1	-0.24E-02	-0.53E-02

Total displacement

X-disp: -0.241E-02

Y-disp: -0.534E-02

Input load used: 500 lbs

NODAL INFORMATION

Node number : 437

Coordinates (X,Y): 5.99 -3.00

Equation numbers : 261 262

Displacements:

Load Case	X-Disp	Y-Disp
1	-0.19E-02	-0.41E-02

Total displacement

X-disp: -0.185E-02

Y-disp: -0.411E-02

Input load used: 480 lbs

MODAL INFORMATION

Mode number : 437

Coordinates (X,Y): 5.99 -3.00

Equation numbers : 261 262

Displacements:

Load Case	X-Disp	Y-Disp
1	-0.88E-03	-0.20E-02

Total displacement

-disp: -0.878E-03

-disp: -0.196E-02

Input load used: 360 lbs

NODAL INFORMATION

Node number : 437

Coordinates (X,Y): 5.99 -3.00

Equation numbers : 261 262

Displacements:

Load Case	X-Disp	Y-Disp
1	-0.44E-03	-0.98E-03

Total displacement

X-disp: -0.439E-03

Y-disp: -0.978E-03

Input load used: 240 lbs

MODAL INFORMATION

mode number : 437

coordinates (X,Y): 5.99 -3.00

equation numbers : 261 262

displacements:

Load Case	X-Disp	Y-Disp
1	-0.22E-03	-0.49E-03

total displacement

-disp: -0.219E-03

-disp: -0.489E-03

Input load used: 120 lbs

SPECIMEN DIMENSIONS

Span : 12 in.
Depth : 3 in.
Thickness : 1.125 in.
Notch Depth : 0.88 in.
Offset : 2 in.
Beam Number : M2S6

NODAL INFORMATION

Node number : 429

Coordinates (X,Y): 2.24 -1.50

Equation numbers : 301 302

Displacements:

Load Case	X-Disp	Y-Disp
1	-0.62E-03	-0.14E-02

Total displacement

X-disp: -0.616E-03

Y-disp: -0.140E-02

Input load used: 240 lbs

NODAL INFORMATION

Node number : 429

Coordinates (X,Y): 2.24 -1.50

Equation numbers : 301 302

Displacements:

Load Case	X-Disp	Y-Disp
1	-0.51E-03	-0.12E-02

Total displacement

X-disp: -0.507E-03

Y-disp: -0.115E-02

Input load used: 200 lbs

NODAL INFORMATION

Node number : 429

Coordinates (X,Y): 2.24 -1.50

Equation numbers : 301 302

Displacements:

Load Case	X-Disp	Y-Disp
1	-0.40E-03	-0.91E-03

Total displacement

X-disp: -0.398E-03

Y-disp: -0.907E-03

Input load used: 160 lbs

NODAL INFORMATION

Node number : 429

Coordinates (X,Y): 2.24 -1.50

Equation numbers : 301 302

Displacements:

Load Case	X-Disp	Y-Disp
1	-0.33E-03	-0.75E-03

Total displacement

X-disp: -0.326E-03

Y-disp: -0.747E-03

Input load used: 120 lbs

NODAL INFORMATION

Node number : 429

Coordinates (X,Y): 2.24 -1.50

Equation numbers : 301 302

Displacements:

Load Case	X-Disp	Y-Disp
1	-0.22E-03	-0.49E-03

Total displacement

X-disp: -0.217E-03

Y-disp: -0.494E-03

Input load used: 80 lbs

NODAL INFORMATION

Node number : 429

Coordinates (X,Y): 2.24 -1.50

Equation numbers : 301 302

Displacements:

Load Case	X-Disp.	Y-Disp
1	-0.14E-03	-0.33E-03

Total displacement

X-disp: -0.145E-03

Y-disp: -0.330E-03

Input load used: 40 lbs

SPECIMEN DIMENSIONS

Span	:	12	in.
Depth	:	3	in.
Thickness	:	1.125	in.
Notch Depth	:	0.88	in.
Offset	:	1	in.
Beam Number	:	C1S3	

NODAL INFORMATION

Node number : 413

Coordinates (X,Y): 1.12 -1.50

Equation numbers : 350 351

Displacements:

Load Case	X-Disp	Y-Disp
1	-0.16E-02	-0.33E-02

Total displacement

X-disp: -0.162E-02

Y-disp: -0.332E-02

Input load used: 200 lbs

NODAL INFORMATION

Node number : 413

Coordinates (X,Y): 1.12 -1.50

Equation numbers : 350 351

Displacements:

Load Case	X-Disp	Y-Disp
1	-0.12E-02	-0.24E-02

Total displacement

X-disp: -0.118E-02

Y-disp: -0.242E-02

Input load used: 185 lbs

NODAL INFORMATION

Node number : 413

Coordinates (X,Y): 1.12 -1.50

Equation numbers : 350 351

Displacements:

Load Case	X-Disp	Y-Disp
1	-0.74E-03	-0.15E-02

Total displacement

X-disp: -0.736E-03

Y-disp: -0.151E-02

Input load used: 160 lbs

NODAL INFORMATION

Node number : 413

Coordinates (X,Y): 1.12 -1.50

Equation numbers : 348 349

Displacements:

Load Case	X-Disp	Y-Disp
1	-0.56E-03	-0.12E-02

Total displacement

X-disp: -0.559E-03

Y-disp: -0.117E-02

Input load used: 120 lbs

NODAL INFORMATION.

Node number : 413

Coordinates (X,Y): 1.12 -1.50

Equation numbers : 348 349

Displacements:

Load Case	X-Disp	Y-Disp
1	-0.34E-03	-0.70E-03

Total displacement

X-disp: -0.336E-03

Y-disp: -0.704E-03

Input load used: 80 lbs

NODAL INFORMATION

Node number : 413

Coordinates (X,Y): 1.12 -1.50

Equation numbers : 348 349

Displacements:

Load Case	X-Disp	Y-Disp
1	-0.22E-03	-0.47E-03

Total displacement

X-disp: -0.224E-03

Y-disp: -0.469E-03

Input load used: 40 lbs

REFERENCES

- (1) Arrea M., and Ingraffea, A.R. 1981. Mixed mode crack propagation in Mortar and Concrete. Dept. of Structural Engineering, Cornell University Report No. 81-13, 143 pp.
- (2) Barr B., Hasso A.B.D. and Khalifa S.M.S. 1987. Study of Mode II fracture of notched beams, SEM-RILEM International Conference, Houston, TX, pp 370-382.
- (3) Bazant Z.P. and Pfeiffer P.A. 1986. Shear Fracture Tests of Concrete. Materials and Structures (Rilem, Paris) Vol. 15, No. 110, pp 111-121.
- (4) Ingraffea R.A. and Panthaki M.J. 1985. Analysis of "Shear Fracture" Tests of Concrete Beams, US-Japan Seminar on Finite Element Analysis of Reinforced Concrete Structures, Tokyo, pp 111-121.
- (5) Jeng Y.S. and Shah S.P. 1987. Mixed-Mode Fracture of Concrete, SEM-RILEM International Conferences Houston, TX, pp 359-1369.
- (6) Isumi M., Mihashi H. and Nomura N. 1985. Toughness of Concrete for Mode II. International Conferences on Fracture Mechanics of Concrete. Lausanne, pp 347-354.
- (7) Rots G.I. and Rene de Borst. 1987. Analysis of Mixed Mode Fracture in Concrete. Journal of Engineering Mechanics Vol 113., no 11, pp 1735-1758.
- (8) Swartz S.E. and Taha N.M. 1987. Preliminary Investigation of the Suitability of the Iosipescu Test Specimen for Determining Mixed Mode Fracture Properties of Concrete. Research, Kansas State University College of Engineering Report #191.
- (9) Van Mier G.M. and Nooru-Mohamed M.B. 1988. Fracture of Concrete Under Tensile and Shear-Like Loading, International Conference on Fracture and Damage of Concrete and Rock, Vienna, pp 433-447.